

FEM Modeling for Biomedical Applications: RF Heating & Microwave Imaging

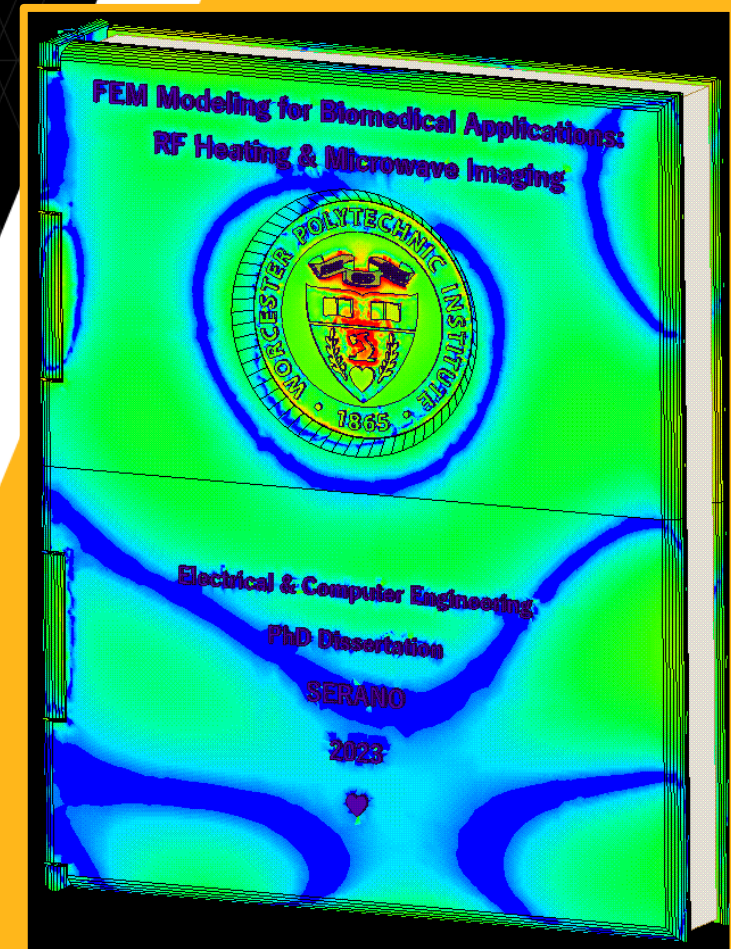
Ph.D. Dissertation Defense
Electrical & Computer Engineering

Peter Serano

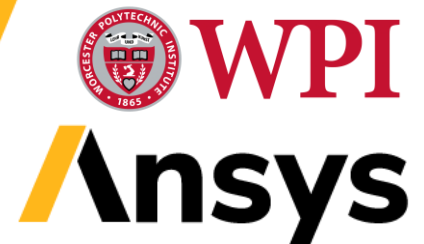
PhD Candidate, WPI ECE

Lead Application Engineer, Ansys Inc.

12/14/23



3D Printable Hardcover Dissertation Binding Made in HFSS



Technical/Personal Background

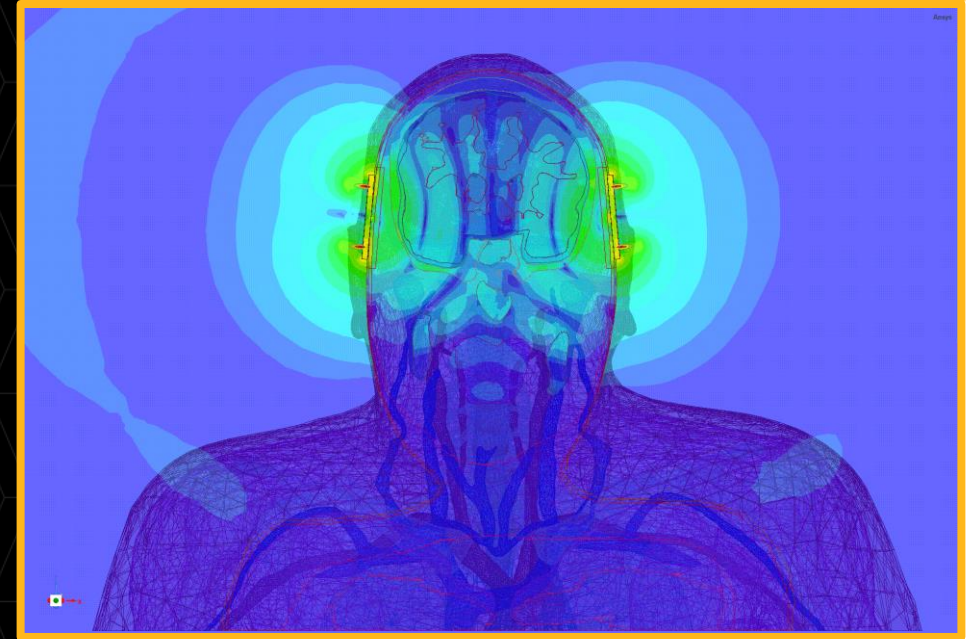
Ph.D. Dissertation Defense
Electrical & Computer Engineering

Peter Serano

PhD Candidate, WPI ECE

Lead Application Engineer, Ansys Inc.

12/14/23



WPI

Ansys

Technical Background



- 2018-Present (Full-Time): Ansys Inc., Washington, DC
 - Lead Application Engineer
- 2017-Present (Part-Time): Rock 'n Repair Shop, Washington, DC
 - Owner / Founder / Manager / Electronics & Instrument Repair Technician
- 2014-2017: U.S. Food and Drug Administration, Silver Spring, MD
 - ORISE Research Fellow, CDRH/OSEL/DBP
- 2011-2014: Athinoula A. Martinos Center for Biomedical Imaging, Charlestown, MA
 - Research Assistant, Analog Brain Imaging Laboratory
 - Research Technician, 15 Tesla MRI Laboratory
- 2010-2011: Bruker Bio-Spin, Billerica, MA
 - RF Engineer: NMR Probe Head Design & Construction
- 2008-2010: InsightMRI, Worcester, MA
 - RF Engineer: RF Coil Design & Construction
- 2002-2009: Worcester Polytechnic Institute, Worcester, MA
 - BS ECE, Music Minor (2006); MS ECE (2009)

Rock'n Repair Shop



5.0 ★★★★★ (140)

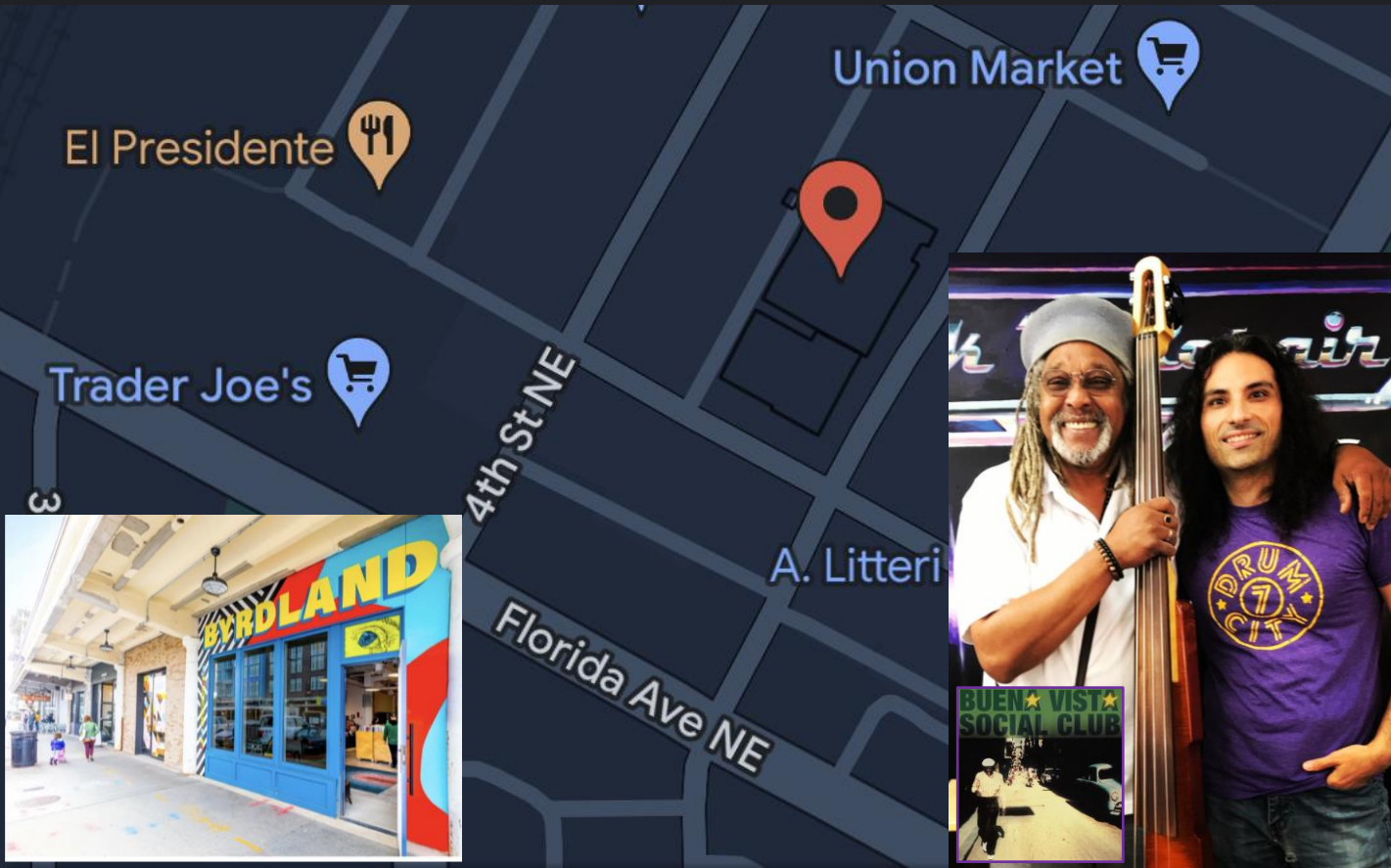
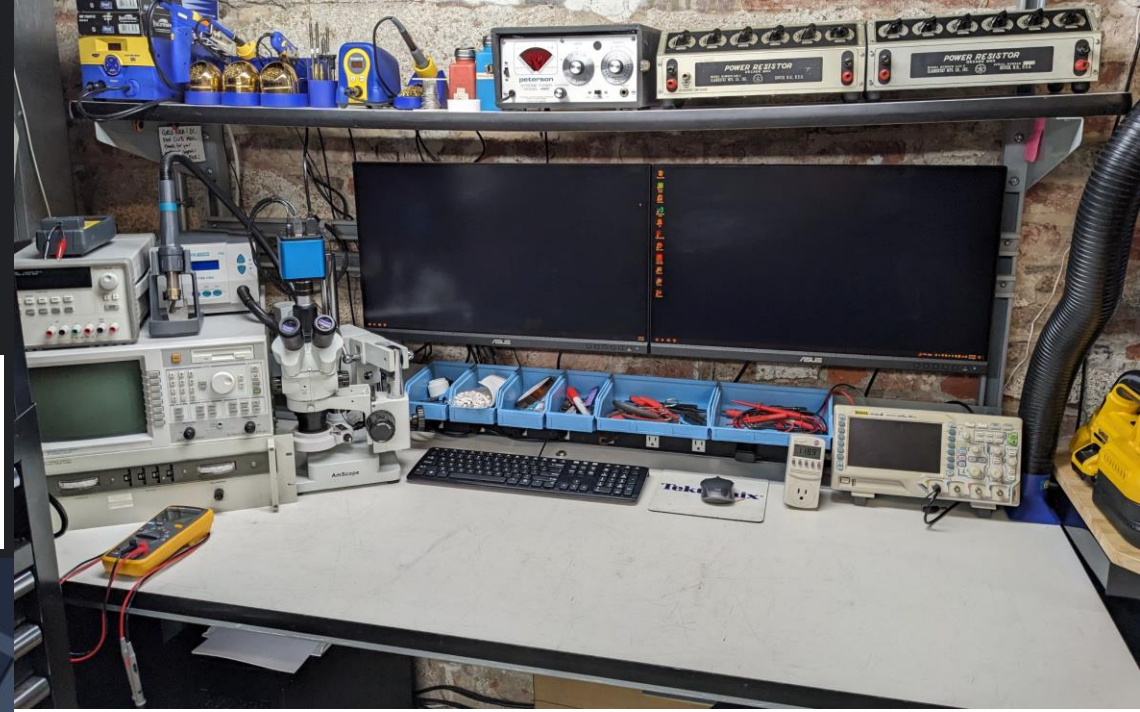
Electronics repair shop

Closed · Opens 12 PM Sat

You manage this Business Profile



1,393 customer interactions



C B.
@ 1 ★ 32 📷 5

★★★★★ 2 years ago

Nice little gem in the heart of DC, owner is very knowledgeable, honest, and down to earth. I definitely recommend taking all of your musical equipment here!!!

Megan D.
@ 2 ★ 5

★★★★★ 5 years ago

Pete is a nice dude and fixed my guitar string last minute.



99 Posts

1,703 Followers

235 Following

Rock'n Repair Shop

DC's Electronics and Instrument Repair Shop
Located inside @byrdlandrecords at Union Market... more

www.rocknrepair.com/contactus

1264 5th St NE, Washington D.C. 20002

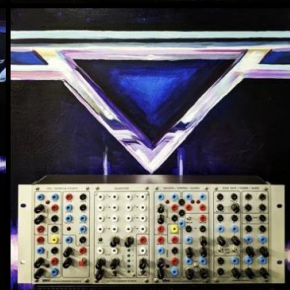
Professional dashboard

118 accounts reached in the last 30 days.

Edit profile

Share profile

Contact



★★★★★ 3 years ago

Super happy with the service at Rock and Repair. Most shops charge \$50-75 just for a diagnostic but Pete was willing to share his knowledge for free and I was able to fix my amp by myself with his advice, iv never experienced a repair shop with this level of service!

Would recommend for any musician who needs a repair!

★★★★★ 5 months ago

I brought my very strange Byzantine chant greek synthesizer that I found in and the owner took very good care of it and me. They took the time to explain the diagnostic process as they went through it and were very fun to learn from and talk to. This is my go-to place for electronic repairs now. Very honest business and brilliant people.

★★★★★ 5 years ago

Peter has saved my professional butt on multiple occasions, rescuing me from hardware and software problems, in person and remotely, with competence, grace, and compassion. Not only does he have the technical skills to fix pretty much everything, but he is also a careful listener. He never condescends to his clients, which is a rare virtue indeed. I hope I never have to work with anyone else ever again for my computer needs, because Peter broke the mold. I can't recommend him highly enough.

★★★★★ 5 years ago

pete fixed a bunch of my modular synths, and did some other stuff on the modular rack, and did a great job fixing a new pick up system on my old acoustic. he also changed a battery for me, without pointing out how silly i was for not knowing the thing had a battery.

★★★★★ 4 years ago

Pete and his team are outstanding! I had a 30 year old string of musical Christmas lights that failed, and even though it is outside of his normal repair focus area, he still offered to take a look at it. Within 30 minutes he had found and repaired 2 problems, and restored the musical string to working condition. This item has strong sentimental value to our family, and in a world of throw out and replace, it was great to find someone willing to take the time to bring things back to life.

★★★★★ 2 years ago

I needed an amp worked on after some problems and these guys were able to fix it (and teach me about what went wrong) in a very fast turnaround time. They are professional, super knowledgeable, and friendly. For amp and electronics repair in DC they are the best shop by far.

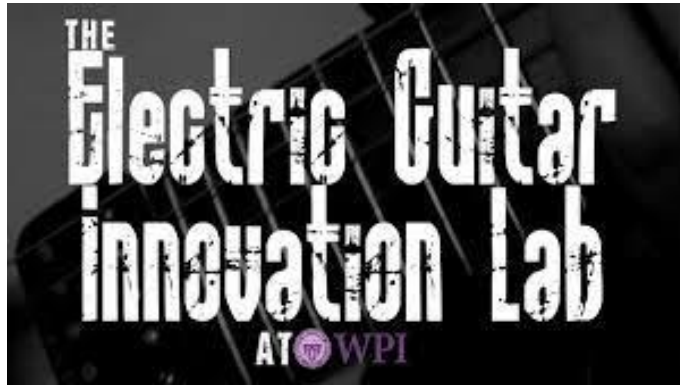
★★★★★ 4 years ago

The best audio repair & instrument tune up shop on town - bar none. Peter is has an encyclopedic knowledge of electronics and acoustics, and is also the a strong contender for "nicest guy in DC". He has fixed two of my guitars and amps in record time. Would give 6 stars if I could.

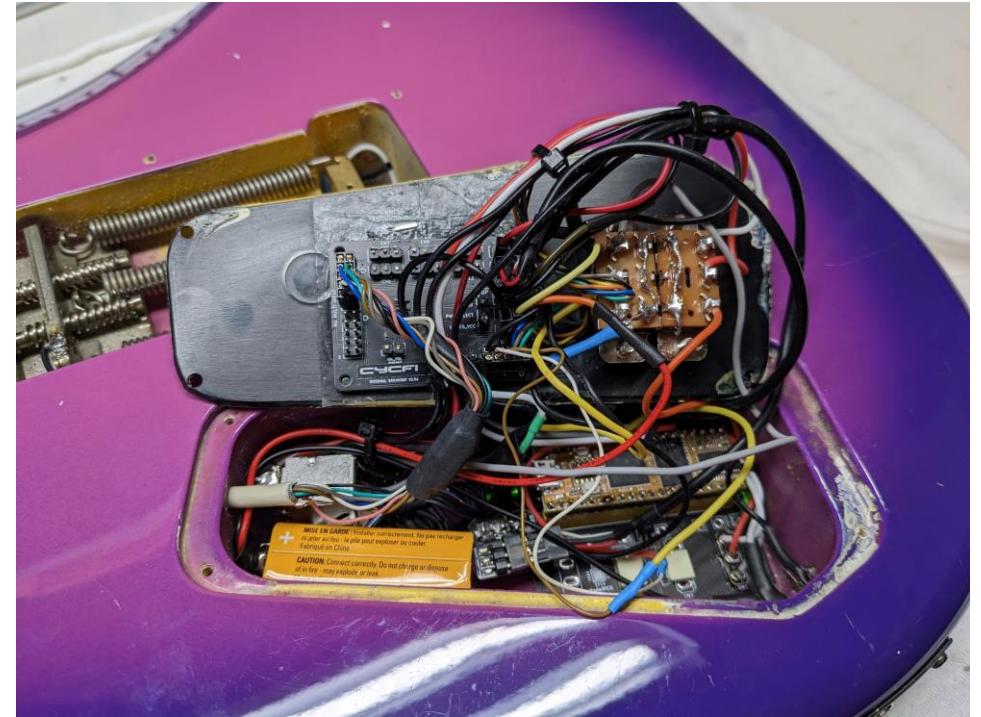
★★★★★ 5 years ago

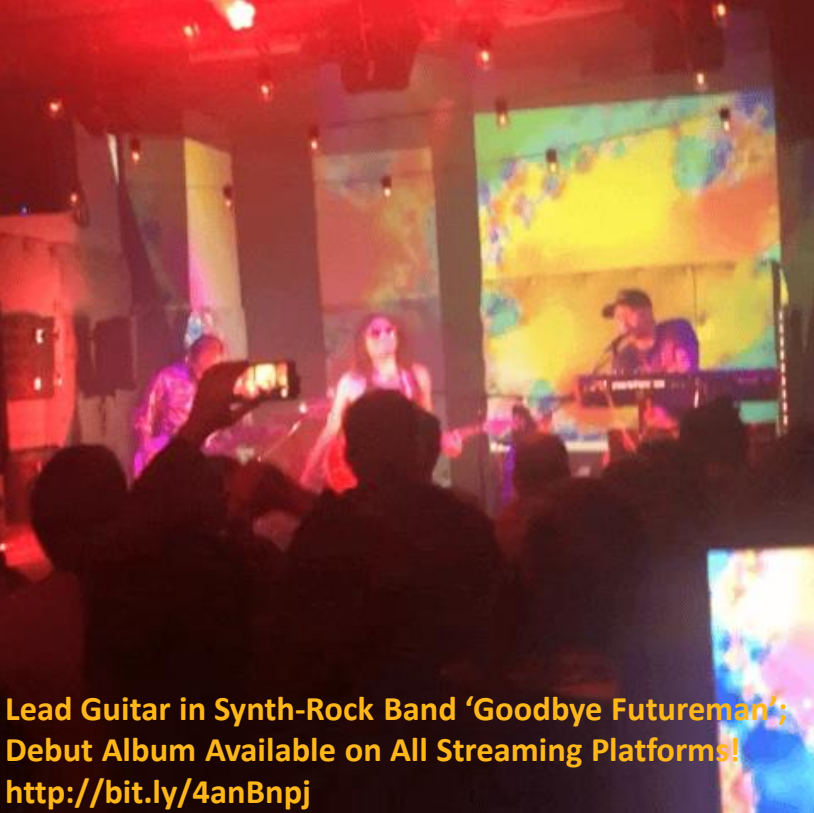
This place is easily my favorite repair shop around. After a few conversations with Pete at 7 Drum City about some guitar mods I wanted, it was easy to notice Pete's expertise and passion for his work. He is also a very friendly person who was patient and willing to answer all the questions I had about what I wanted to do with my guitar. Wanting to learn more about the process to satisfy my own curiosity, I brought in my Fender Strat to have new Mother's Milk pickups installed and to replace some older parts, and asked Pete if I could get a walk-through of the installation. Not only did he explain every step of the process as he worked on my guitar, he even taught me how to solder some of the parts using his own tools, and gave me advice on how to take care of smaller problems at home to avoid unnecessary trips to the repair shop. It's been a few months since I got this job done and my guitar sounds better than it ever has. Basically, Pete's a stand up guy who's highly skilled and running a top quality repair shop that won't break the bank. I definitely recommend this place to anyone who needs work done on their equipment.

Collaboration with WPI Electric Guitar Innovation Lab (EGIL)

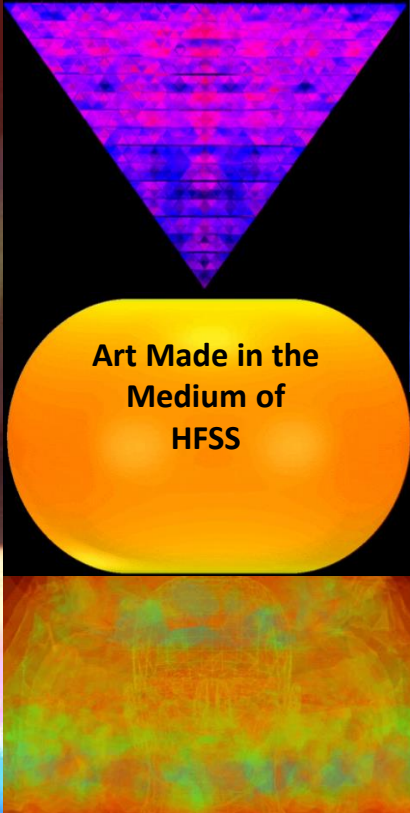


- Embedded WPI EGIL's DSP + Microcontroller Platform into My Guitar
 - Custom PCB Design Currently Being Developed!
- Enables Modulation of Digital FX w/
 - Accelerometer & Gyroscope Input (Movement of Guitar Body)
 - Infrared Distance Sensor Input (Varying Hand Placement Above Sensor)

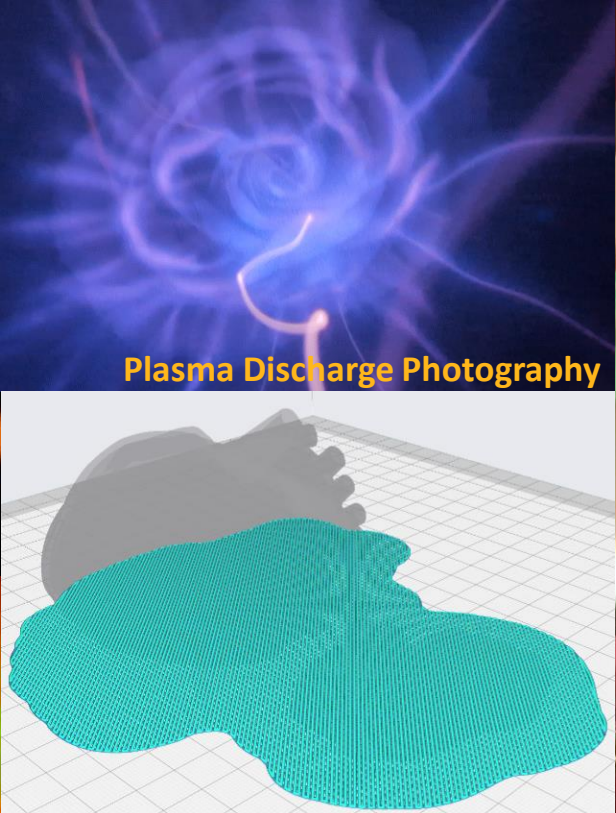




Lead Guitar in Synth-Rock Band 'Goodbye Futureman';
Debut Album Available on All Streaming Platforms!
<http://bit.ly/4anBnpj>



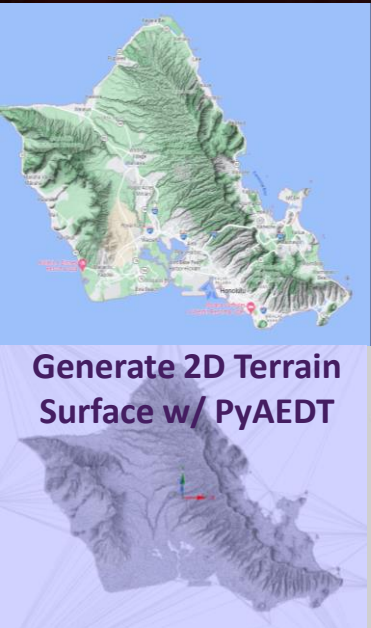
Art Made in the
Medium of
HFSS



Plasma Discharge Photography



World's First Penguin-Based MIDI Controller



Generate 2D Terrain
Surface w/ PyAEDT

```
# Calculate the distance z value
dist_z = np.abs(original_mesh_vectors[:, :, 2])

# Identify the extents in x and y
min_x, max_x = np.min(original_mesh_vectors[:, :, 1]), np.max(original_mesh_vectors[:, :, 1])
min_y, max_y = np.min(original_mesh_vectors[:, :, 3]), np.max(original_mesh_vectors[:, :, 3])

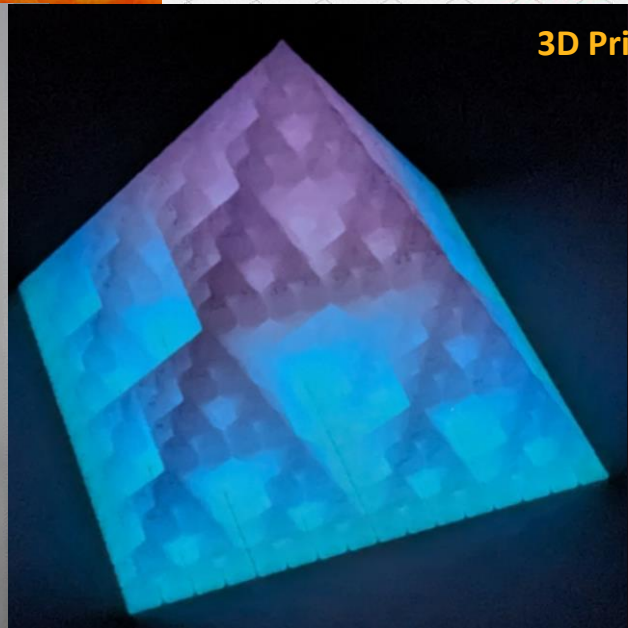
# Extract unique points at X and Y extents
x_min_points = np.unique(original_mesh_vectors[is_close(original_mesh_vectors[:, :, 1], min_x), :], axis=0)
x_max_points = np.unique(original_mesh_vectors[is_close(original_mesh_vectors[:, :, 1], max_x), :], axis=0)
y_min_points = np.unique(original_mesh_vectors[is_close(original_mesh_vectors[:, :, 3], min_y), :], axis=0)
y_max_points = np.unique(original_mesh_vectors[is_close(original_mesh_vectors[:, :, 3], max_y), :], axis=0)

# Sort points by their y (for X extents) and X (for Y extents) for proper printing
x_min_points = x_min_points[x_min_points[:, 1].argsort()]
x_max_points = x_max_points[x_max_points[:, 1].argsort()]
y_min_points = y_min_points[y_min_points[:, 3].argsort()]
y_max_points = y_max_points[y_max_points[:, 3].argsort()]

# Generate side wall faces for points on X extents (YZ plane)
x_side_faces = []
for x_points in [x_min_points, x_max_points]:
    for i in range(len(x_points) - 1):
        p1 = x_points[i]
        p2 = x_points[i+1]
        pt_base = [p1[0], p1[1], min_z]
        pt_base = [p2[0], p2[1], min_z]
        x_side_faces.append([p1, p2, pt_base])
    x_side_faces.append([p1, p2_base, pt_base])

# Generate side wall faces for points on Y extents (XZ plane)
y_side_faces = []
for y_points in [y_min_points, y_max_points]:
    for i in range(len(y_points) - 1):
        p1 = y_points[i]
```

+ Custom Python
Code to Generate
3D Printable STL



3D Printing!



Development of an FDA Approved Medical Device Development Tool (MDDT):

*'Computation Tool For Temperature Rise
Prediction Near An Orthopedic Femoral Nail
Implant During A 1.5 T MRI Scan '*

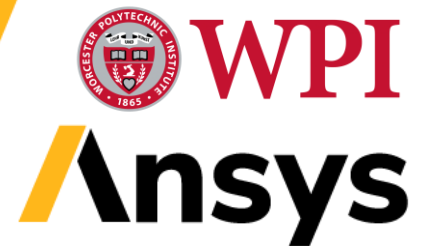
*Ph.D. Dissertation Defense
Electrical & Computer Engineering*

Peter Serano

PhD Candidate, WPI ECE

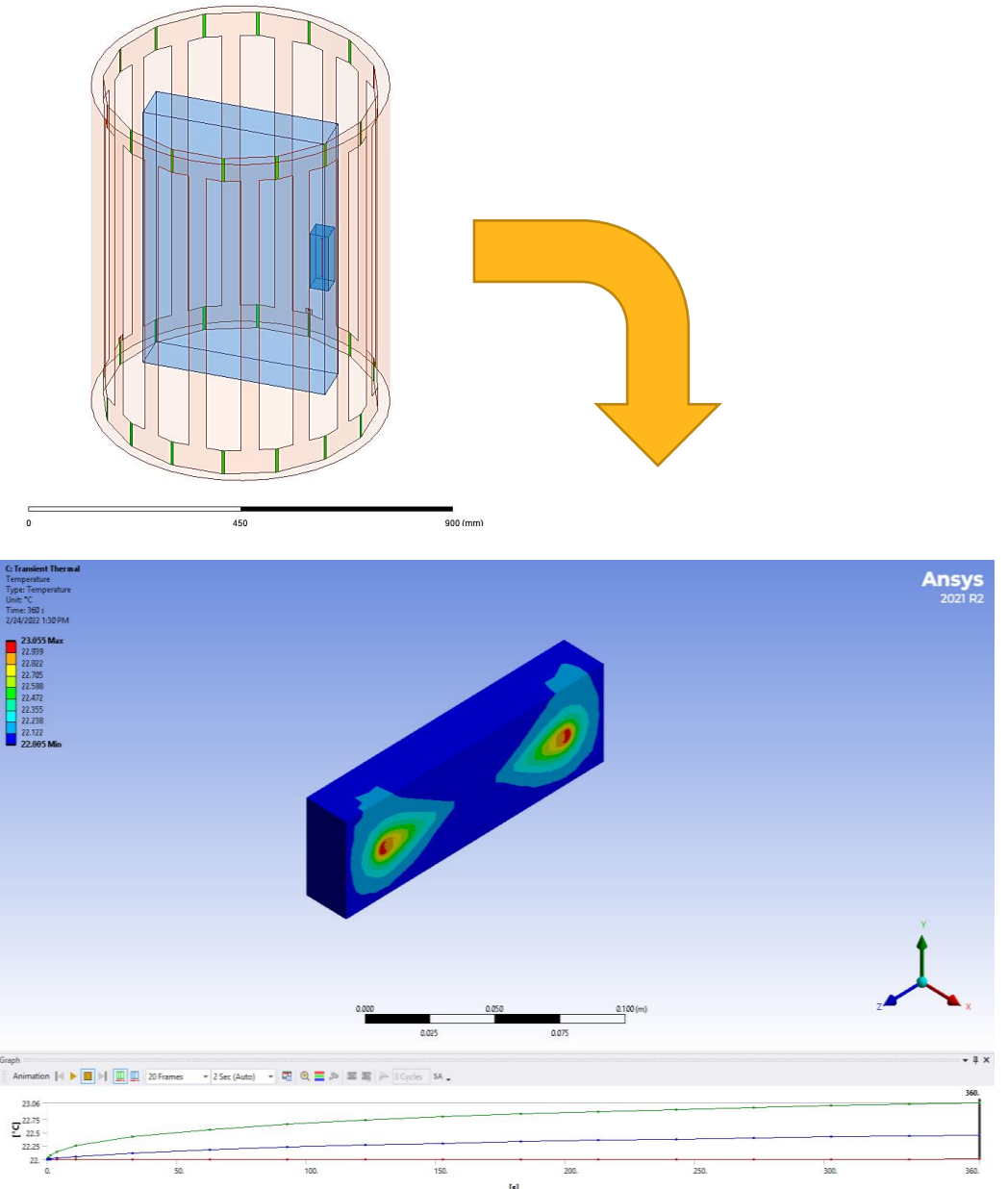
Lead Application Engineer, Ansys Inc.

12/14/23



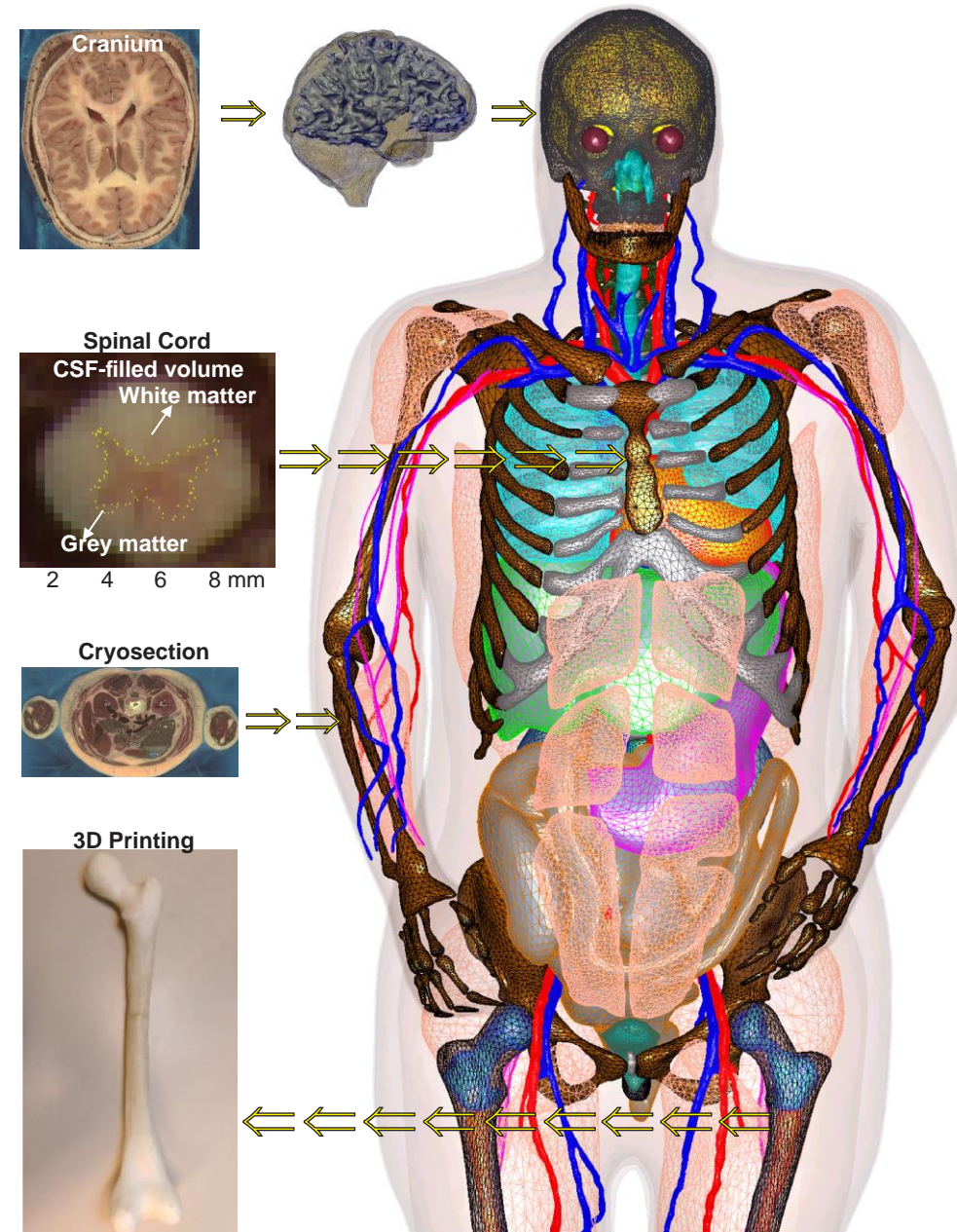
Motivation

- Produce a validated, efficient methodology to simulate MRI-induced heating in a non-homogenous, anatomically correct human body model
- Demonstrate multi-physics simulation methodology for comparisons against 1.5T MRI with published experimental data
- Provide complete test-bed (human body model and software solution) to medical device development community to explore techniques and accelerate design decisions



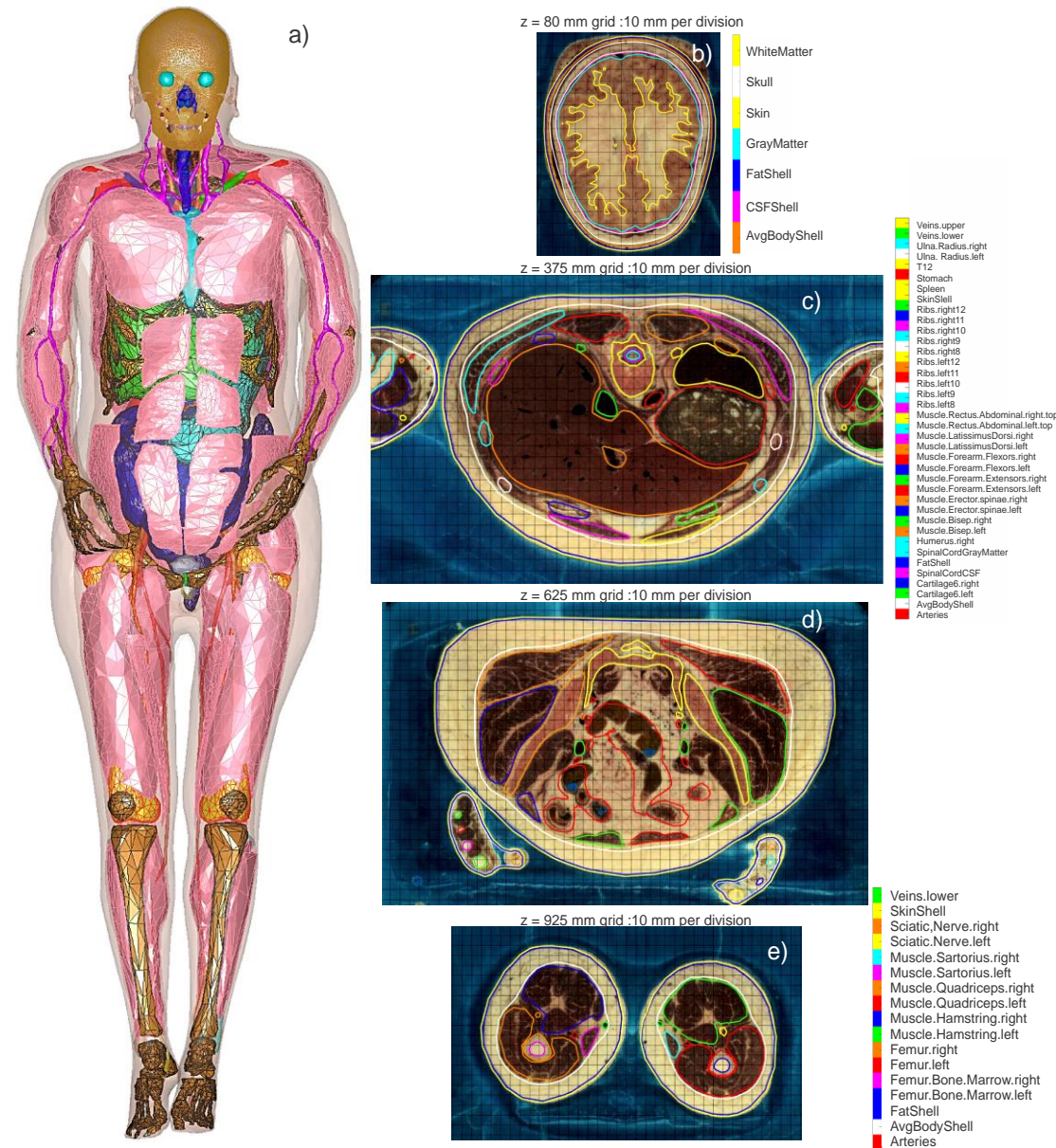
Ansys VHP Female Model v5.0

- Created by NEVA Electromagnetics (Yarmouth, MA)
 - Manual/semi-manual segmentation using ITK-Snap
- Based on the Visible Human Project[®] of the U.S. National Library of Medicine cryosection imagery
 - Modeled after 59-year-old female patient with BMI ~30
 - Optimized for use in wide variety of low and high frequency electromagnetic applications
 - 249 individual CAD based structures
- Compatible with AEDT + Mechanical & Fluent via Workbench
- Available in Two Resolutions:
 - 640k Facets (0.5mm - 3.0mm Surface Deviation)
 - 160k Facets (3.0mm - 7.0mm Surface Deviation)



Anslys VHP Female Model v5.0

- Anatomical validation completed by board of subject matter experts in human physiology and specialization areas
 - MATLAB tool available to provide real-time structure viewing for independent user examination and evaluation
- Latest enhancements include:
 - Greater resolution of reproductive system – new segmentation and mesh integration underway by Mallika Anand, MD, BIDMC and research group
 - Library of orthopedic implants
 - Highly detailed ear canals
 - Multiple body shells to modulate BMI



RF Induced Heating of Implanted Medical Devices in MRI

Objective

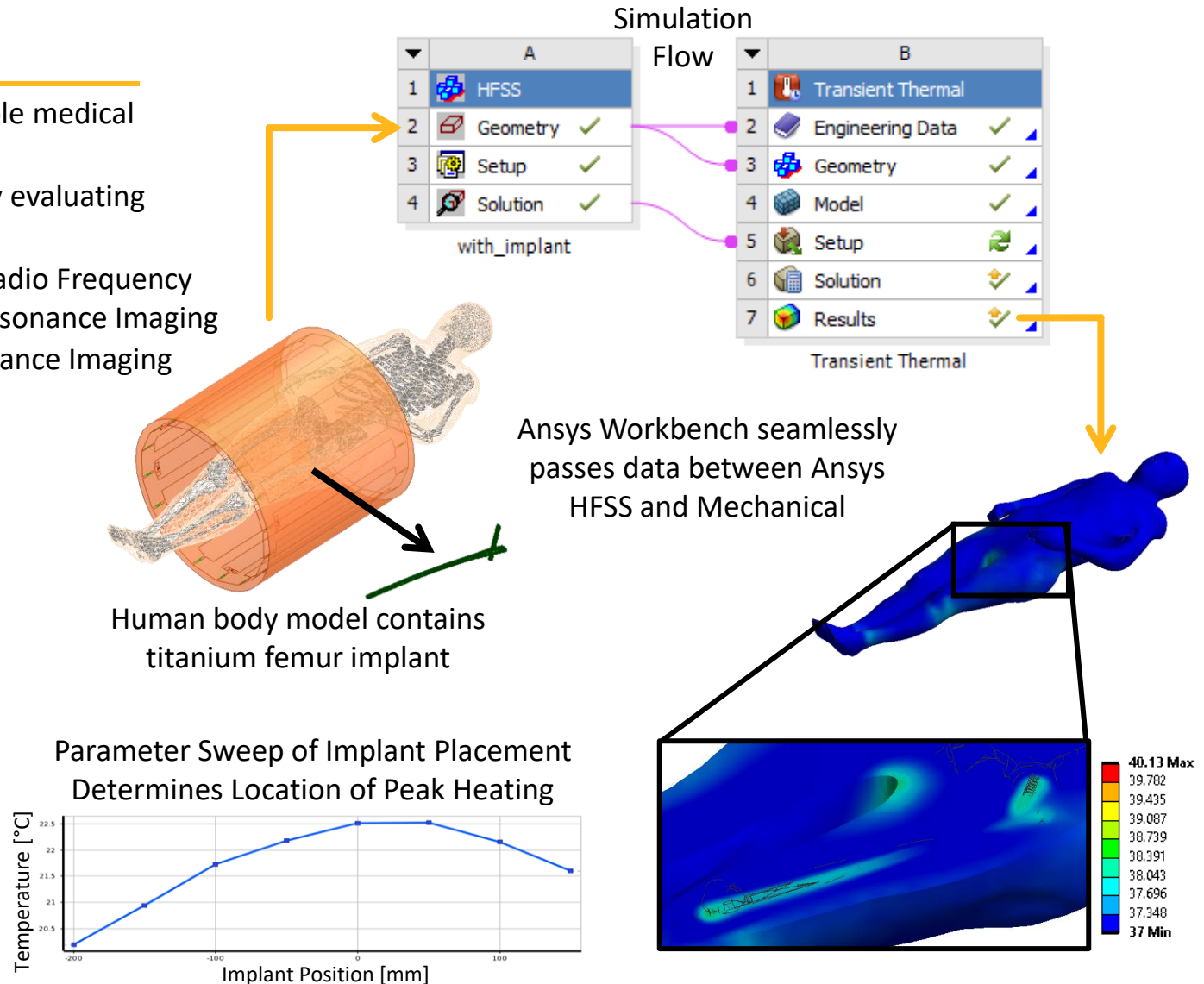
- Accurately predict temperature changes on and near implantable medical devices in magnetic resonance environments
- Ensure safety of patients with implants undergoing MRI scan by evaluating standardized regulatory requirements via simulation:
 - **ASTM F2182**: Standard Test Method for Measurement of Radio Frequency Induced Heating Near Passive Implants During Magnetic Resonance Imaging
 - **ISO/TS 10974**: Assessment of the Safety of Magnetic Resonance Imaging for Patients with an Active Implantable Medical Device

Approach

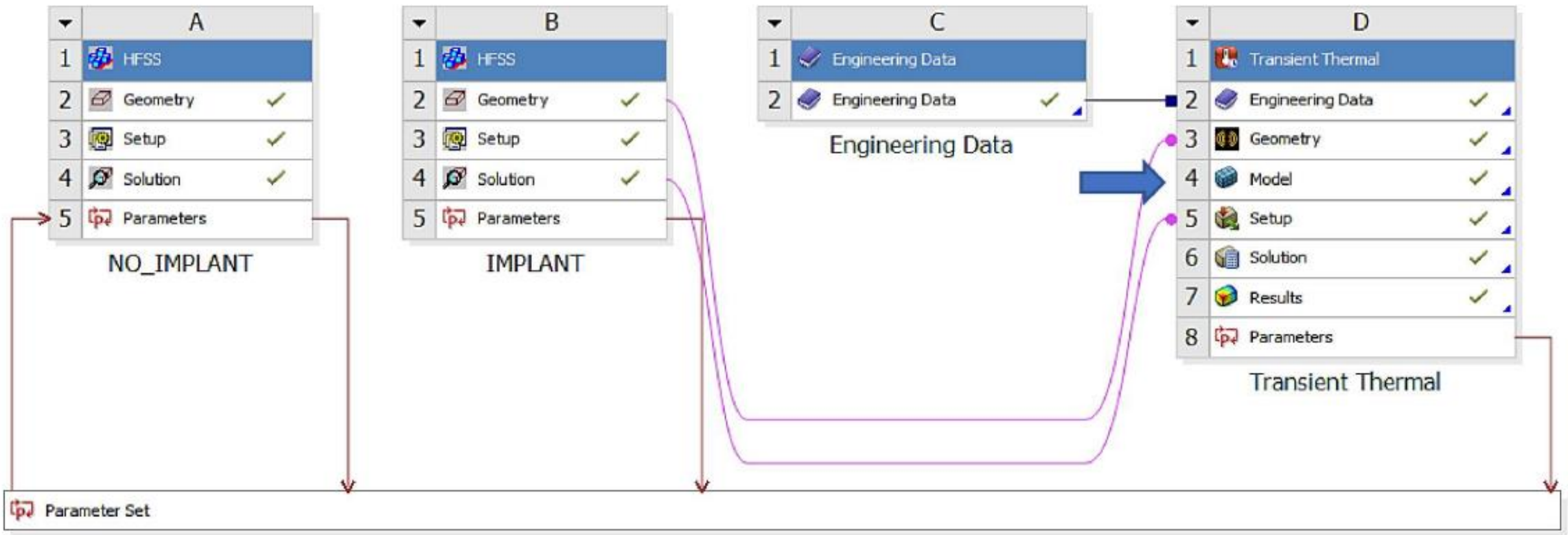
- Unified simulation environment links Ansys HFSS to Ansys Mechanical to simulate temperature rise due to EM losses in tissue and implant during exposure to RF fields of MRI.
- Parameterized models allow for rapid evaluation of patient landmark, device placement, and device-specific variations.

Value

- Efficient process for evaluating temperature rise on or near implanted medical devices in realistic human body models
 - Provide design insights into sources of temperature rise to help identify MRI safe implant designs
 - Perform in-silico testing prior to or in lieu of physical measurements

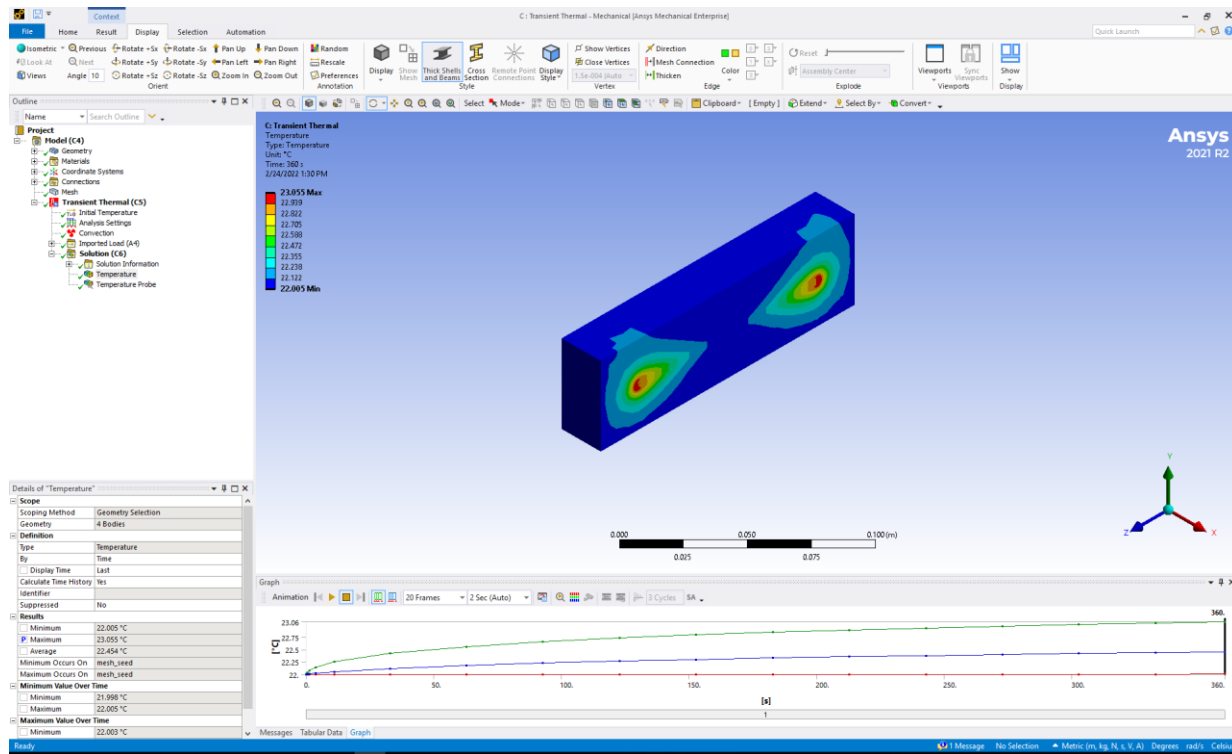


EM-Thermal Co-Simulation Workflow Overview



Validation Case #1a: Simulating ASTM F2182 Standard in Gel

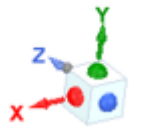
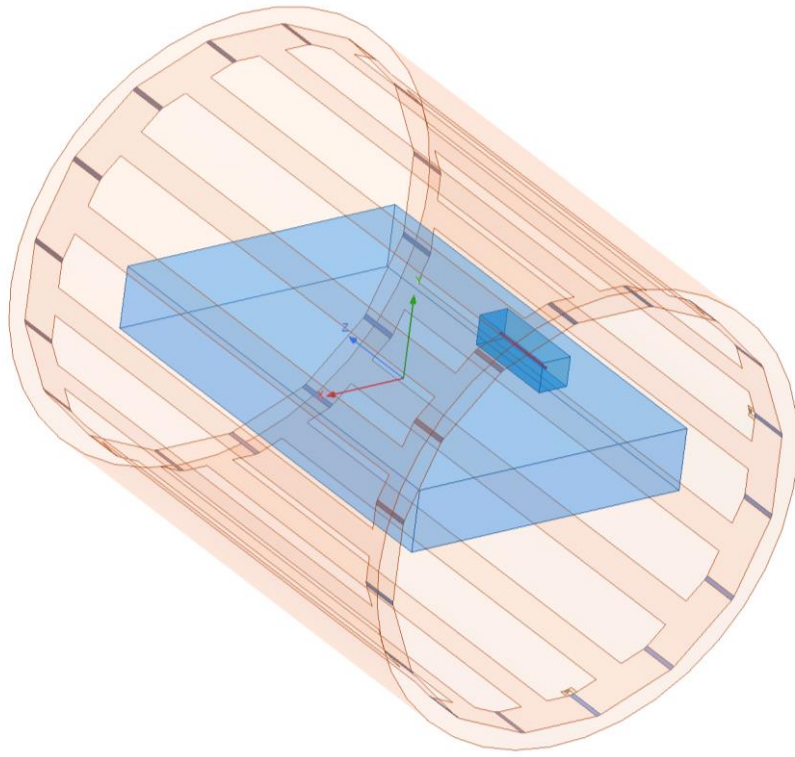
Component	Dimensions	Density (kg/m)	Electrical Conductivity (S/m)	Relative permittivity	Thermal conductivity (W/(m*K))	Specific heat (J/(kg*K))
Phantom enclosure	65 x 42 x 12 cm 12 mm thickness	1180	0	3.14	0.2	1780
Phantom gel	65 x 42 x 9 cm	1000	0.47	78	0.6	4184
Implant (Ti alloy rod)	3.2 mm diam x 10 cm long	4430	5.95×10^5	1	6.7	526.3
1.5 T RF coil	Height: 82 cm Inner diameter: 59.4 cm	N/A	Infinite	N/A	N/A	N/A



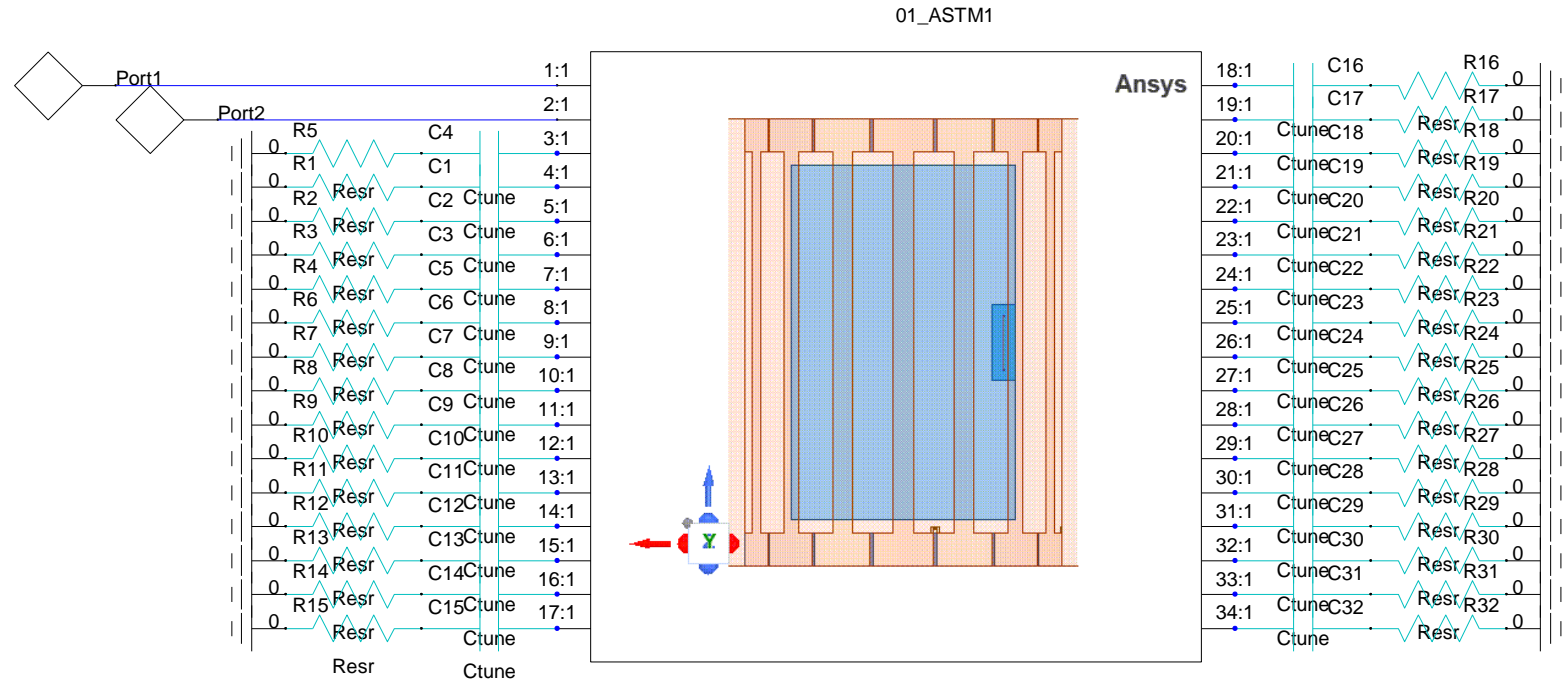
- Results predict a whole-body SAR of 3.6 W/kg and temperature rise of 11° C
- Within one standard deviation of values reported in a peer-reviewed interlaboratory task group

Computational modeling of RF-induced heating due to a titanium-alloy rod: An Interlaboratory Comparison for the ASTM F2182 task group; Murdock et al.; Proc. Intl. Soc. Mag. Reson. Med. 27 (2019)

FEM + Circuit Co-Simulation Model of "Birdcage" RF Coil

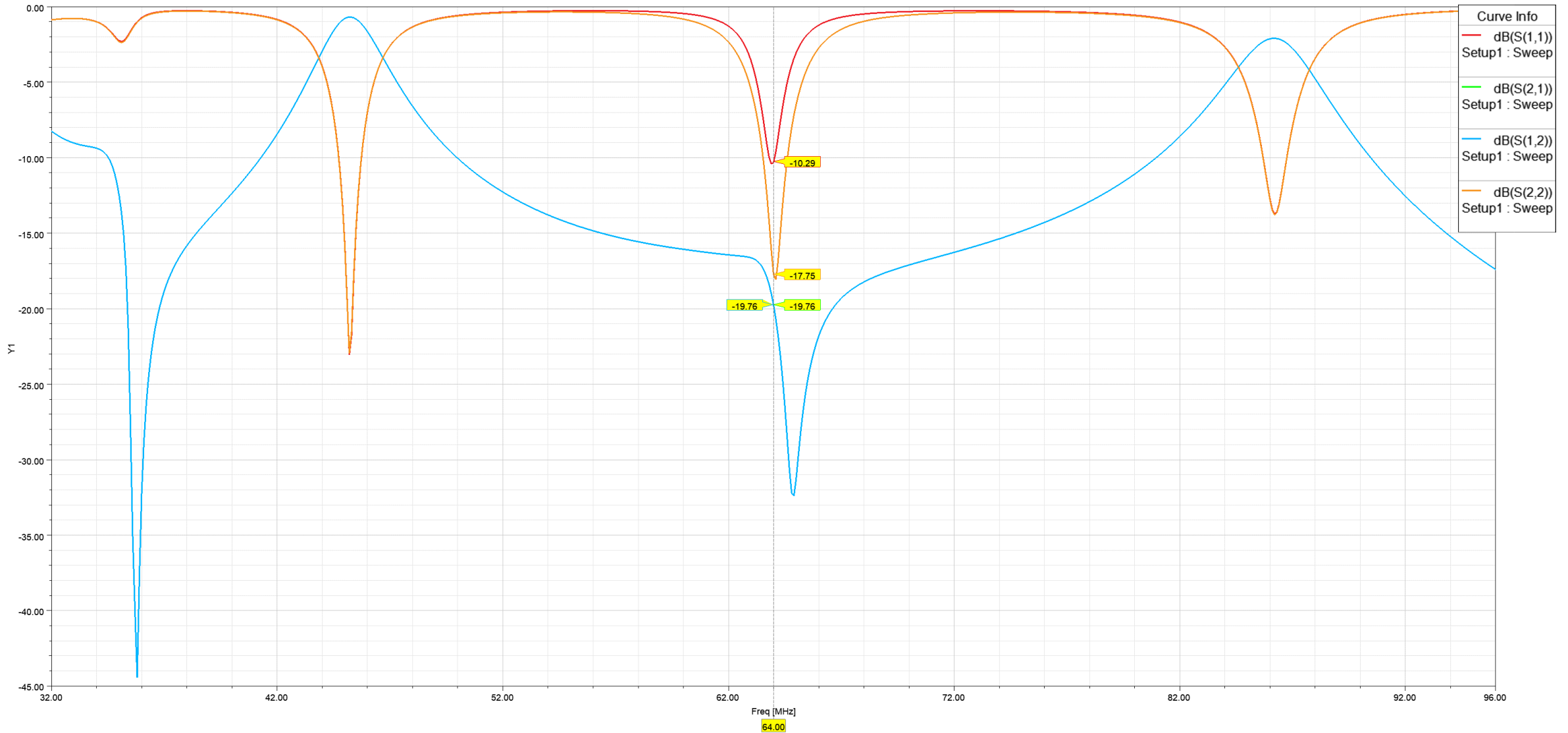


0 200 400 (mm)

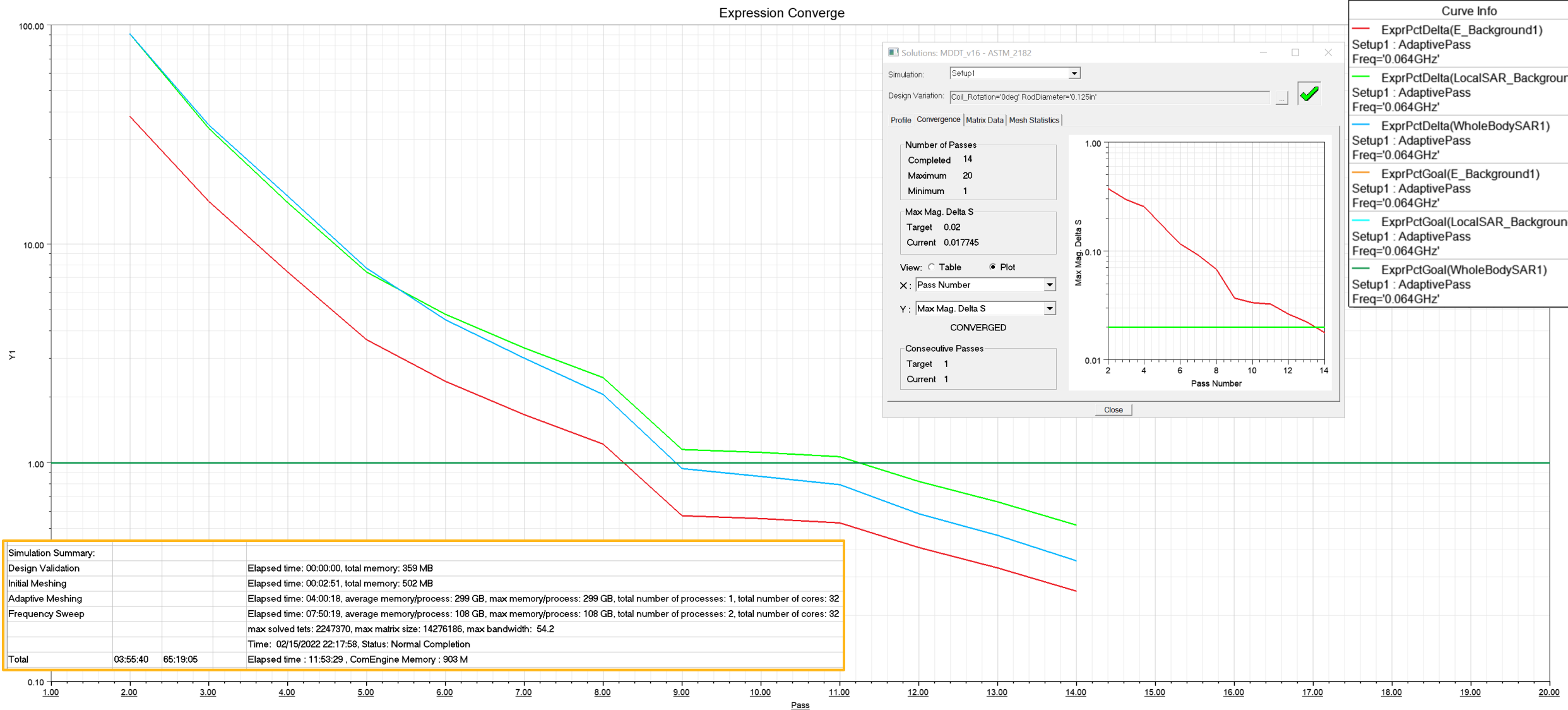


Design Properties
 Ctune = 105pF
 Resr = 0.1ohm
 Vin = 76.78V

S-Parameters: Tuned & Matched for Quadrature Excitation

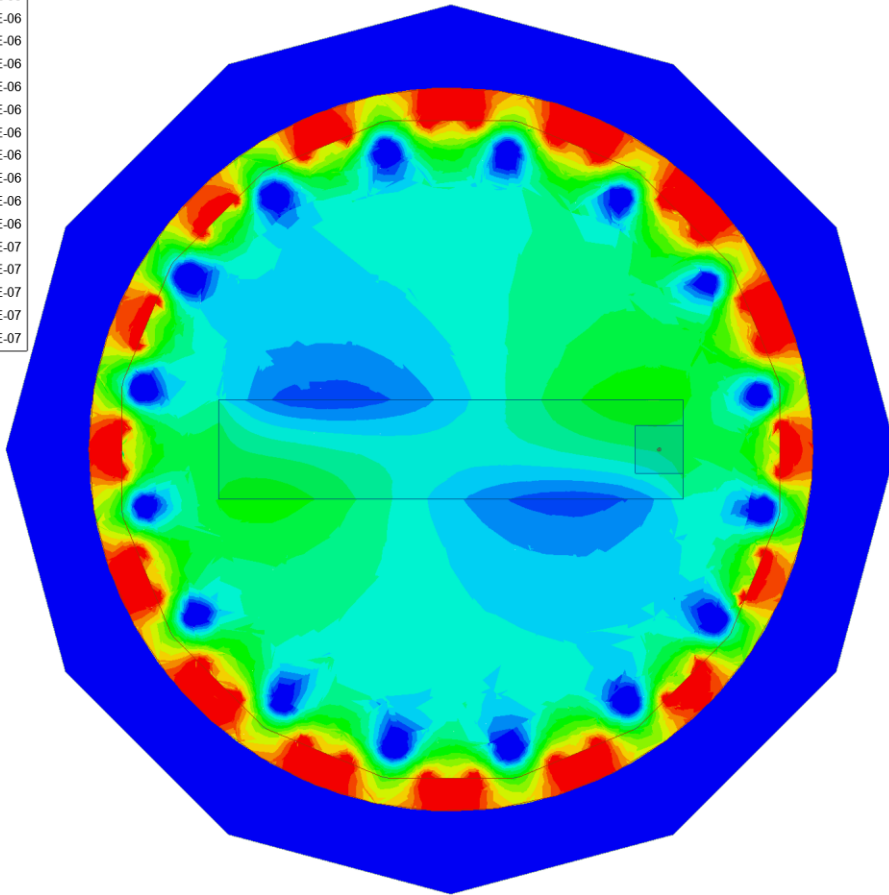
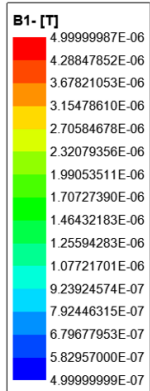


S-Parameter [$\Delta S < 0.02$] + Near Field Convergence [$\Delta SAR < 1\%$]

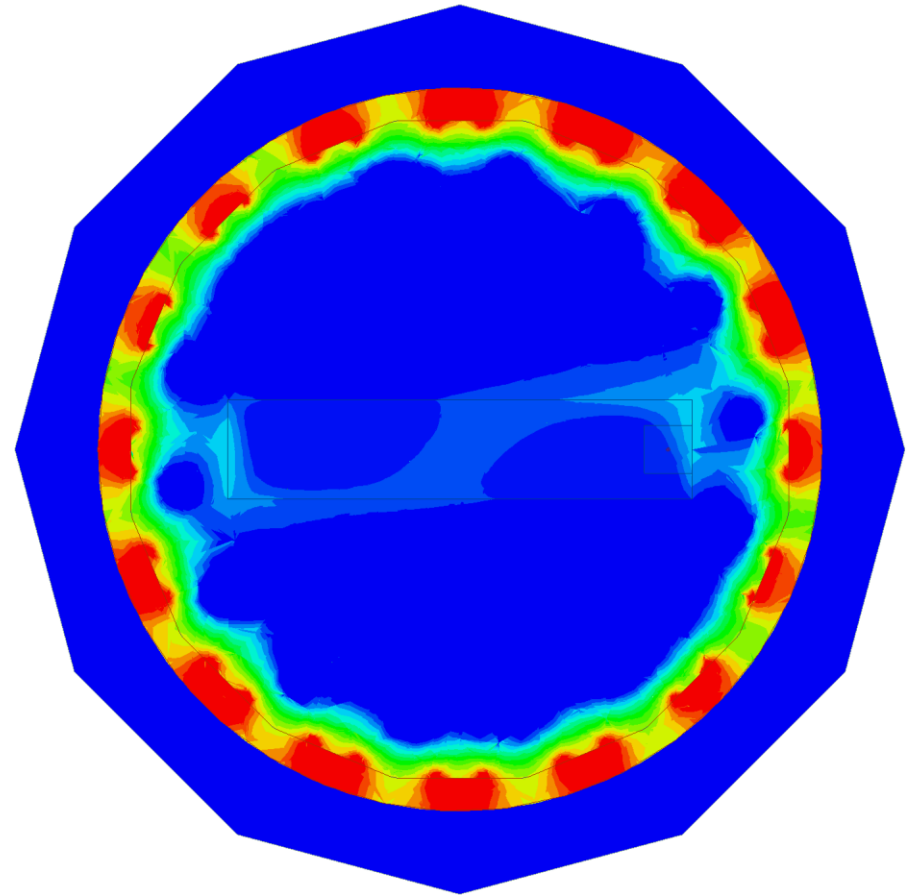


Calibrate Power Input:

Adjust Input Voltage to Set $|B_1^+| = 1 \mu\text{T}$ at Coil's Isocenter

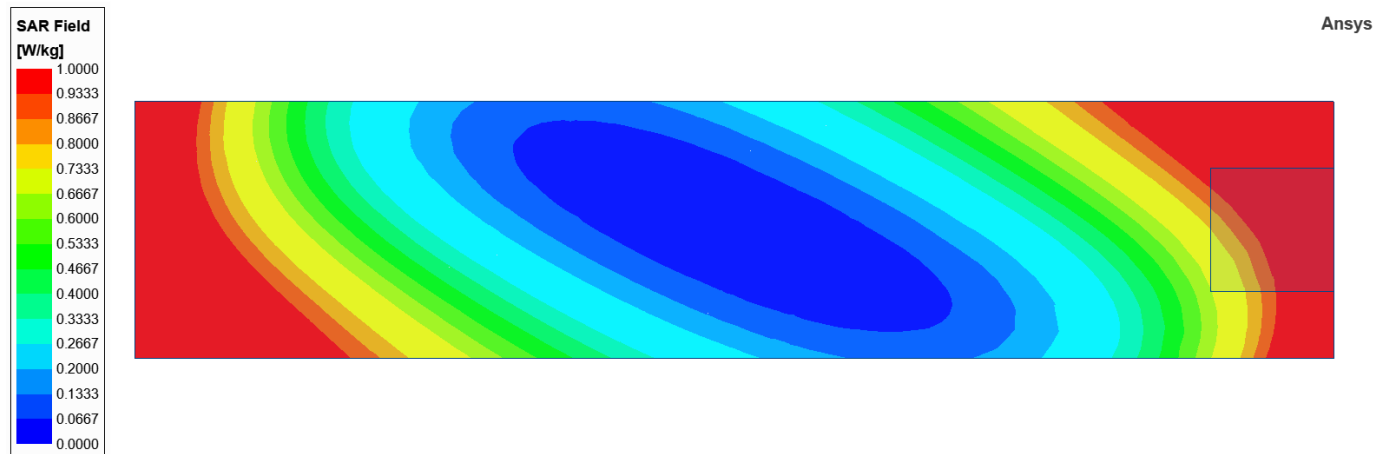
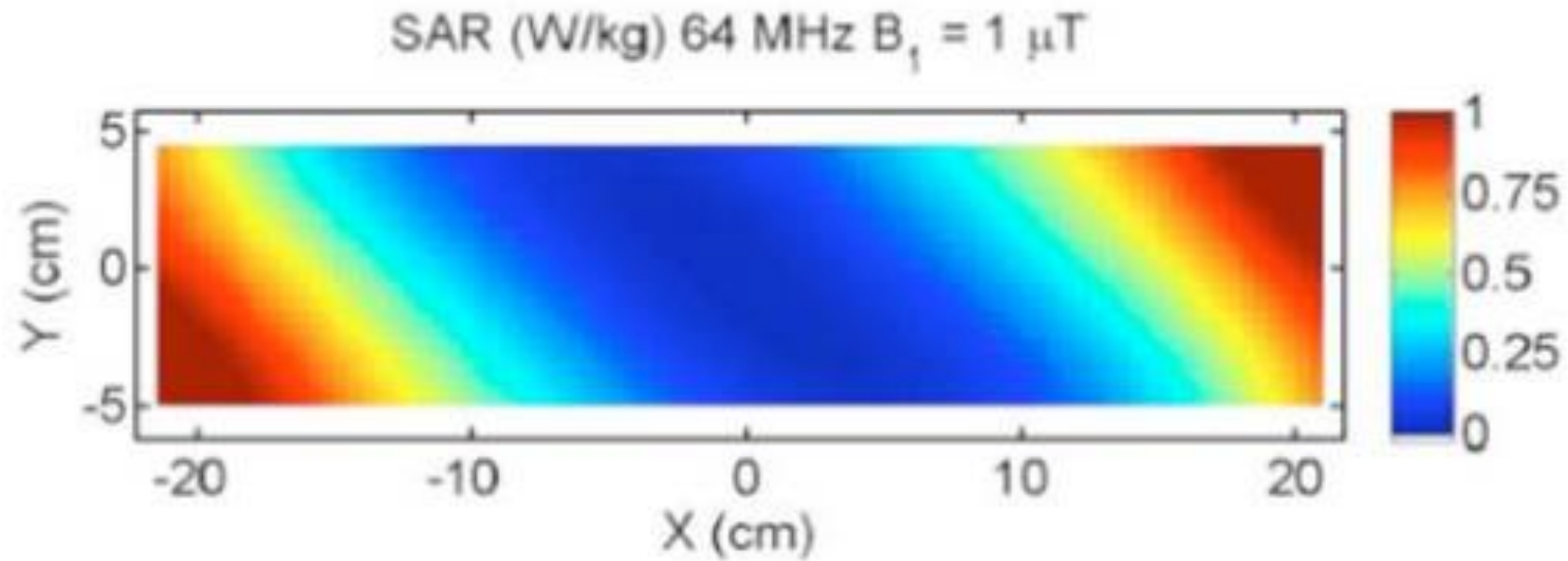


$|B_1^+|$

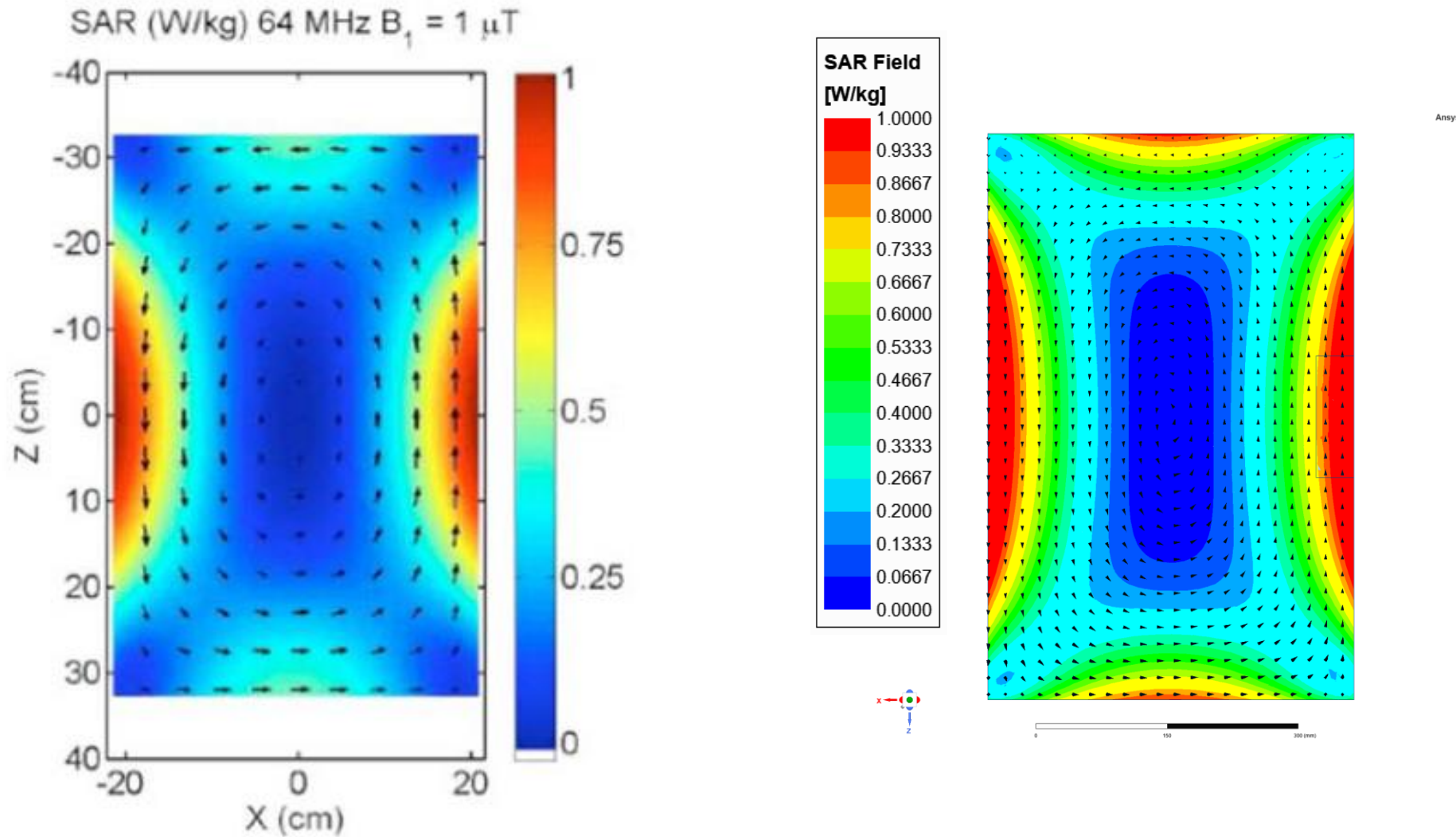


$|B_1^-|$

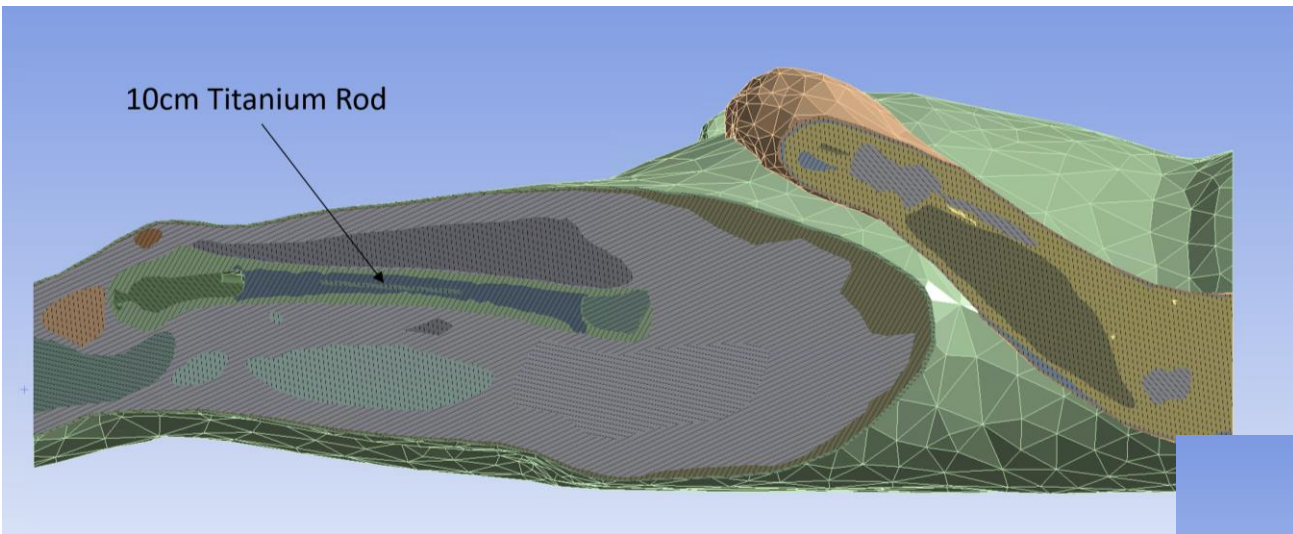
Local SAR – Comparison w/ ASTM Standard



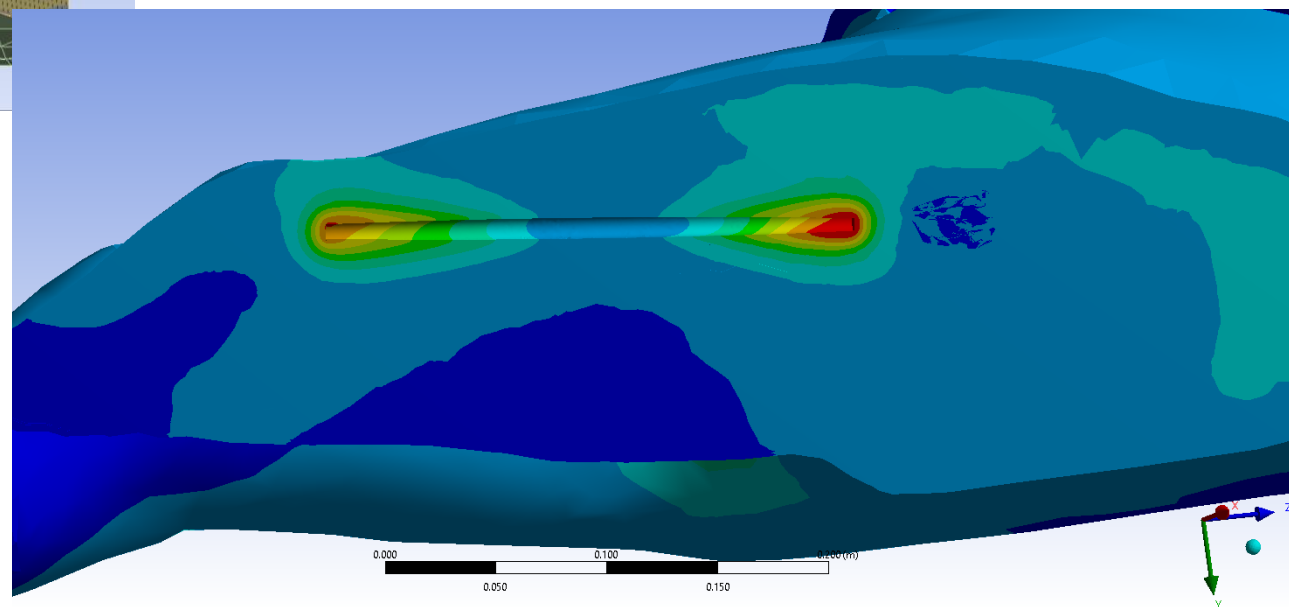
Local SAR – Comparison w/ ASTM Standard



Validation Case #1b: Simulating ASTM F2182 Rod in VHP Phantom

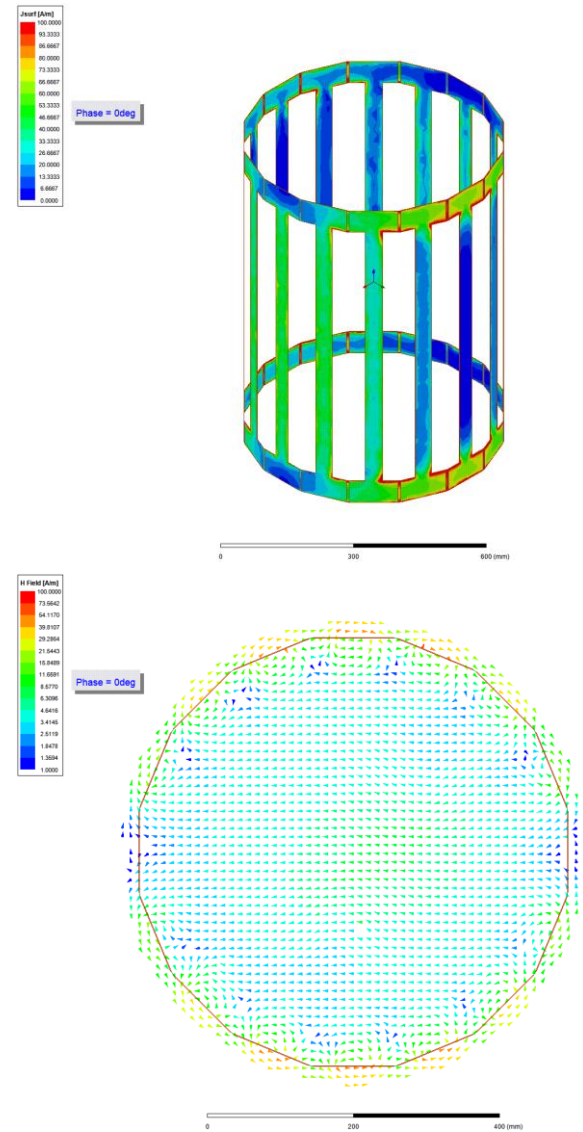


- Temperature rise again in line with standards

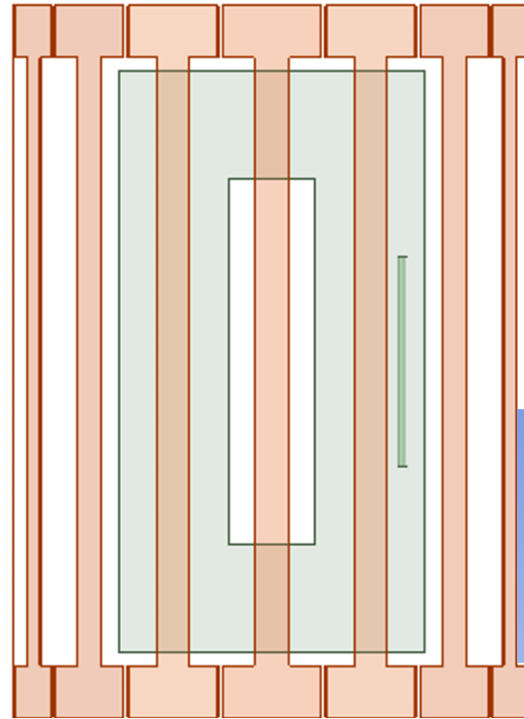


Computational modeling of RF-induced heating due to a titanium-alloy rod: An Interlaboratory Comparison for the ASTM F2182 task group; Murdock et al.; Proc. Intl. Soc. Mag. Reson. Med. 27 (2019)

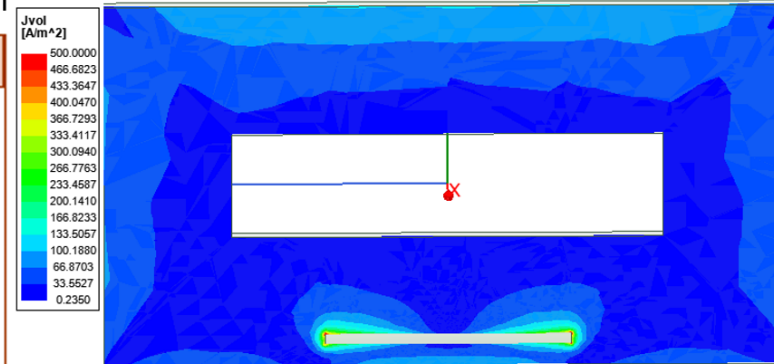
Validation Case #2a: Gel with Embedded Rod in 1.5T MRI



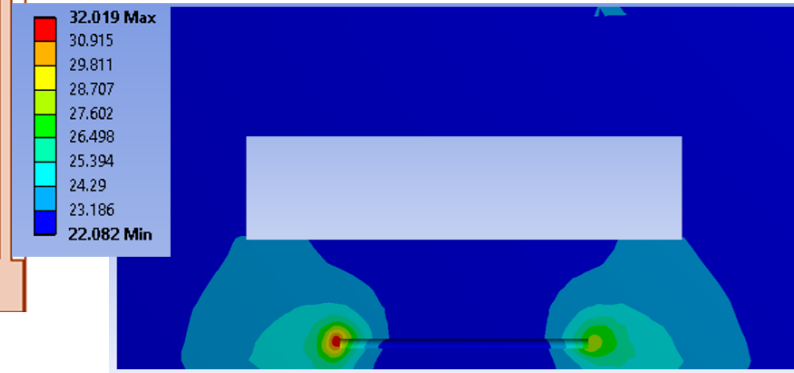
Rod and Phantom in 1.5T MRI Coil



Simulated Current Density



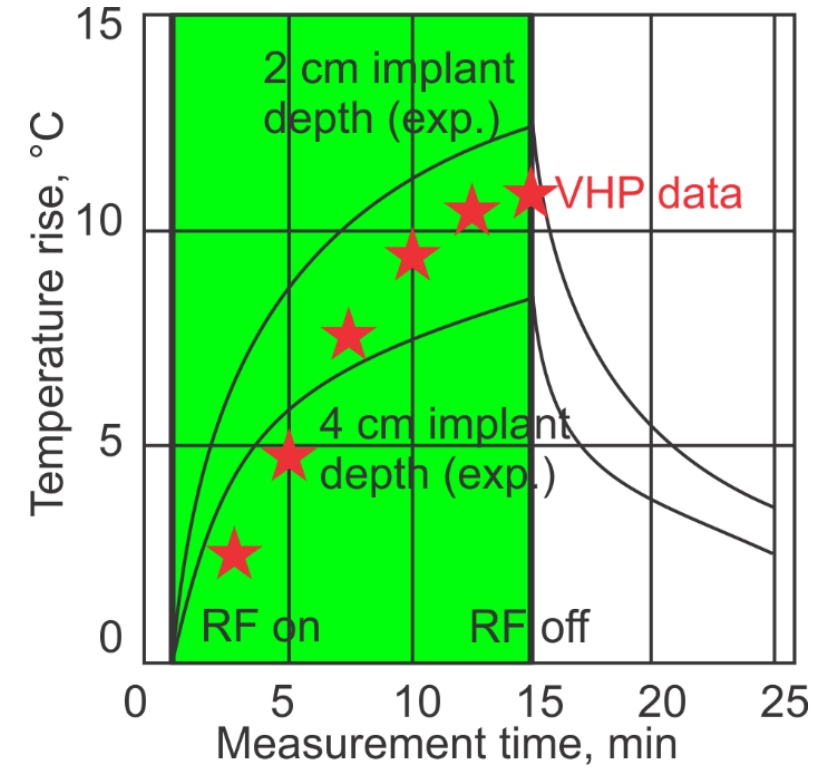
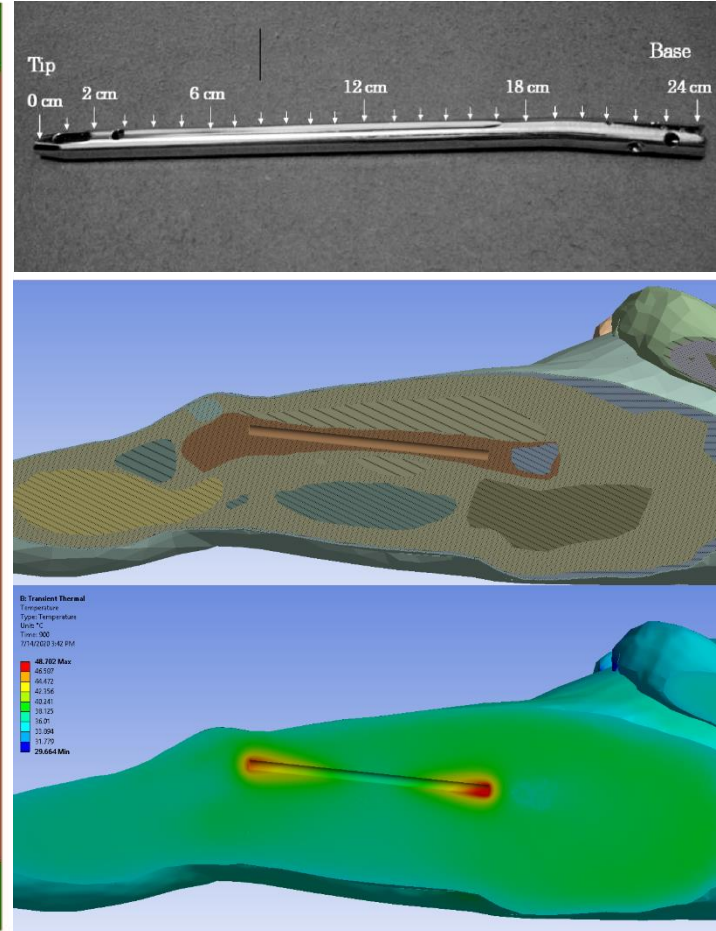
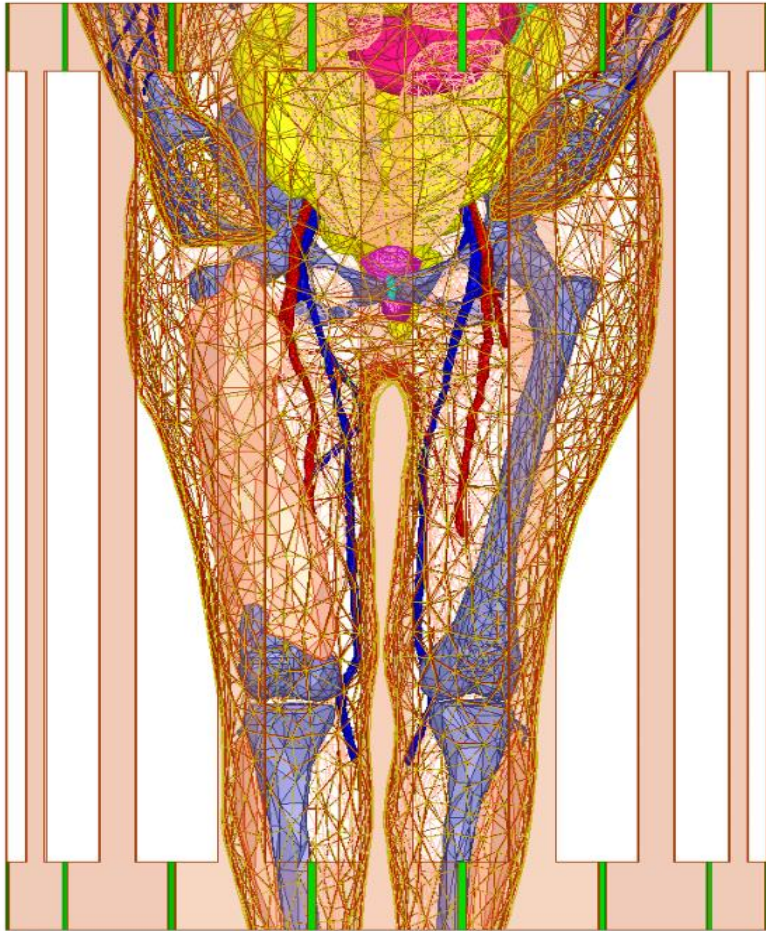
Simulated Temperature Rise



- Simulate realistically loaded MRI birdcage coil with simple gel phantom and embedded metallic rod
- Good agreement with experimental results – current density and temperature rise

Muranaka H, Horiguchi T, Usui S, Ueda Y, Nakamura O, Ikeda F, Iwakura K, Nakaya G. 2006. Evaluation of RF heating on humerus implant in phantoms during 1.5 T MRI imaging and comparisons with electromagnetic simulation. Magn Reson Med Sci. 5(2):79-88. PMID: 17008764.
 Muranaka H, Horiguchi T, Usui S, Ueda Y, Nakamura O, Ikeda F. 2007. Dependence of RF heating on SAR and implant position in a 1.5T MR system. Magn Reson Med Sci. 6(4):199-209. PMID: 18239357.
 Muranaka H, Horiguchi T, Ueda Y, Tanki N. 2011. Evaluation of RF heating due to various implants during MR procedures. Magn Reson Med Sci. 10(1):11-19. PMID 21441723.

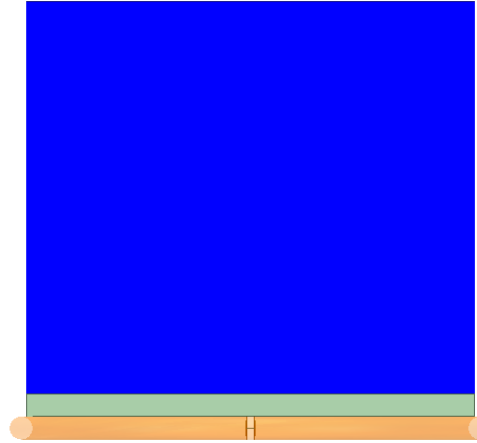
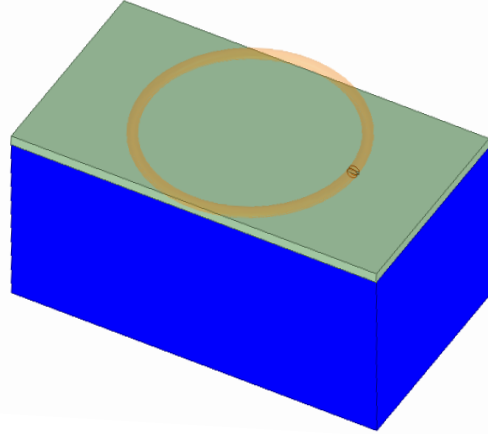
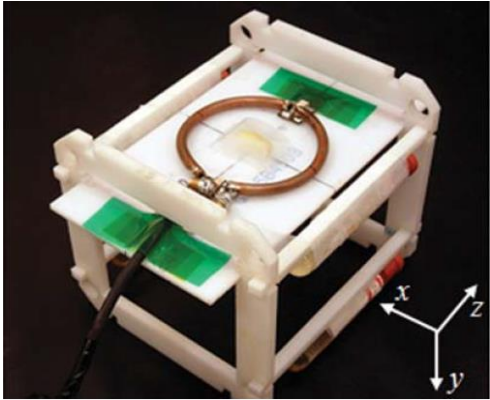
Validation Case #2b: VHP Female with Embedded Rod in 1.5T MRI



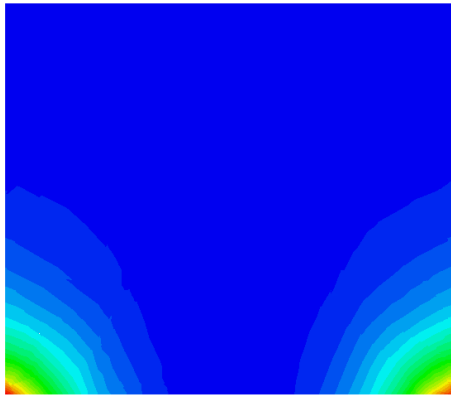
VHP results in relative agreement – differences attributed to variation in rod depth (vs constant depth of phantom) and changes in material properties

Muranaka H, Horiguchi T, Ueda Y, Tanki N. 2011. Evaluation of RF heating due to various implants during MR procedures. Magn Reson Med Sci. 10(1):11-19. PMID 21441723.

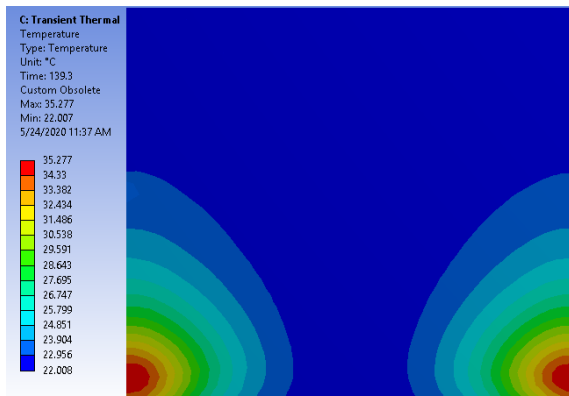
Validation Case #3a: Surface Coil on Agar Phantom – SAR Characterization at 165 MHz



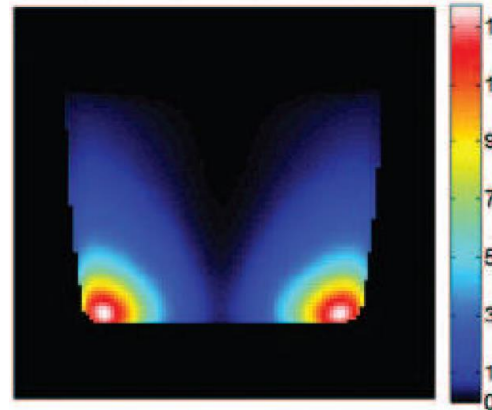
- While not at the desired 1.5T frequency, very few *in vivo* experiments are available
- Just a simple Agar block, this case establishes both the workflow (model construction, initial simulation in HFSS, corresponding heat simulation in Thermal) and simulation results
- Good correlation with both SAR (~1100 W/kg) and change in heat (~13° C)



Simulated SAR



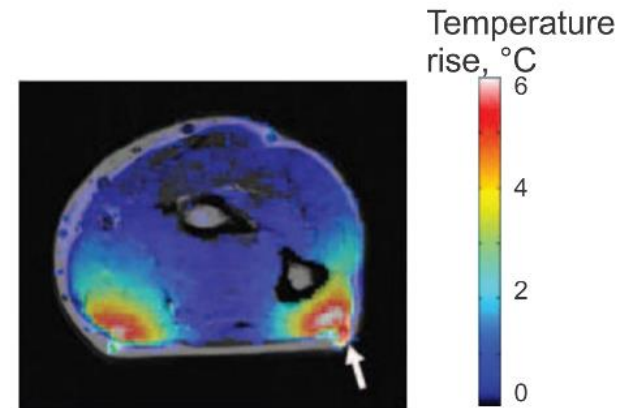
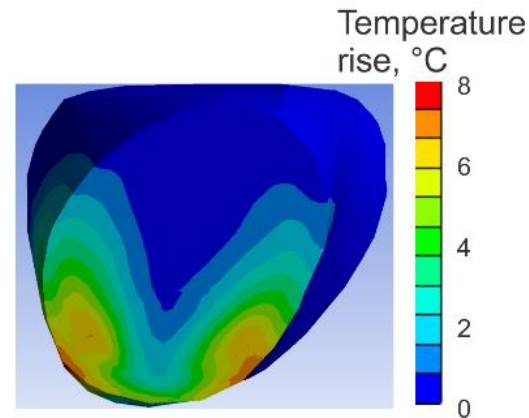
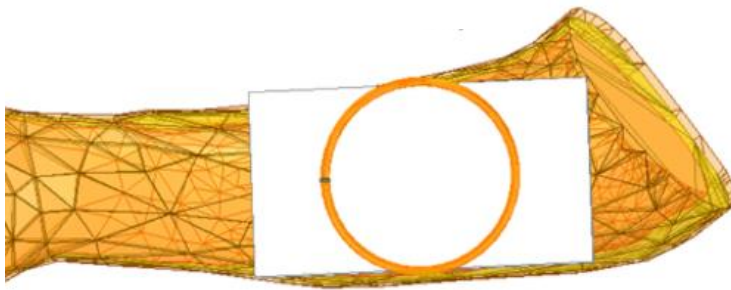
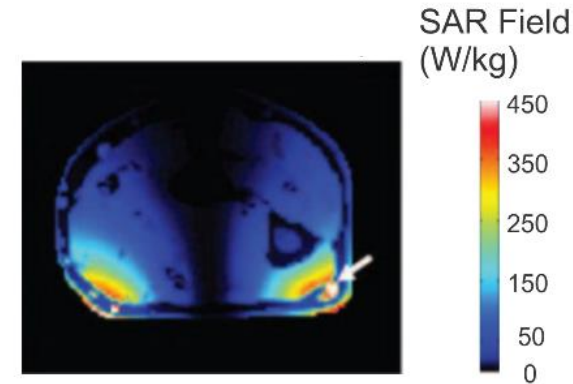
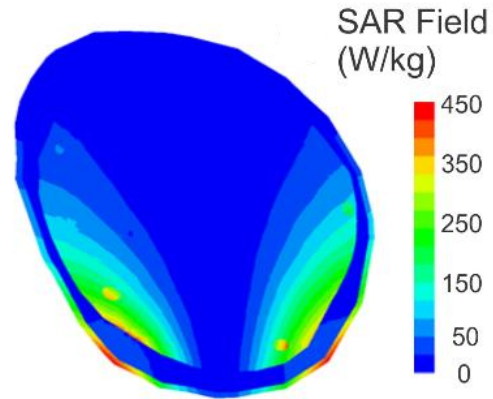
Simulated Temp Rise



Measured Temp Rise

Oh S, Ryu Y-C, Carluccio G, Sica CT, Collins CM. 2014. Measurement of SAR-induced temperature increase in a phantom and in vivo with comparison to numerical simulation. Magn. Reson. Med. 71(5):1923–1931. PMID 23804188.1

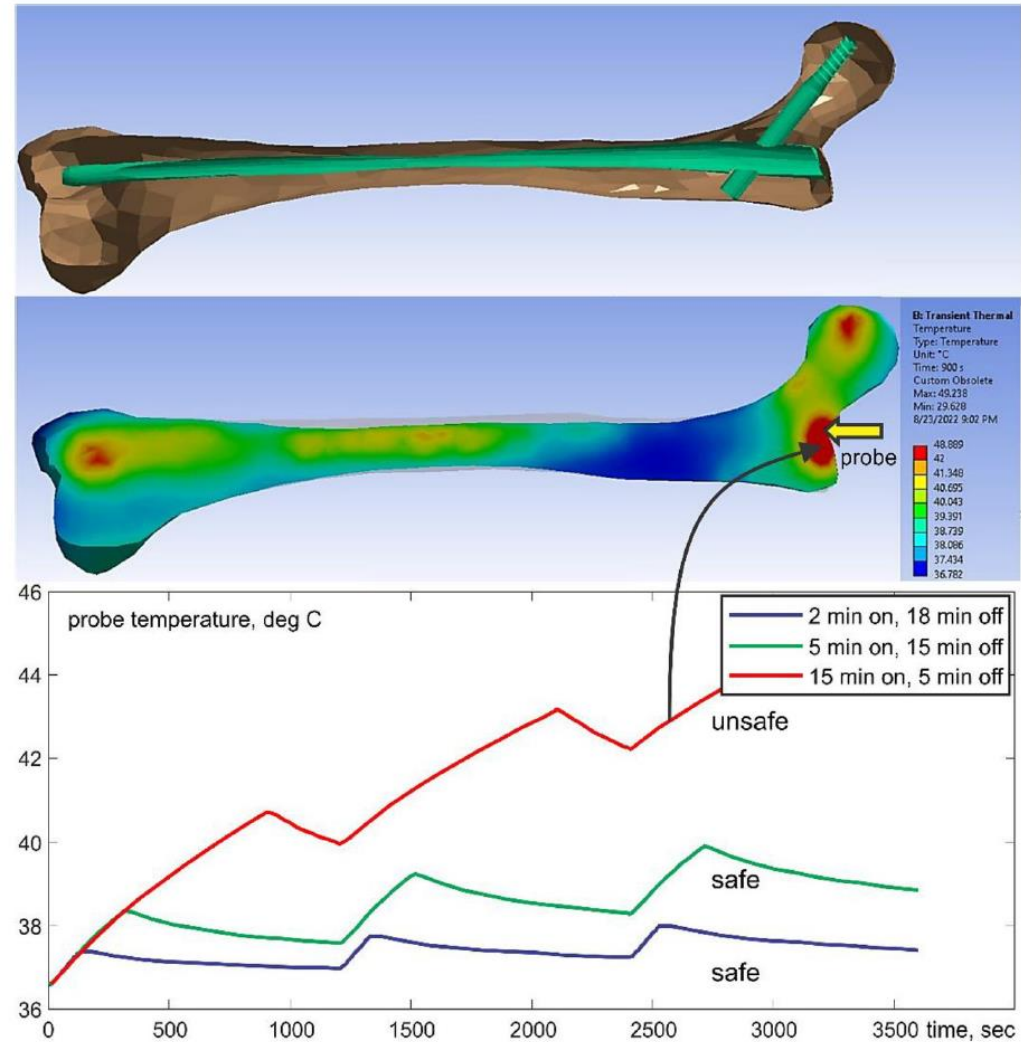
Validation Case #3b: Surface Coil on Human Forearm – SAR Characterization at 165 MHz



- Adding in forearm with corresponding bones, blood vessels, nerves, etc.
- Good correlation with both SAR (~450 W/kg) and change in heat (~6.6° C)

Oh S, Ryu Y-C, Carluccio G, Sica CT, Collins CM. 2014. Measurement of SAR-induced temperature increase in a phantom and in vivo with comparison to numerical simulation. Magn. Reson. Med. 71(5):1923–1931. PMID 23804188.1

Accessing Specific MRI Scan Sequence Timing:



Publications in PLOS ONE & eLife:

PLOS ONE

RESEARCH ARTICLE

Visible Human Project® female surface based computational phantom (Nelly) for radio-frequency safety evaluation in MRI coils

Gregory M. Noetscher^{1,2,4*}, Peter Serano^{3,4,6}, William A. Wartman^{1,6}, Kyoko Fujimoto^{4,6}, Sergey N. Makarov^{1,2,4,6}

1 Department of Electrical and Computer Engineering, Worcester Polytechnic Institute, Worcester, Massachusetts, United States of America, **2** NEVA Electromagnetics, LLC, Yarmouth Port, Massachusetts, United States of America, **3** Ansys, Inc., Canonsburg, Pennsylvania, United States of America, **4** Athinoula A. Martinos Center for Biomedical Imaging, Massachusetts General Hospital, Charlestown, Massachusetts, United States of America, **5** Center for Devices and Radiological Health, US Food and Drug Administration, Silver Spring, Maryland, United States of America

* These authors contributed equally to this work.
* gnoet@wpi.edu



Abstract

Quantitative modeling of specific absorption rate and temperature rise within the human body during 1.5 T and 3 T MRI scans is of clinical significance to ensure patient safety. This work presents justification, via validation and comparison, of the potential use of the Visible Human Project (VHP) derived Computer Aided Design (CAD) female full body computational human model for non-clinical assessment of female patients of age 50–65 years with a BMI of 30–36 during 1.5 T and 3 T based MRI procedures. The initial segmentation validation and four different application examples have been identified and used to compare to numerical simulation results obtained using VHP Female computational human model under the same or similar conditions. The first application example provides a simulation-to-simulation validation while the later three application examples compare with measured experimental data. Given the same or similar coil settings, the computational human model generates meaningful results for SAR, B1 field, and temperature rise when used in conjunction with the 1.5 T birdcage MRI coils or at higher frequencies corresponding to 3 T MRI. Notably, the deviation in temperature rise from experiment did not exceed 2.75° C for three different heating scenarios considered in the study with relative deviations of 10%, 25%, and 20%. This study provides a reasonably systematic validation and comparison of the VHP-Female CAD v.3.0–5.0 surface-based computational human model starting with the segmentation validation and following four different application examples.

OPEN ACCESS

Citation: Noetscher GM, Serano P, Wartman WA, Fujimoto K, Makarov SN (2021) Visible Human Project® female surface based computational phantom (Nelly) for radio-frequency safety evaluation in MRI coils. PLOS ONE 16(12): e0260922. <https://doi.org/10.1371/journal.pone.0260922>

Editor: Muhammad Zubair, Information Technology University, PAKISTAN

Received: July 21, 2021

Accepted: November 19, 2021

Published: December 10, 2021

Copyright: This is an open access article distributed under the terms of the [Creative Commons Attribution License](https://creativecommons.org/licenses/by/4.0/), which permits unrestricted use, distribution, and reproduction in any medium, provided the original author and source are credited.

Data Availability Statement: All models used in this study may be obtained via the following URL: <https://www.nevaelectromagnetics.com/>

Funding: The authors received no specific funding for this work.

Competing Interests: The authors have declared that no competing interests exist.

Introduction

Quantitative assessment of radio frequency (RF) absorption experienced by a patient undergoing a Magnetic Resonance Imaging (MRI) procedure is prohibitively difficult to obtain due to

PLOS ONE | <https://doi.org/10.1371/journal.pone.0260922> December 10, 2021 1/21

eLife SHORT REPORT

An in silico testbed for fast and accurate MR labeling of orthopedic implants

Gregory M Noetscher^{1*†}, Peter J Serano^{2†}, Marc Horner³, Alexander Prokop³, Jonathan Hanson⁴, Kyoko Fujimoto⁵, James Brown⁶, Ara Nazarian⁷, Jerome Ackerman^{8,9}, Sergey N Makarov^{1,2,4,6}

1Electrical & Computer Eng. Dept, Worcester Polytechnic Institute, Worcester, United States; **2**Ansys, Canonsburg, United States; **3**Dassault Systèmes Deutschland GmbH, Darmstadt, Germany; **4**Neva Electromagnetics, LLC, Holden, United States; **5**GE HealthCare, Chicago, United States; **6**Micro Systems Engineering, Inc, an affiliate of Biotronik, Lake Oswego, United States; **7**Musculoskeletal Translational Innovation Initiative, Department of Orthopedic Surgery, Beth Israel Deaconess Medical Center and Harvard Medical School, Boston, United States; **8**Harvard Medical School, Boston, United States; **9**Athinoula A Martinos Center for Biomed. Imaging, Massachusetts General Hospital, Charlestown, United States

Abstract One limitation on the ability to monitor health in older adults using magnetic resonance (MR) imaging is the presence of implants, where the prevalence of implantable devices (orthopedic, cardiac, neuromodulation) increases in the population, as does the pervasiveness of conditions requiring MRI studies for diagnosis (musculoskeletal diseases, infections, or cancer). The present study describes a novel multiphysics implant modeling testbed using the following approaches with two examples: (1) an in silico human model based on the widely available Visible Human Project (VHP) cryo-section dataset; (2) a finite element method (FEM) modeling software workbench from Ansys (Electronics Desktop/Mechanical) to model MR radio frequency (RF) coils and the temperature rise modeling in heterogeneous media. The in silico VHP-Female model (250 parts with an additional 40 components specifically characterizing embedded implants and resultant surrounding tissues) corresponds to a 60-year-old female with a body mass index of 36. The testbed includes the FEM-compatible in silico human model, an implant embedding procedure, a generic parameterizable MRI RF birdcage two-port coil model, a workflow for computing heat sources on the implant surface and in adjacent tissues, and a thermal FEM solver directly linked to the MR coil simulator to determine implant heating based on an MR imaging study protocol. The primary target is MR labeling of large orthopedic implants. The testbed has very recently been approved by the US Food and Drug Administration (FDA) as a medical device development tool for 1.5 T orthopedic implant examinations.

eLife assessment

This manuscript will provide a **valuable** method to evaluate the safety of MR in patients with orthopedic implants, which is required in clinics. A strength of the work is that the in-silicon testbed is **solid**, based on the widely available human project, and validated. In addition, the toolbox will be open for clinical practice.

Introduction

One limitation on the ability to monitor health in older adults using magnetic resonance (MR) imaging studies is the presence of implants, where the prevalence of implantable devices (orthopedic, cardiac, neuromodulation) increases in the population, as does the pervasiveness of conditions requiring MRI

***For correspondence:** gnoet@wpi.edu

†These authors contributed equally to this work

Competing interest: See page 9

Funding: See page 9

Sent for Review: 06 July 2023

Preprint posted: 18 July 2023

Reviewed preprint posted: 15 September 2023

Reviewed preprint revised: 07 November 2023

Version of Record published: 14 December 2023

Reviewing Editor: Peng Liu, Icahn School of Medicine at Mount Sinai, United States

© Copyright Noetscher, Serano et al. This article is distributed under the terms of the [Creative Commons Attribution License](https://creativecommons.org/licenses/by/4.0/), which permits unrestricted use and redistribution provided that the original author and source are credited.

Noetscher, Serano et al. eLife 2023;12:RP90440. DOI: <https://doi.org/10.7554/eLife.90440> 1 of 12

FDA Medical Device Development Tool (MDDT)

Tool (Link to SEBQ)	Product Area(s)	MDDT Category	Date Qualified
Computational Tool Comprising Visible Human Project Based Anatomical Female CAD Model and Ansys HFSS/Mechanical FEM Software for Temperature Rise Prediction near an Orthopedic Femoral Nail Implant during a 1.5 T MRI Scan	Orthopedic, MR Safety Labeling	Non-clinical Assessment Model	03/30/2023

The FDA's Medical Device Development Tools (MDDT) program is intended to facilitate device development, timely evaluation of medical devices, and promote innovation by providing a more efficient and predictable means for collecting the necessary information to support regulatory submissions and associated decision-making.

<https://www.fda.gov/medical-devices/medical-device-development-tools-mddt>

A Novel Approach to Reducing Non-Through Body Energy Transfer in Microwave Imaging Systems

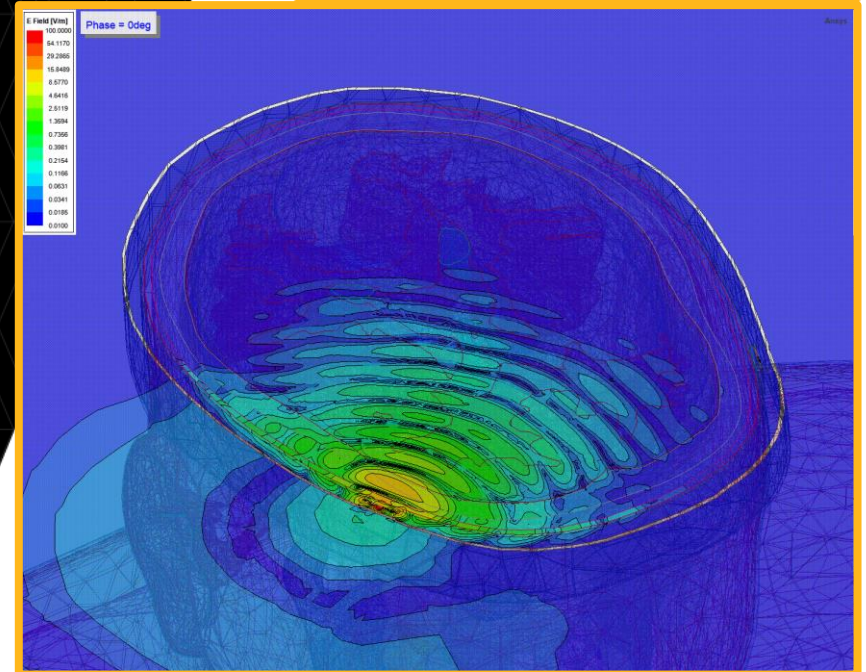
Ph.D. Dissertation Defense
Electrical & Computer Engineering

Peter Serano

PhD Candidate, WPI ECE

Lead Application Engineer, Ansys Inc.

12/14/23



WPI

Ansys

Microwave Imaging

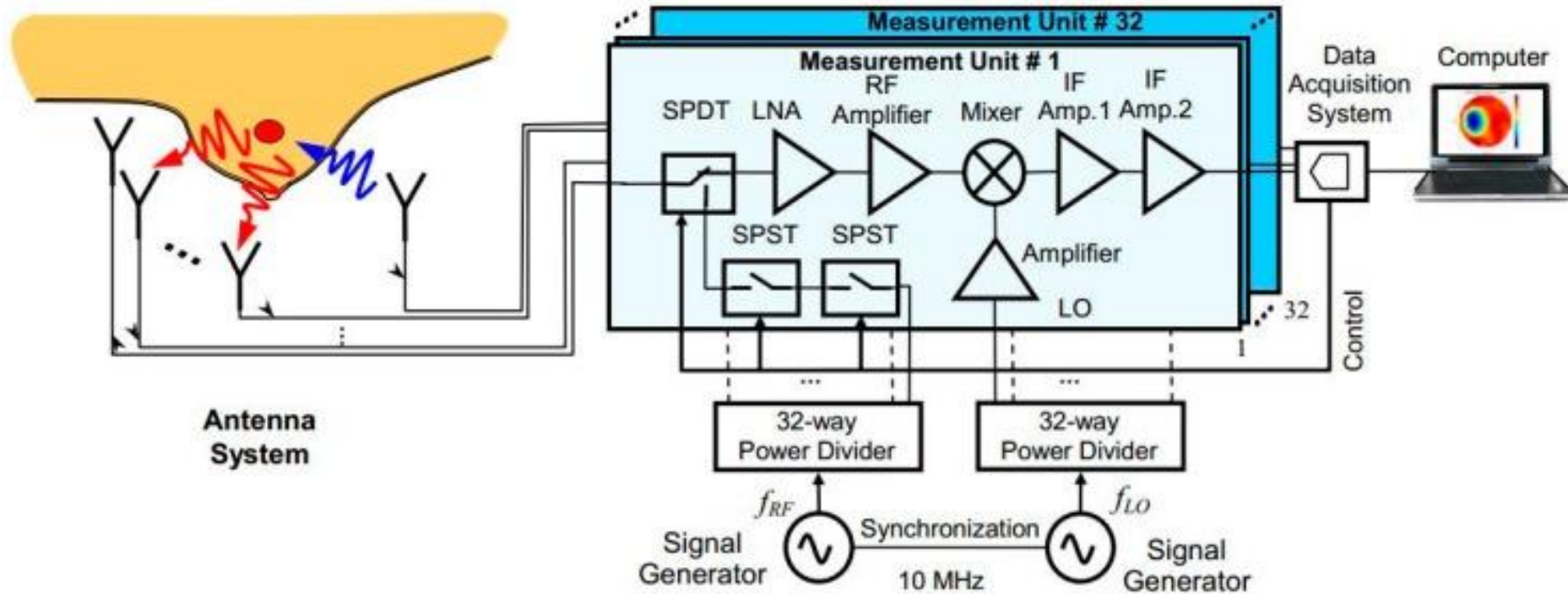
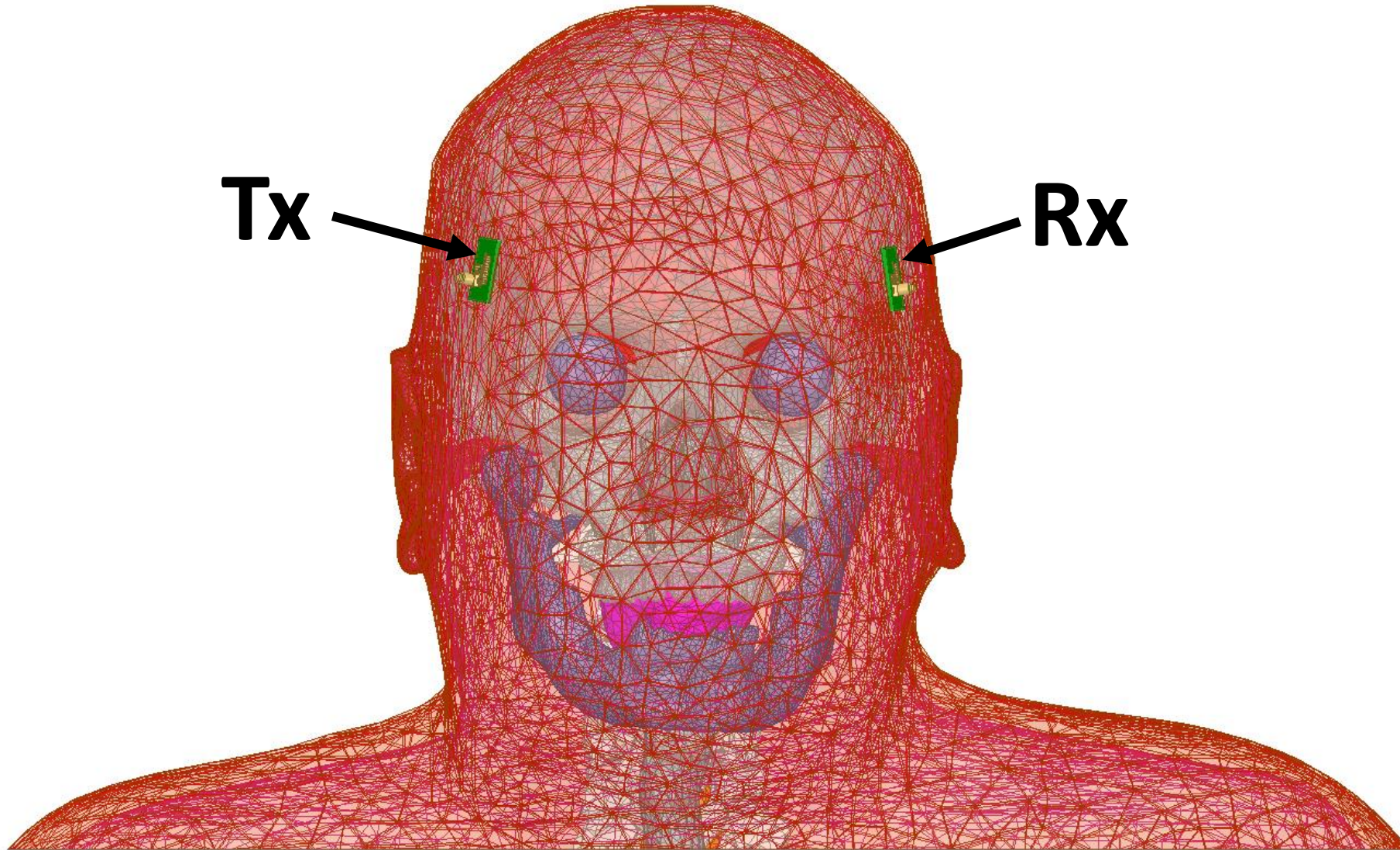


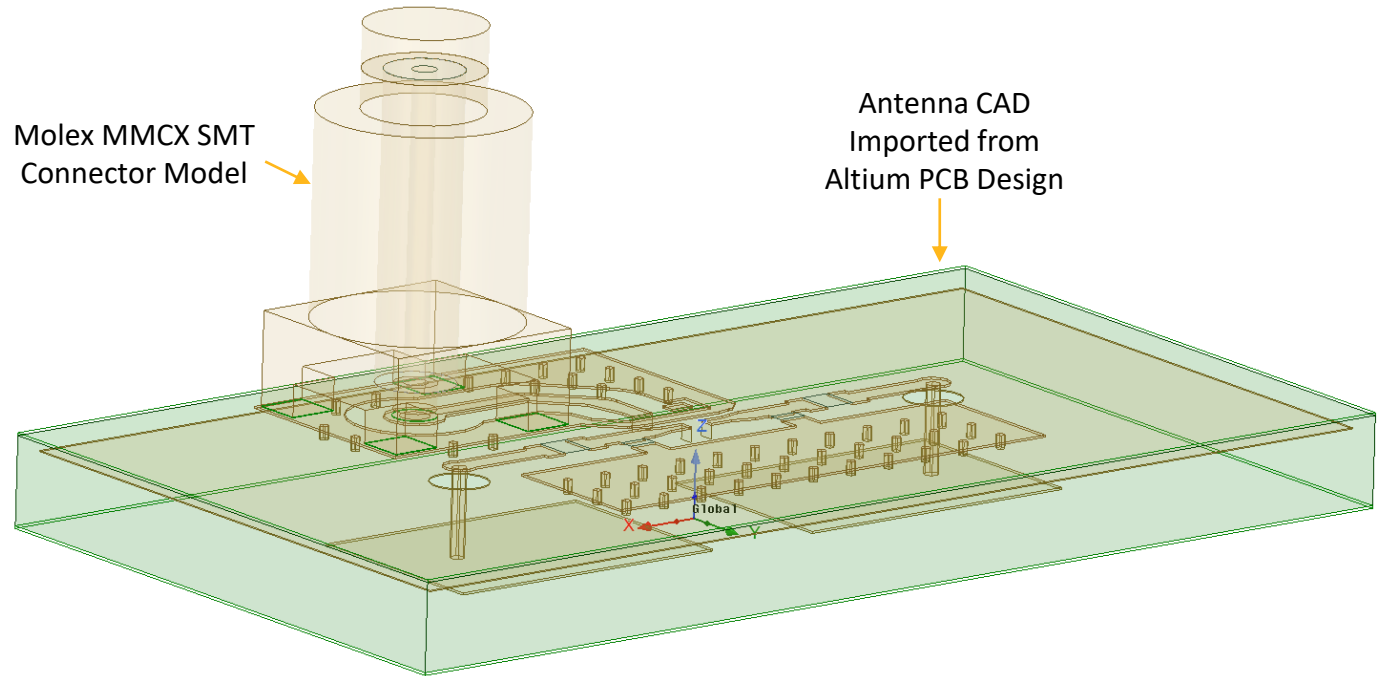
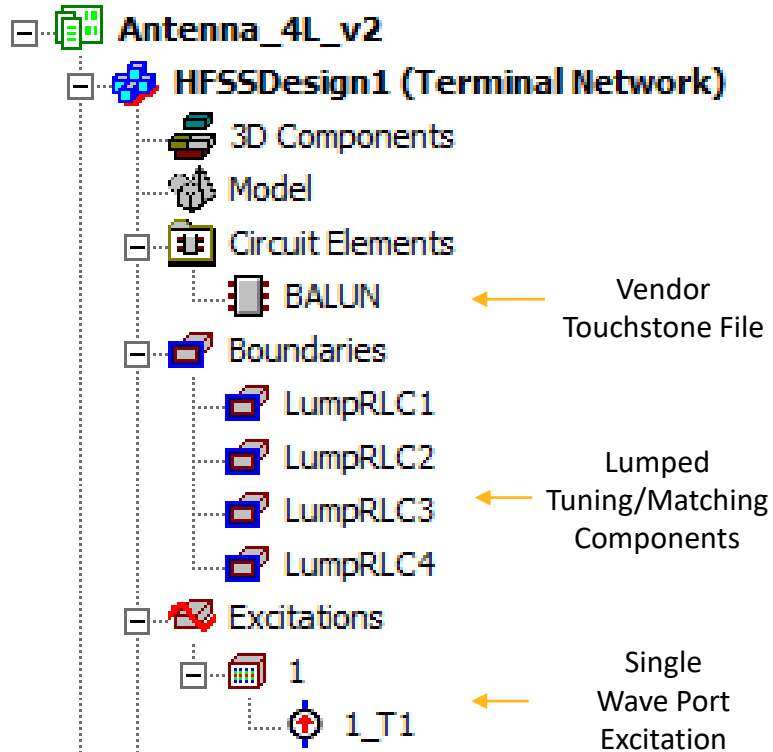
Image Source: Mahmud, et. al; "Ultra-Wideband (UWB) Antenna Sensor Based Microwave Breast Imaging: A Review"

Single Tx/Rx Microwave Imaging System

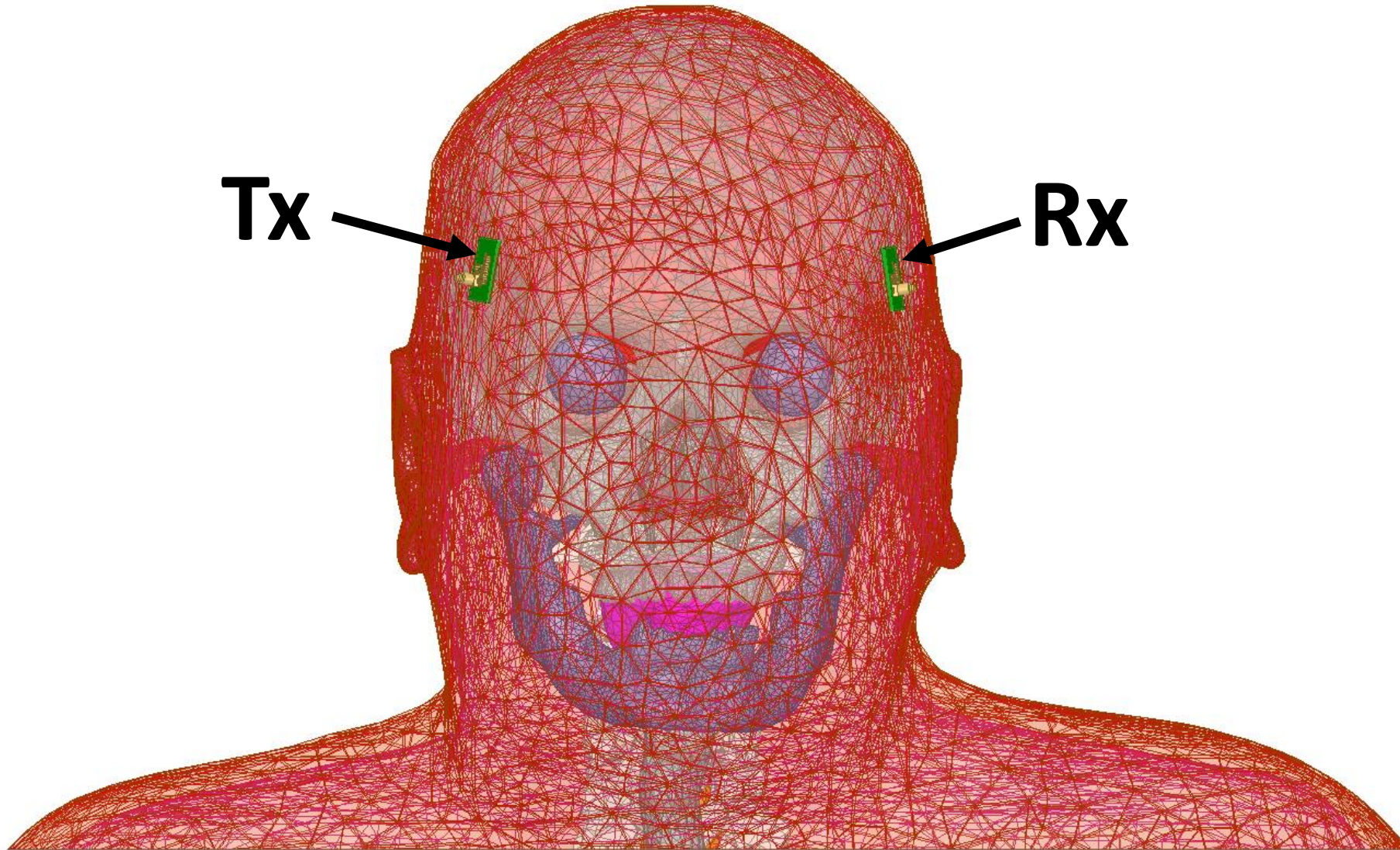


Dual Anti-Phase Patch Antenna (Modeled as HFSS 3D Component)

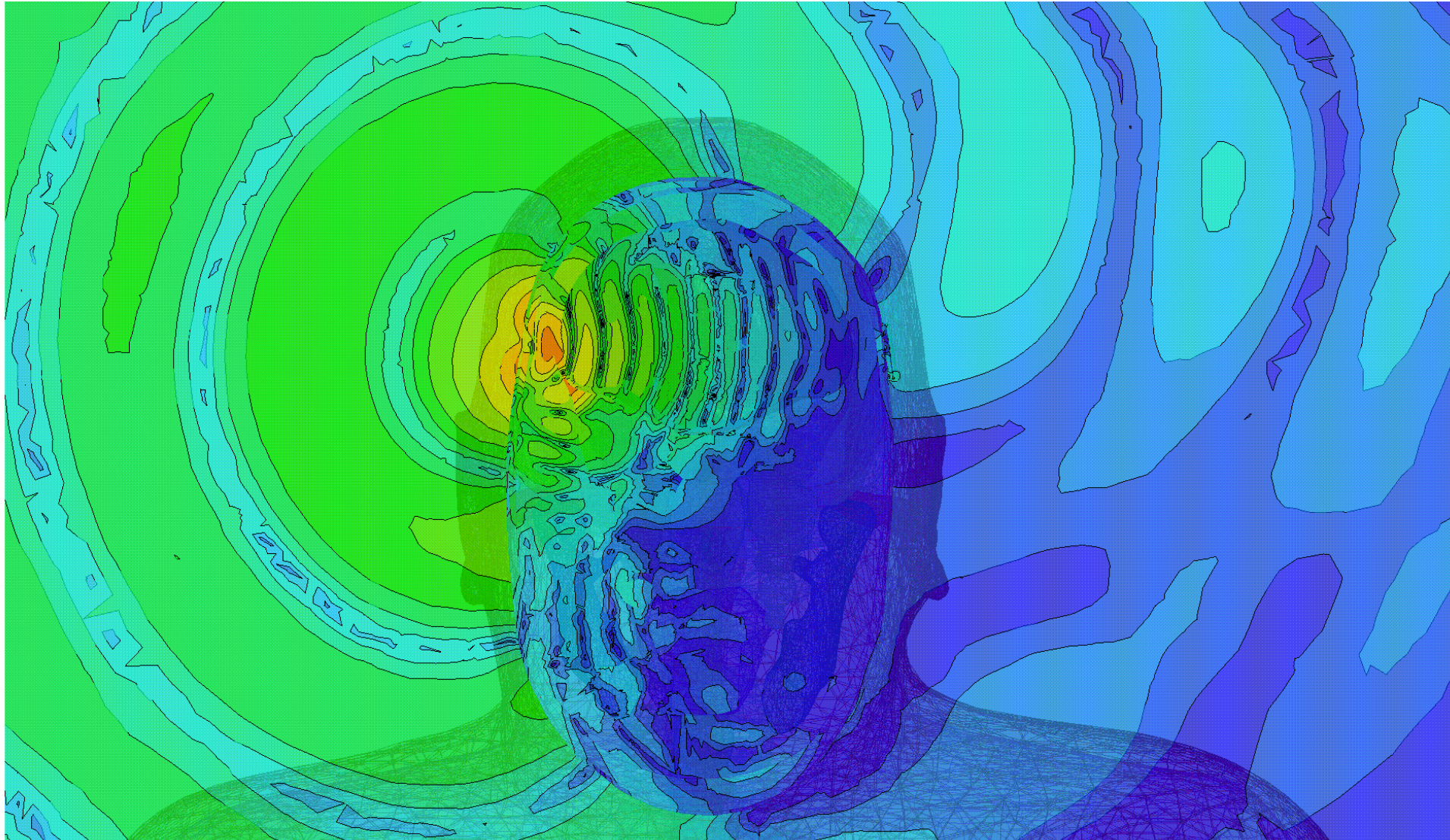
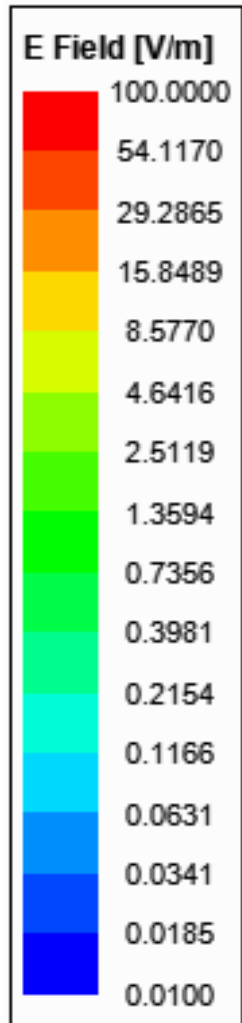
Ansys



Single Tx/Rx Microwave Imaging System



Problem: On-Body Antenna Radiates Excessively Outside The Body (DUT)



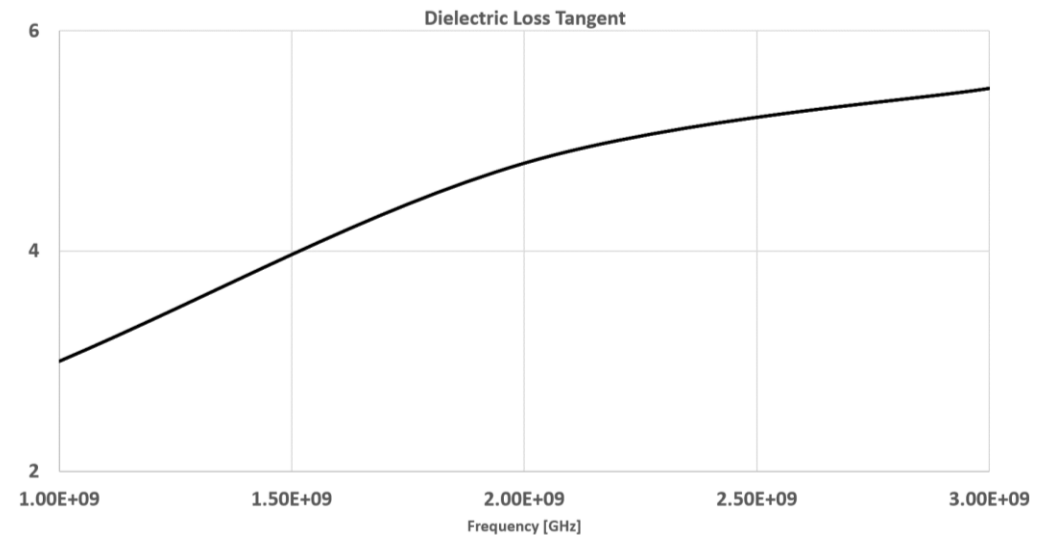
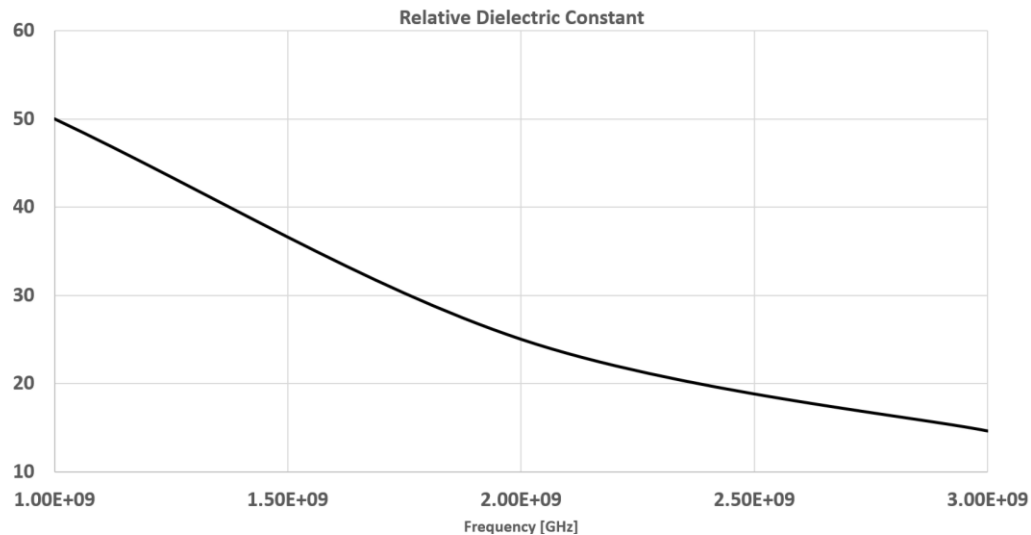
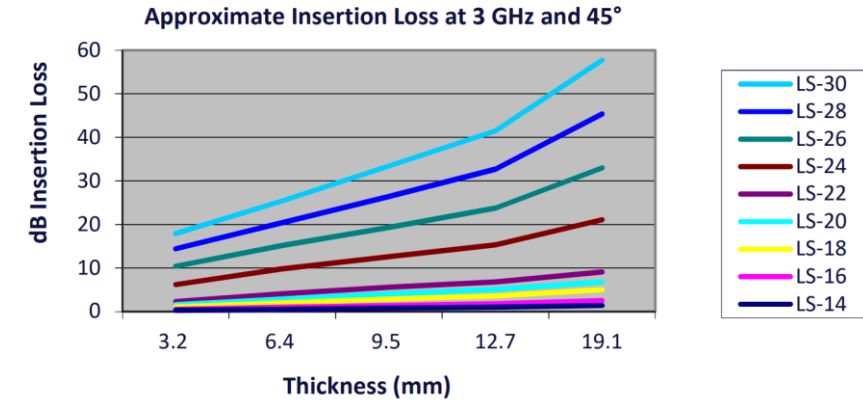
Proposed Solution Utilizing New RF Absorbing Foams

Eccosorb® LS

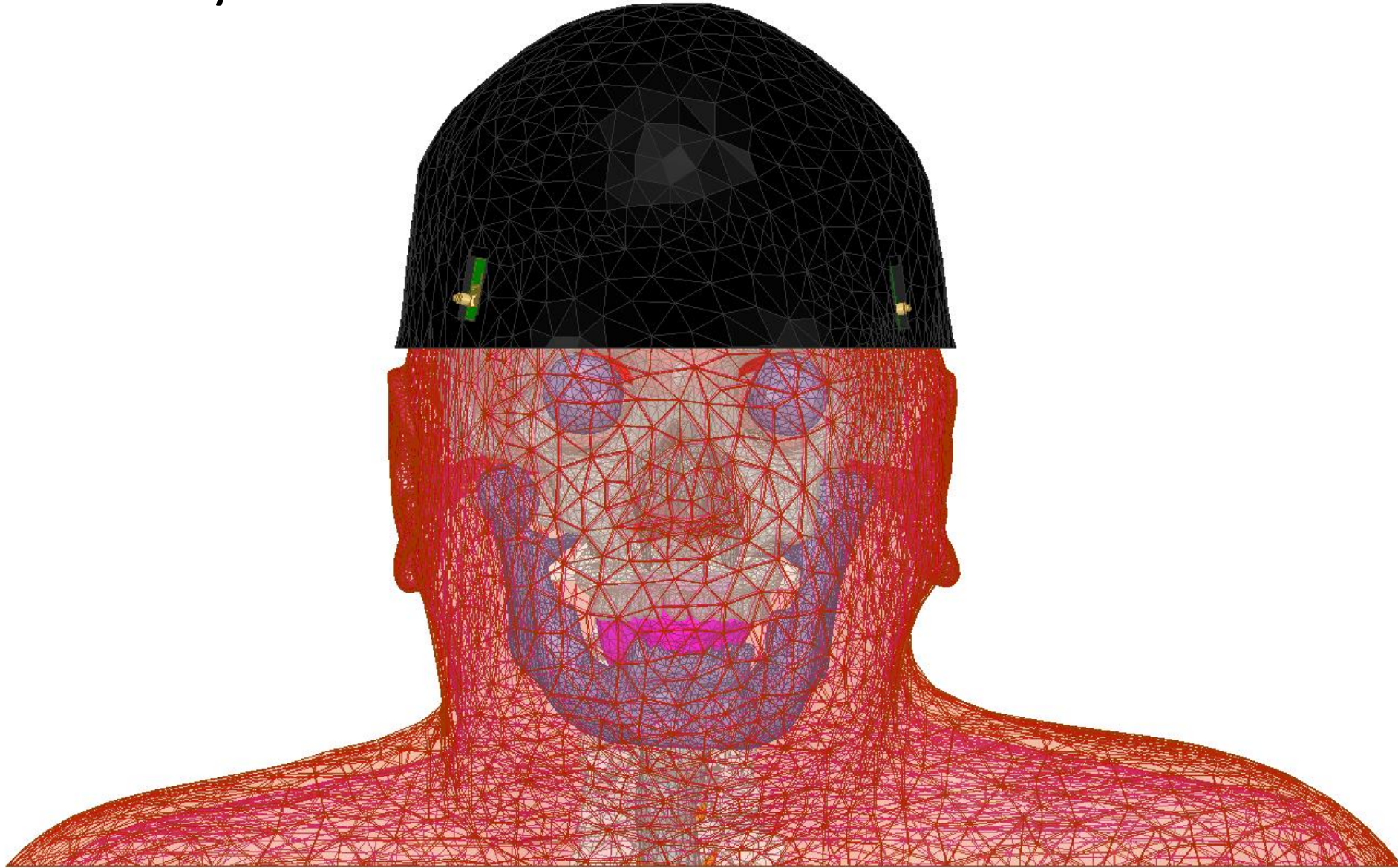
APPLICATIONS

- Eccosorb LS is used to lower cavity Q's in RF amplifiers, oscillators, cabinets containing microwave devices, computer housings, LNB's and isolation of antennas by insertion loss.
- Eccosorb LS is also used to reduce surface currents on radiating elements and outer ground-plane type surfaces.
- Reflectivity of an object (metal or otherwise) can be reduced somewhat by applying one or more layers of Eccosorb LS to its surface.

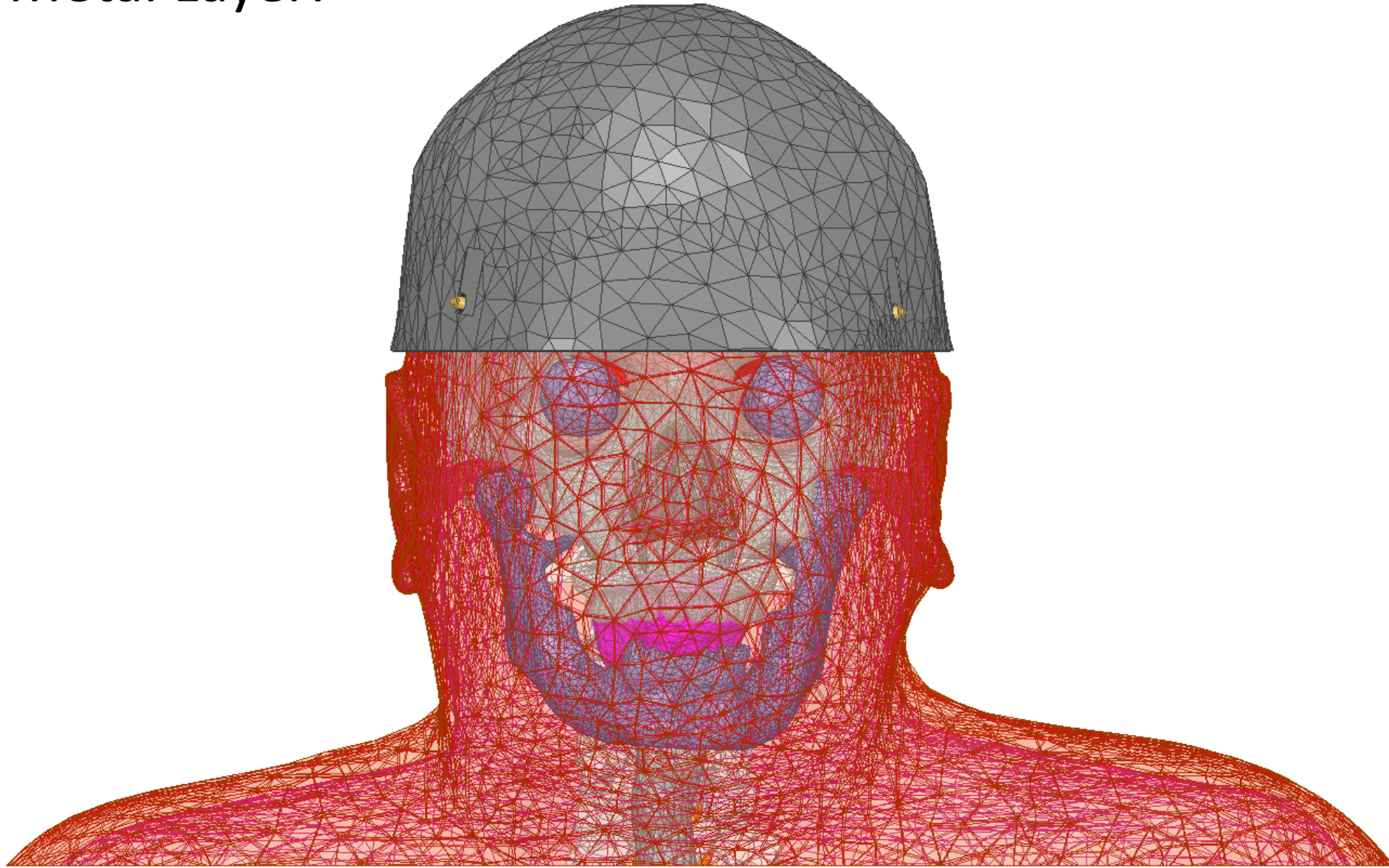
Lossy, Flexible, Foam Microwave Absorber



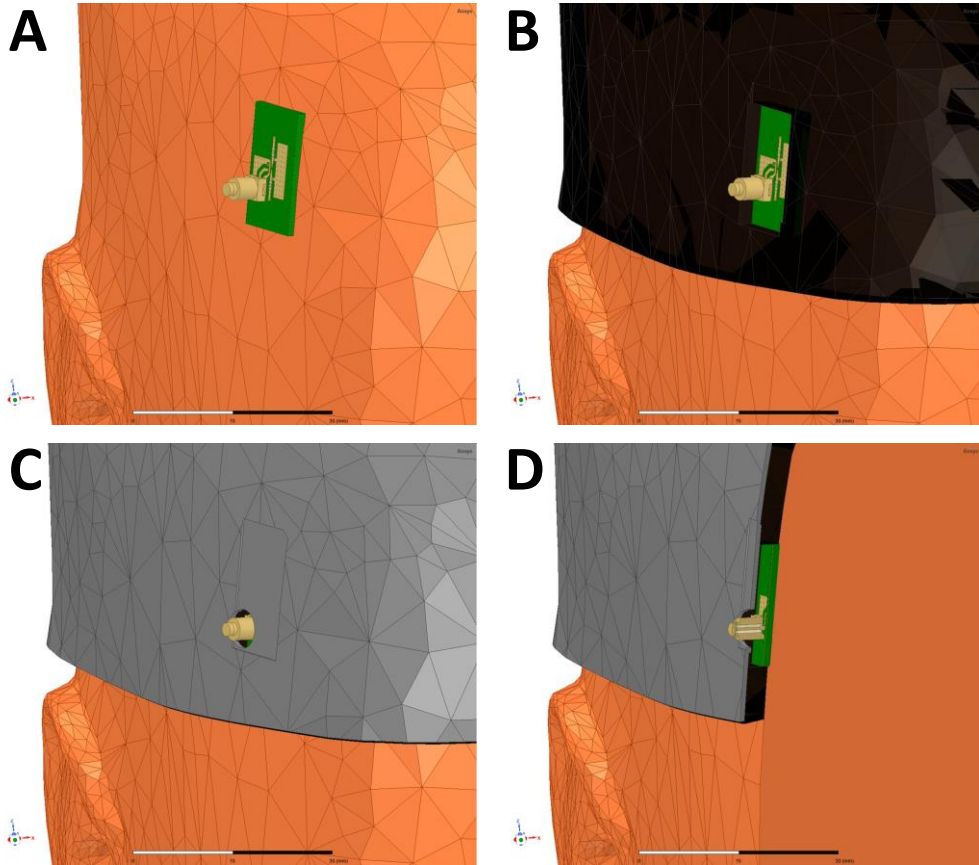
/ Inner Foam Layer:



/ Outer Metal Layer:

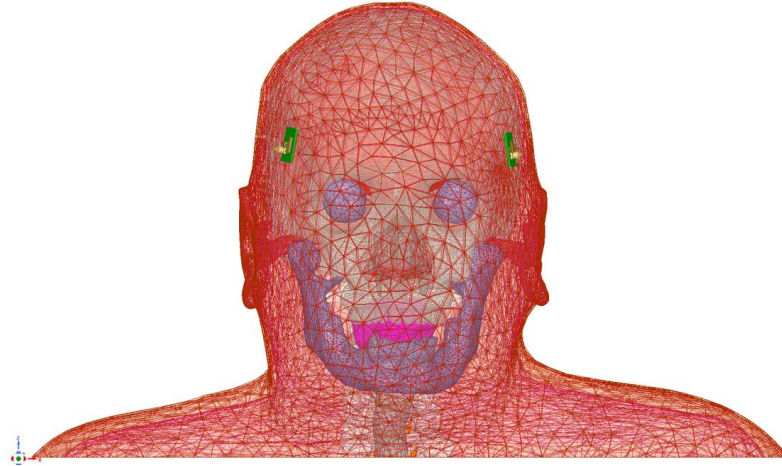


Foam + Metal Cap: HFSS Model (Left); Constructed Prototype (Right)

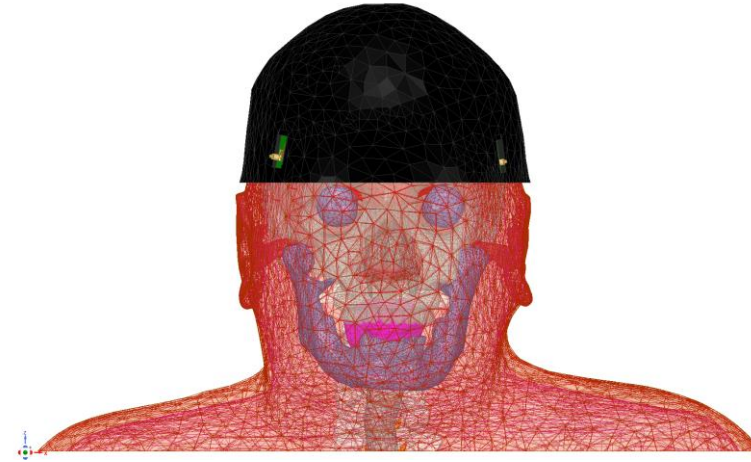


/ HFSS Models:

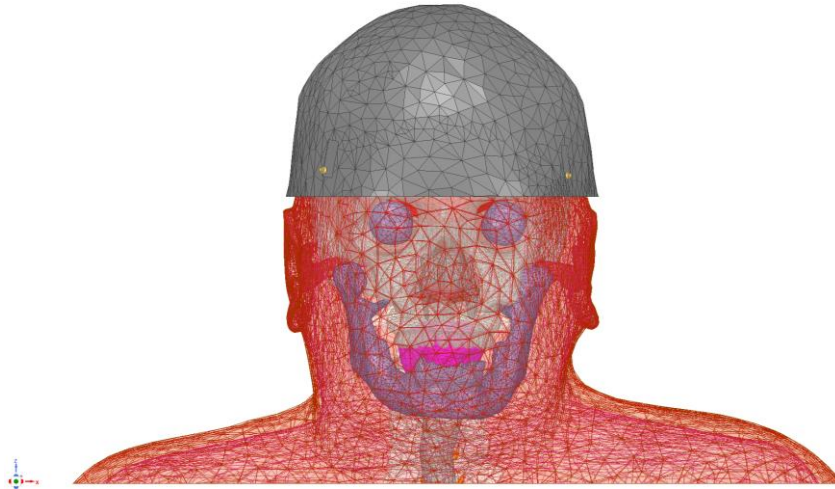
NO FOAM / NO METAL



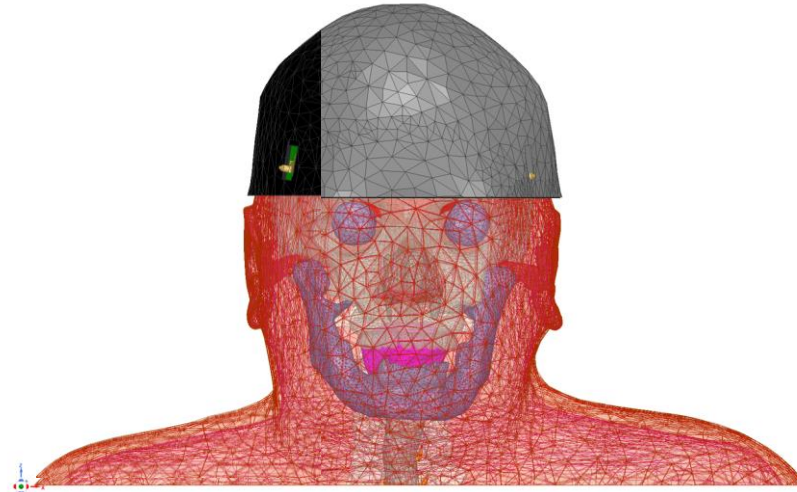
FOAM / NO METAL



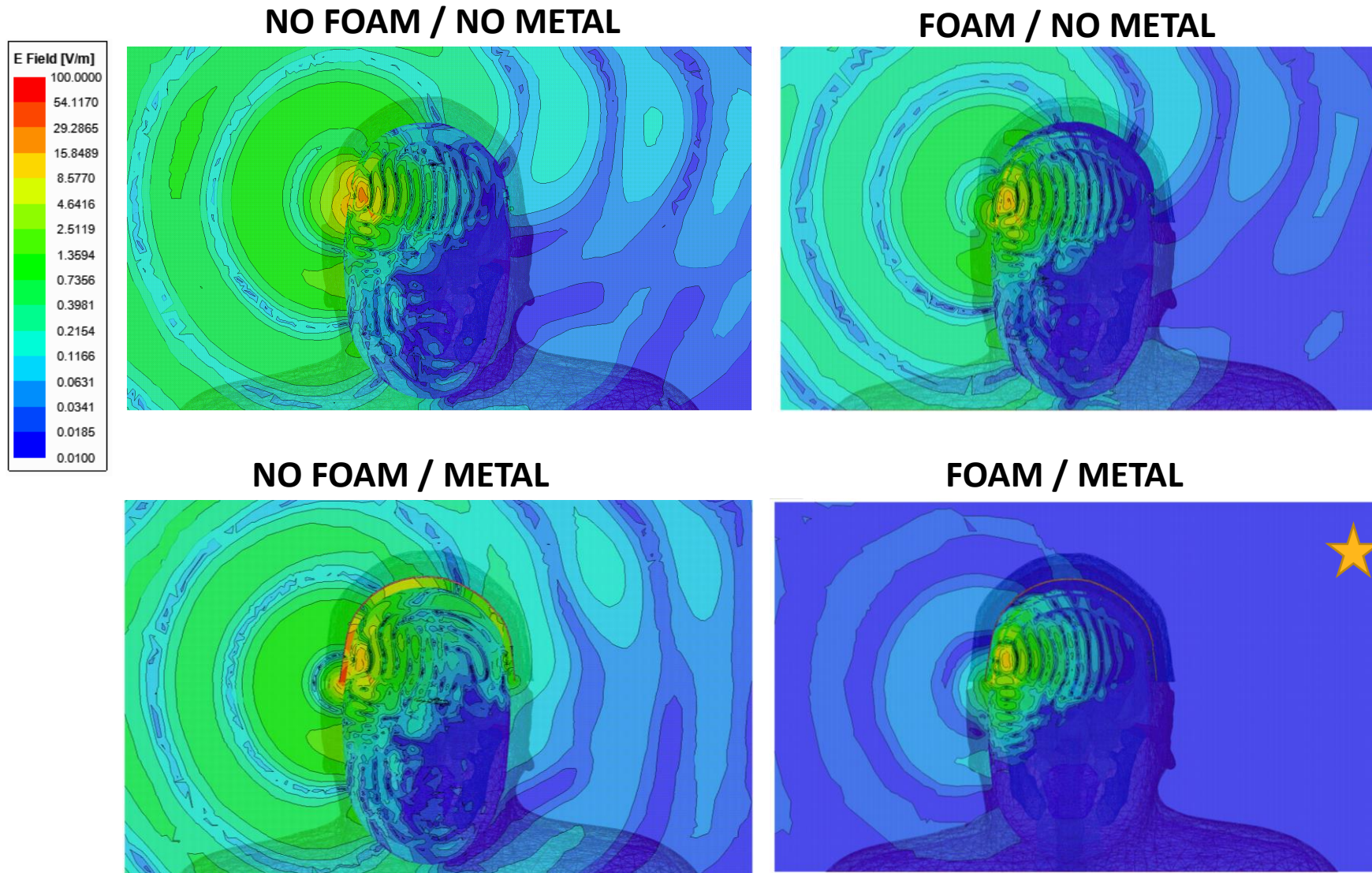
NO FOAM / METAL



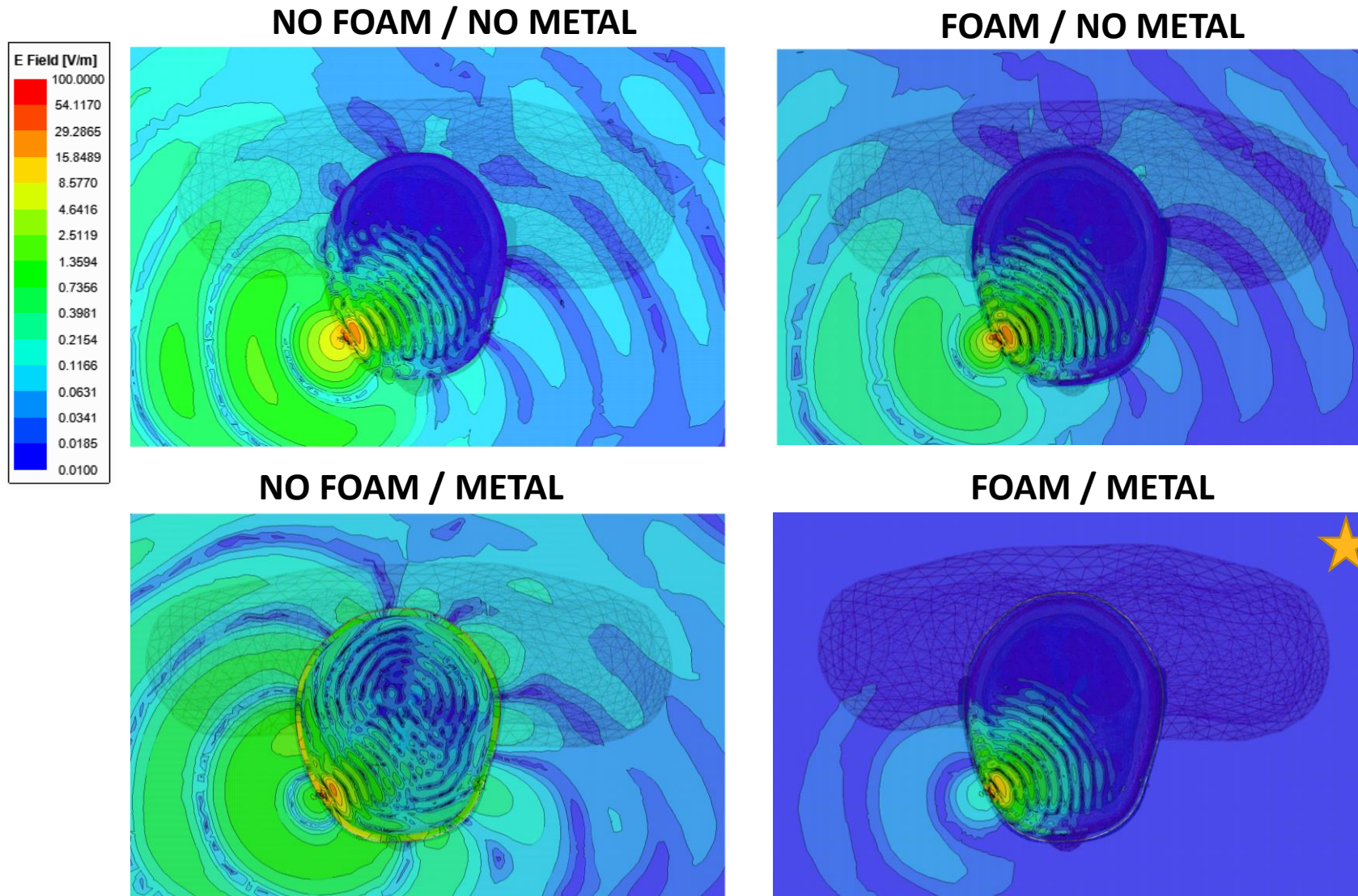
FOAM / METAL



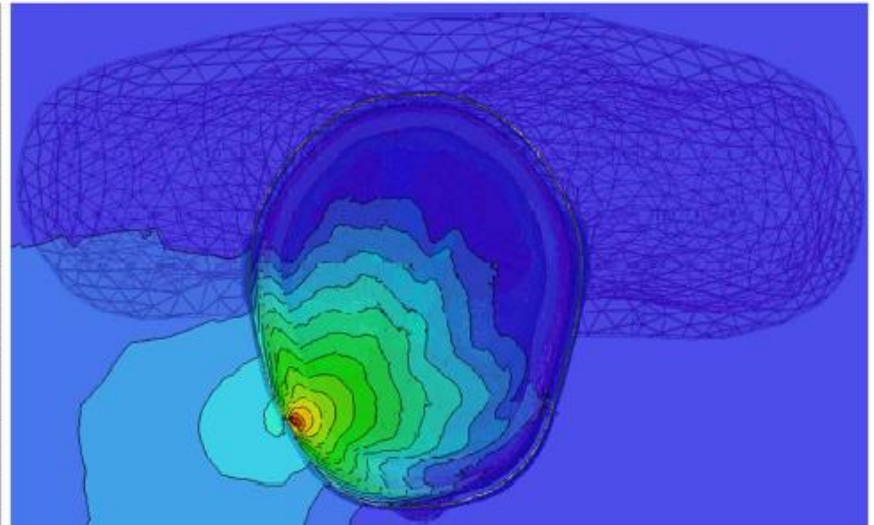
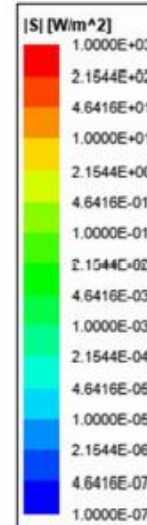
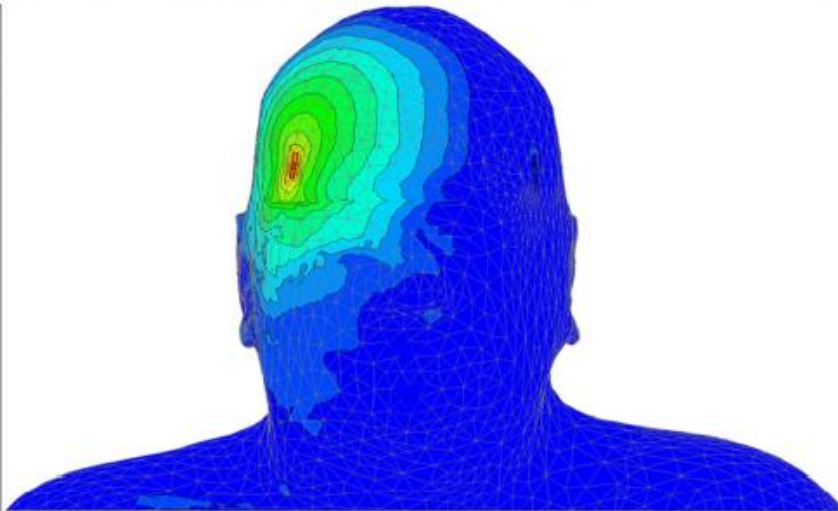
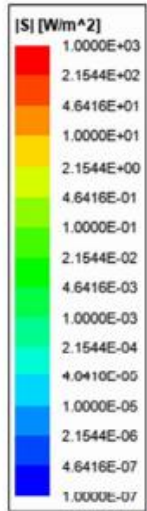
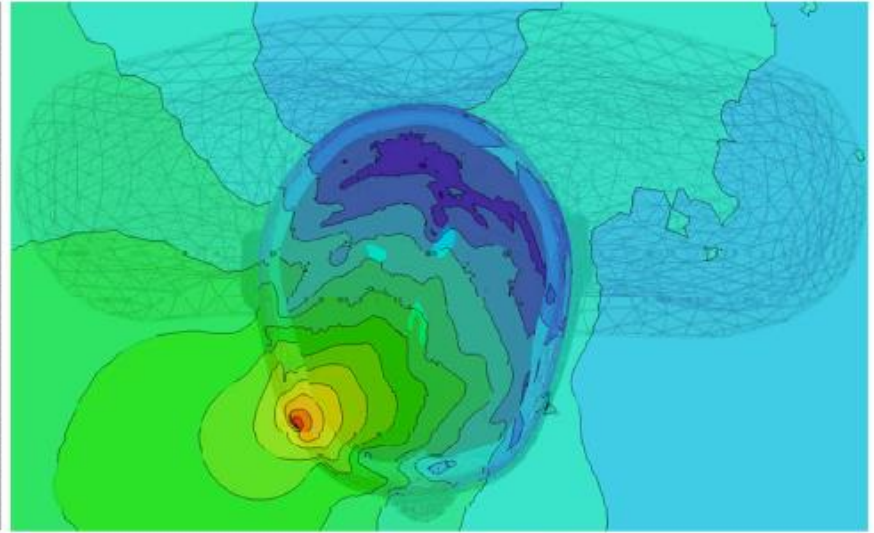
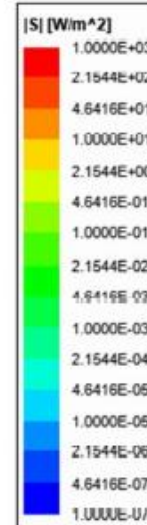
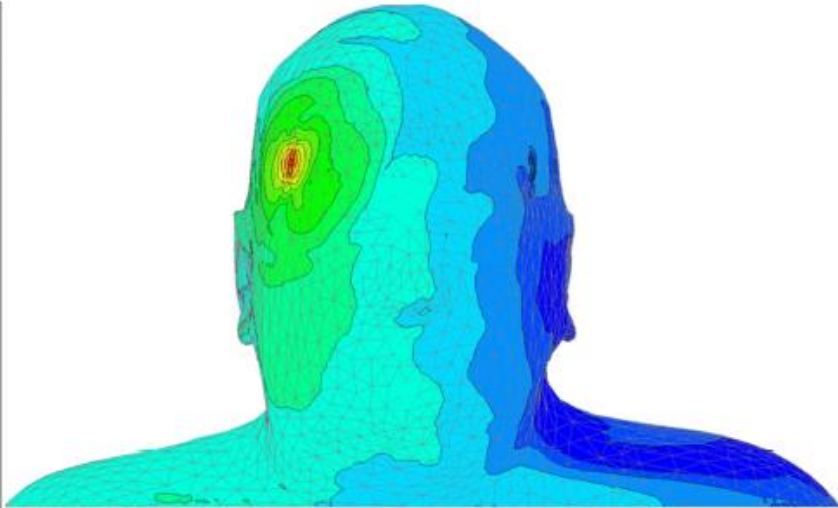
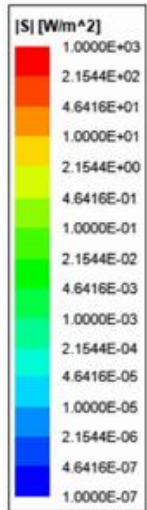
/ |E| Field vs. Input Excitation Phase – Coronal Plane



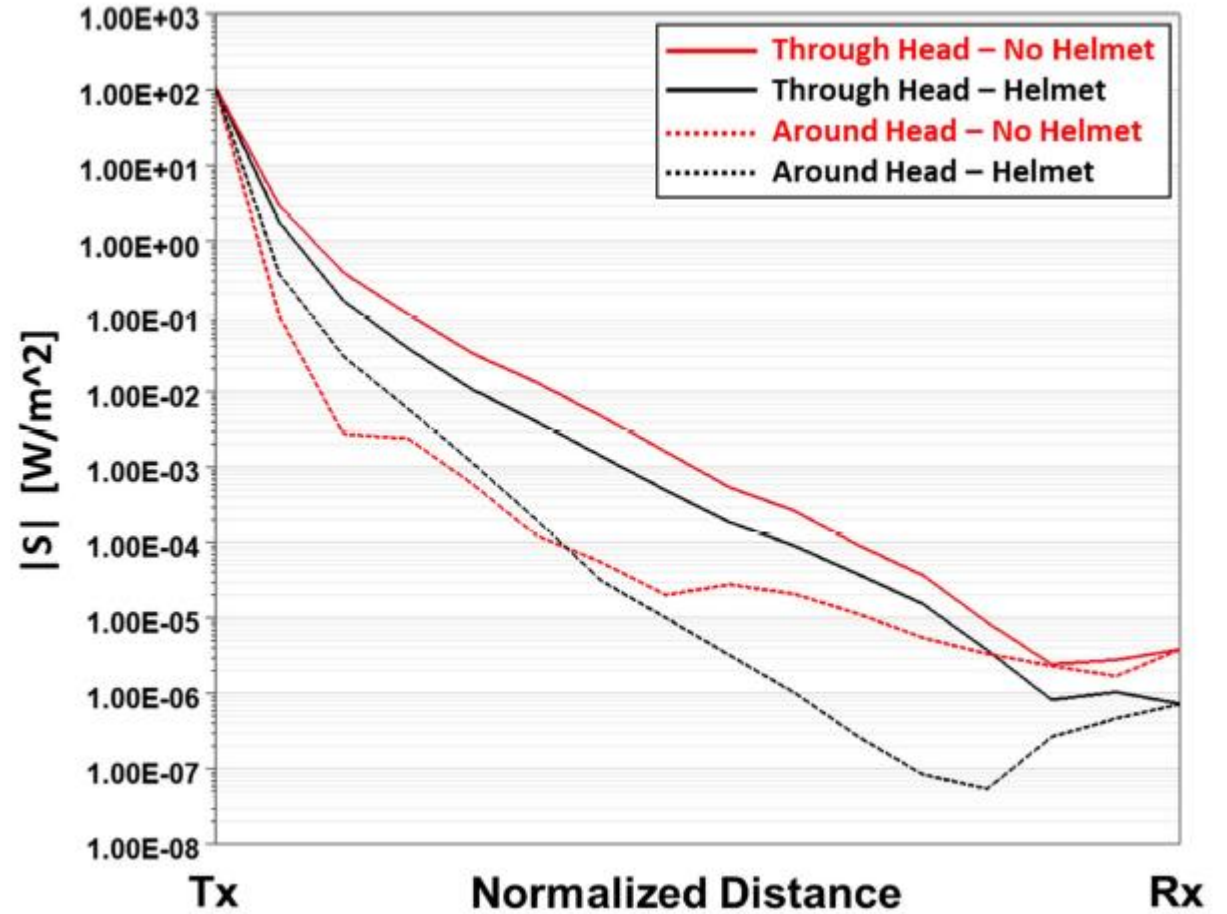
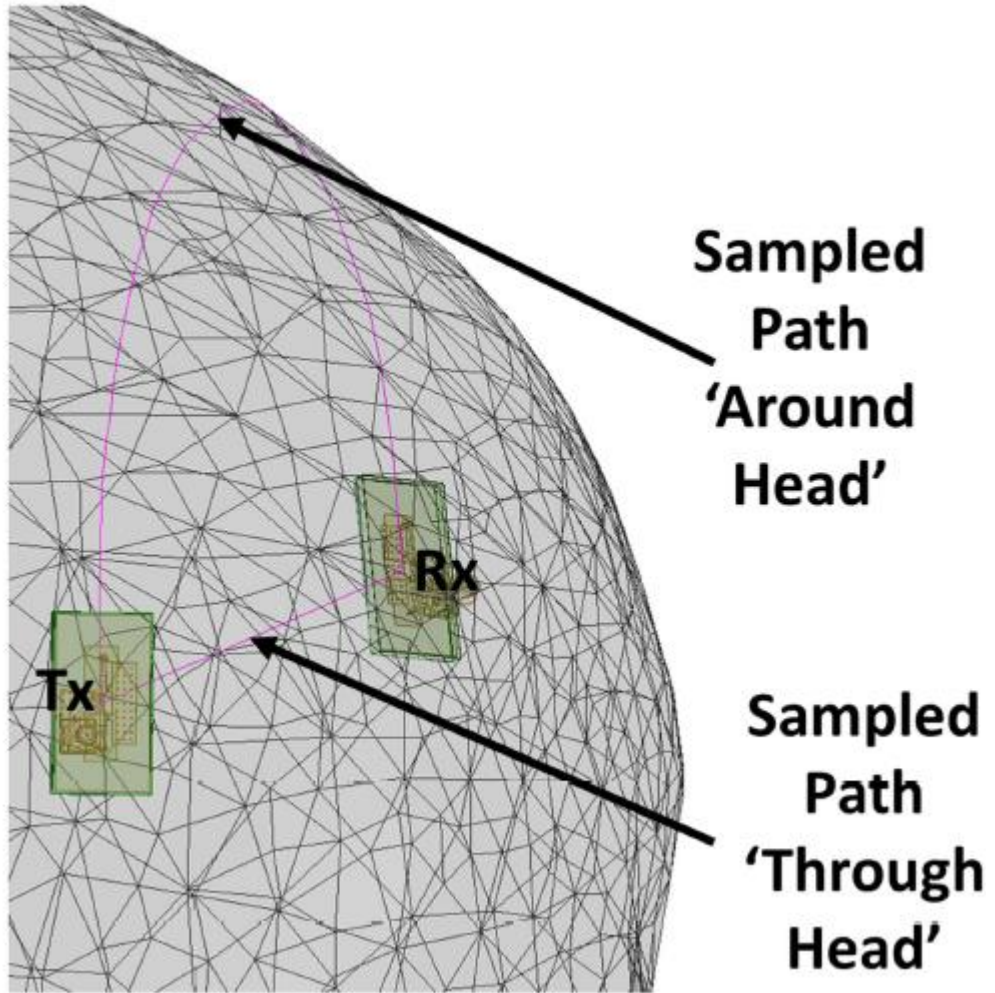
/ |E| Field vs. Input Excitation Phase – Transverse Plane



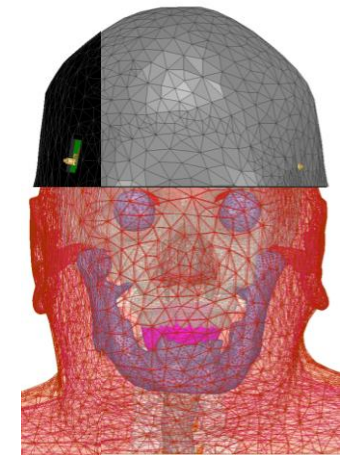
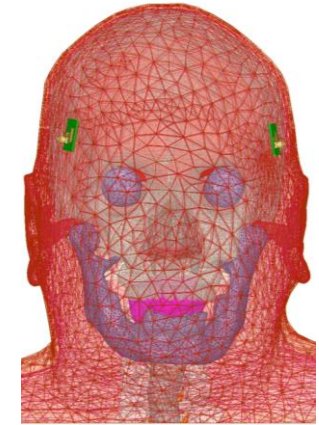
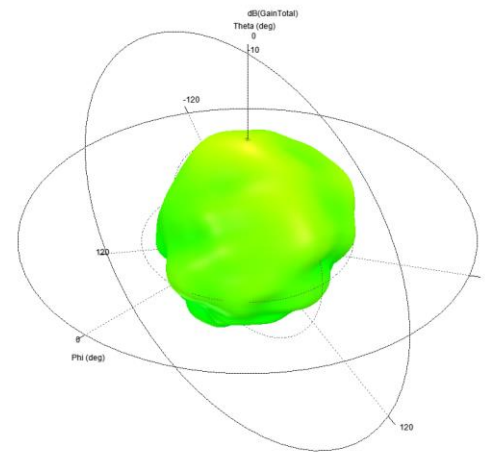
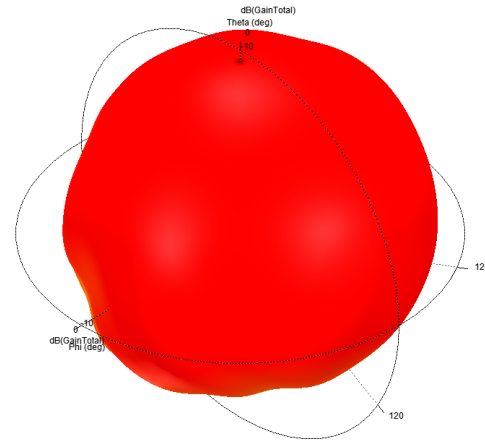
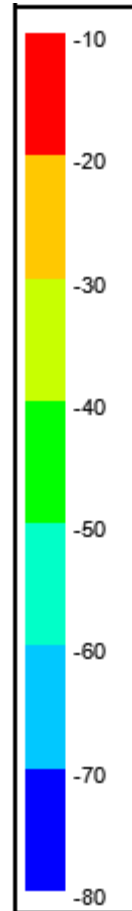
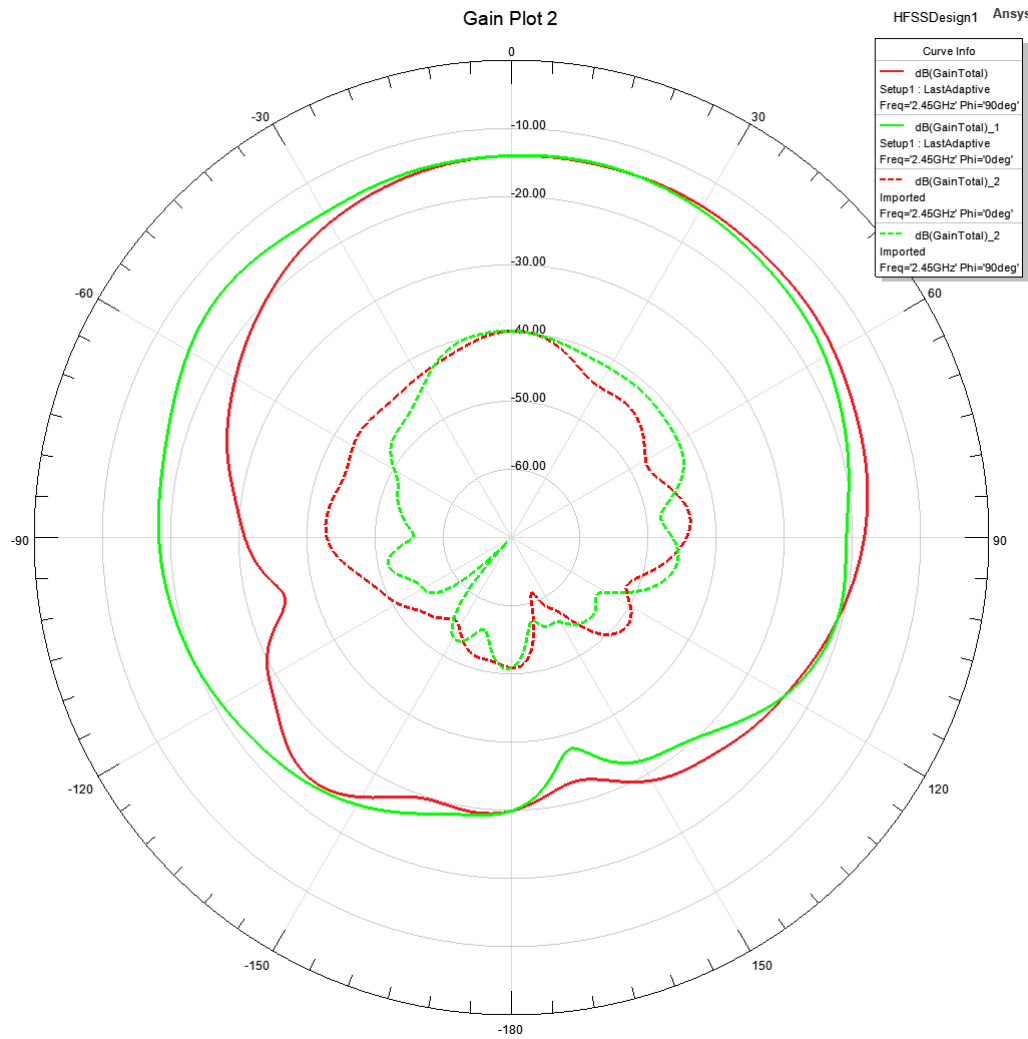
Poynting Vector Magnitude: Body Surface (Left); Through Head (Right)



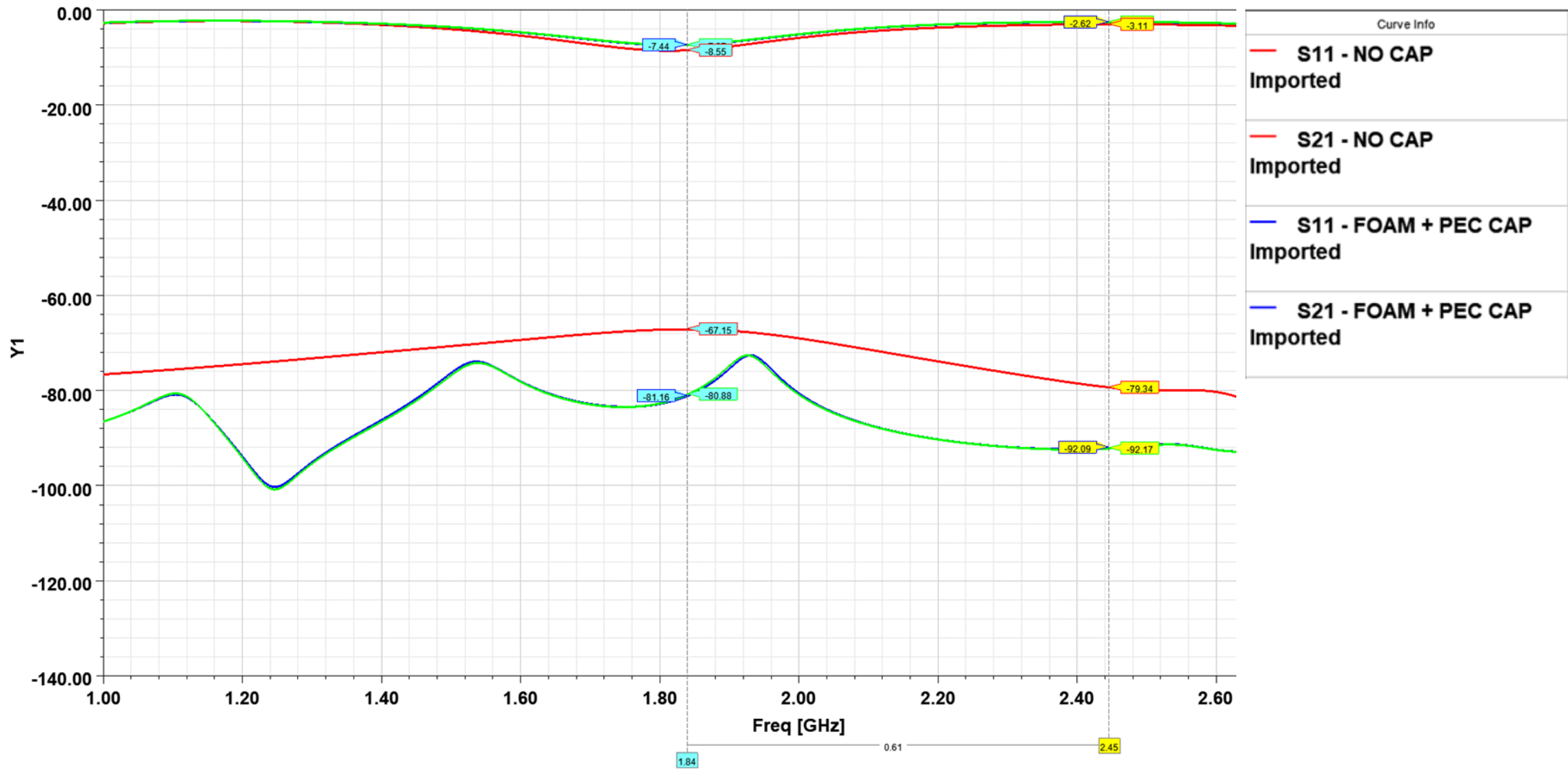
Poynting Vector Magnitude: Through vs. Around Head



Far Field Gain Pattern

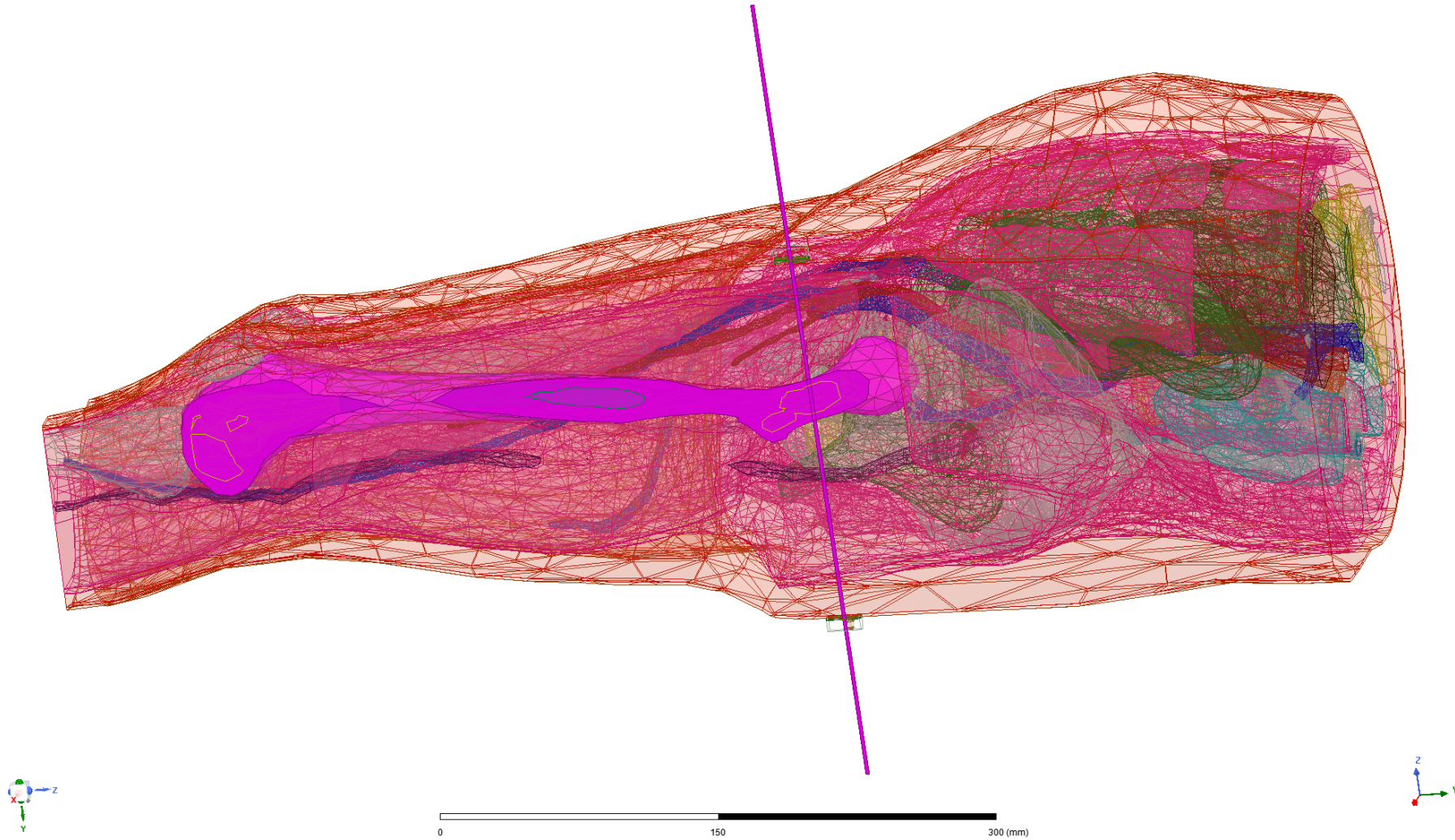


S Parameters: Reduced S21 Coupling \propto Increase in SNR

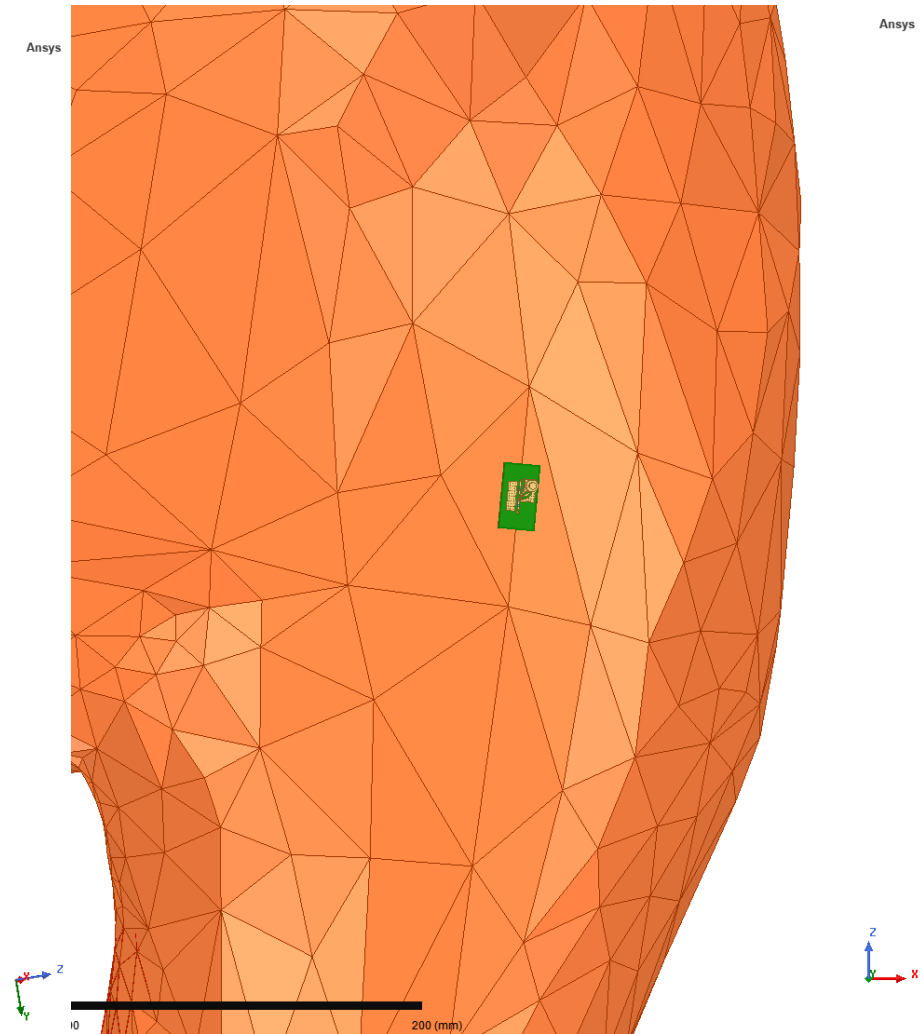
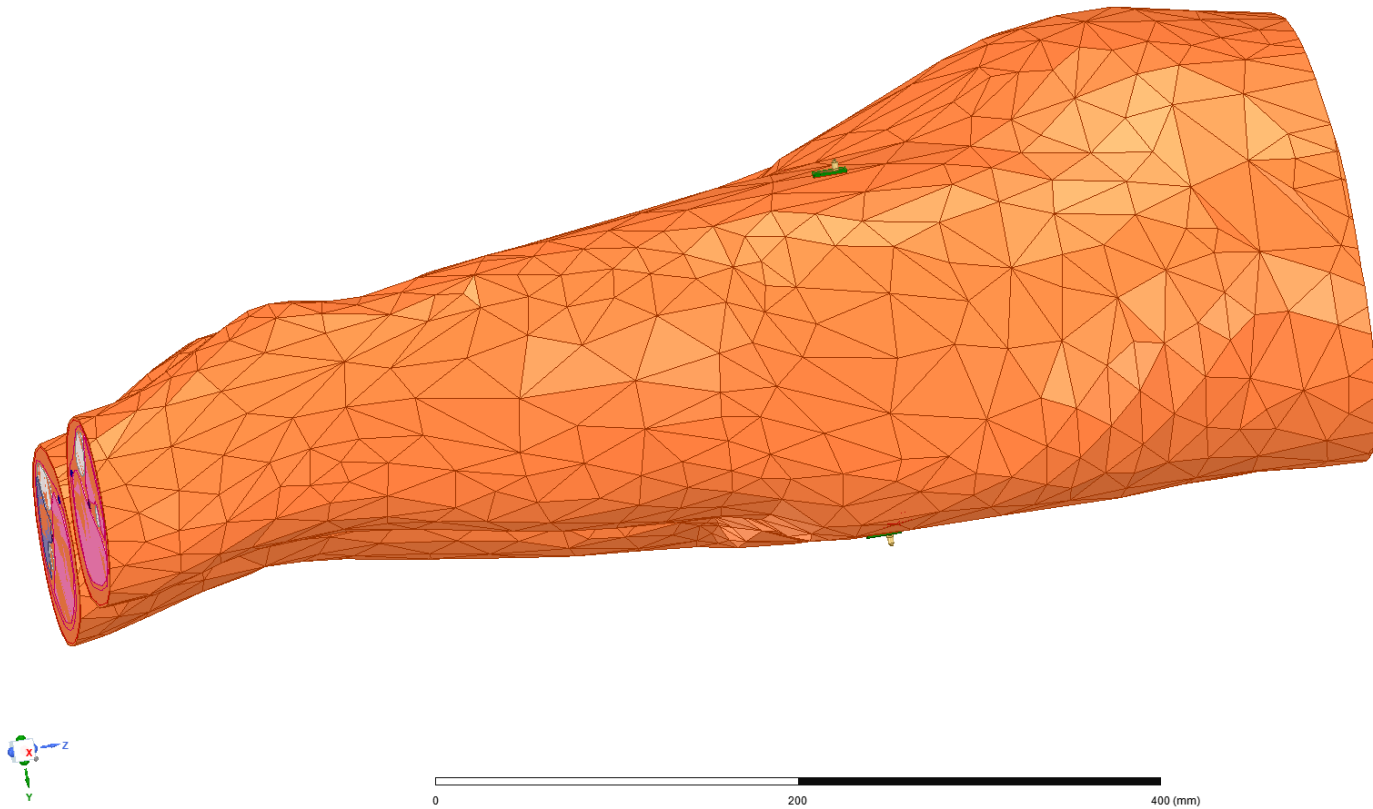


Case 2: MW Imaging of the Femur

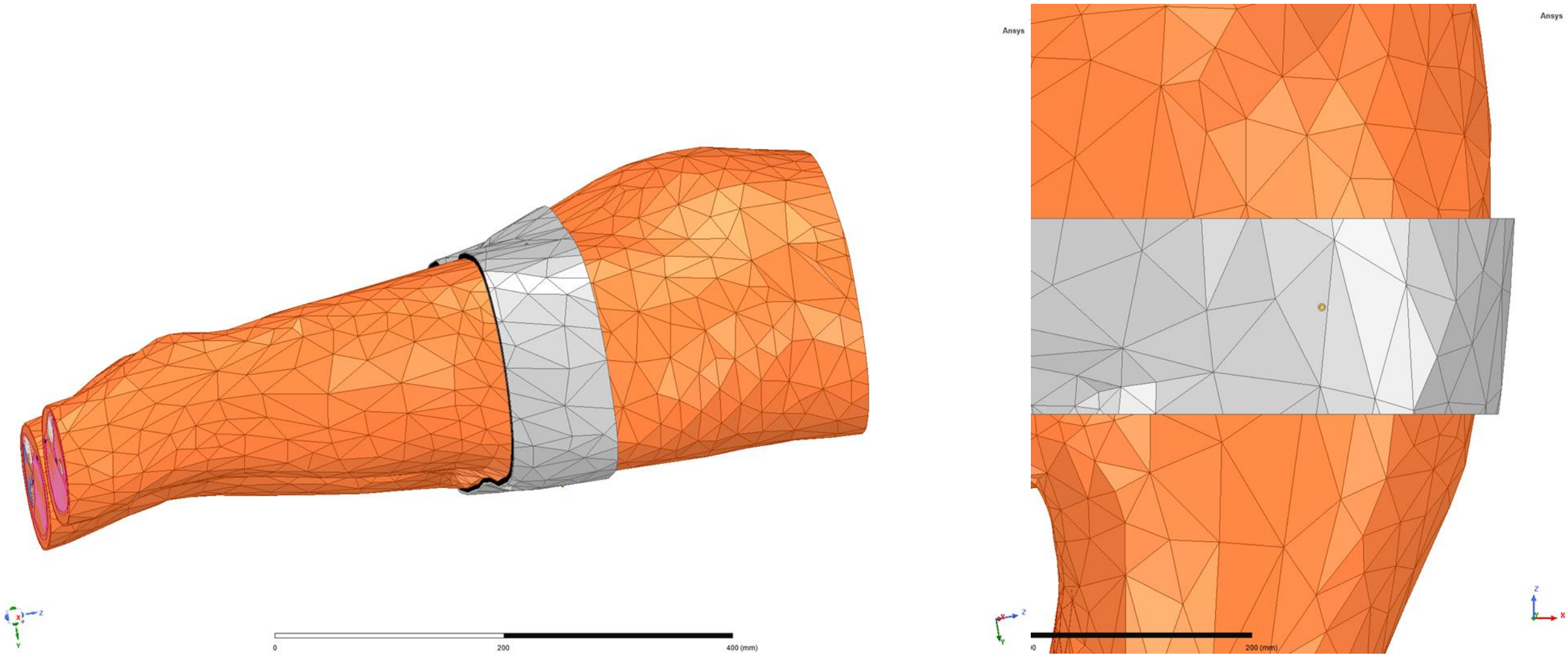
Ansys



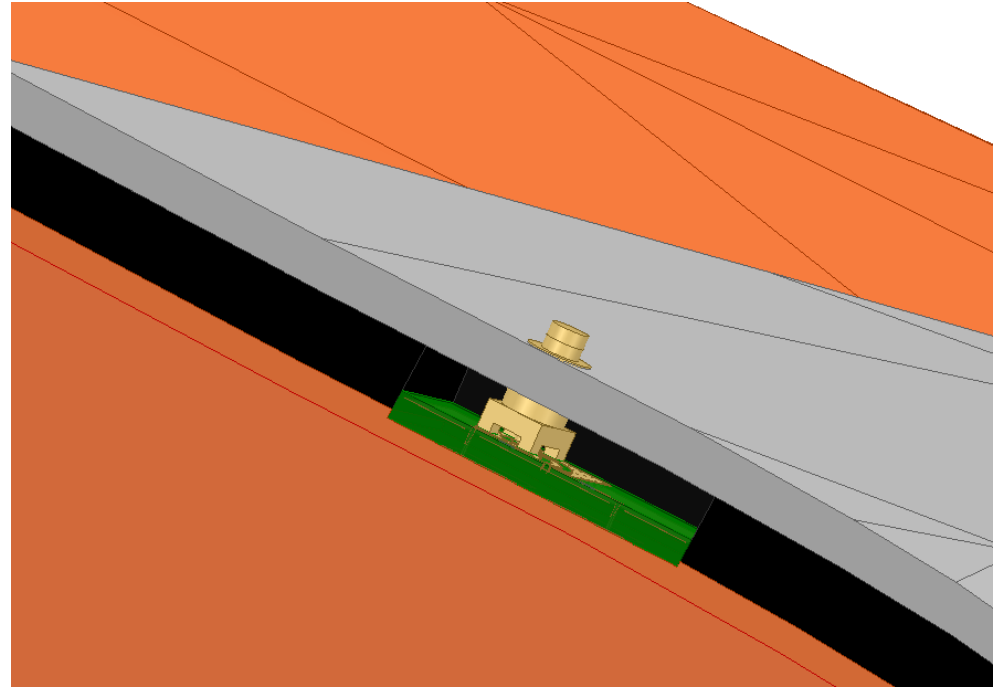
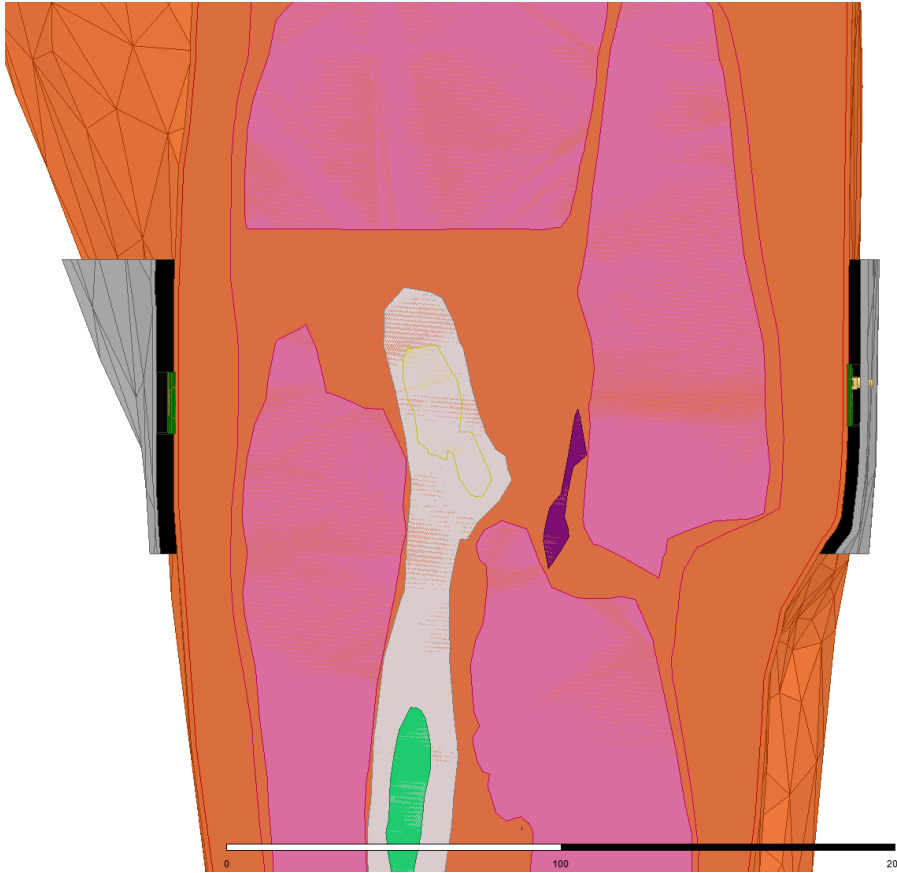
Antennas on VHP Hips



Antennas on VHP Hips with Foam + Metal Belt



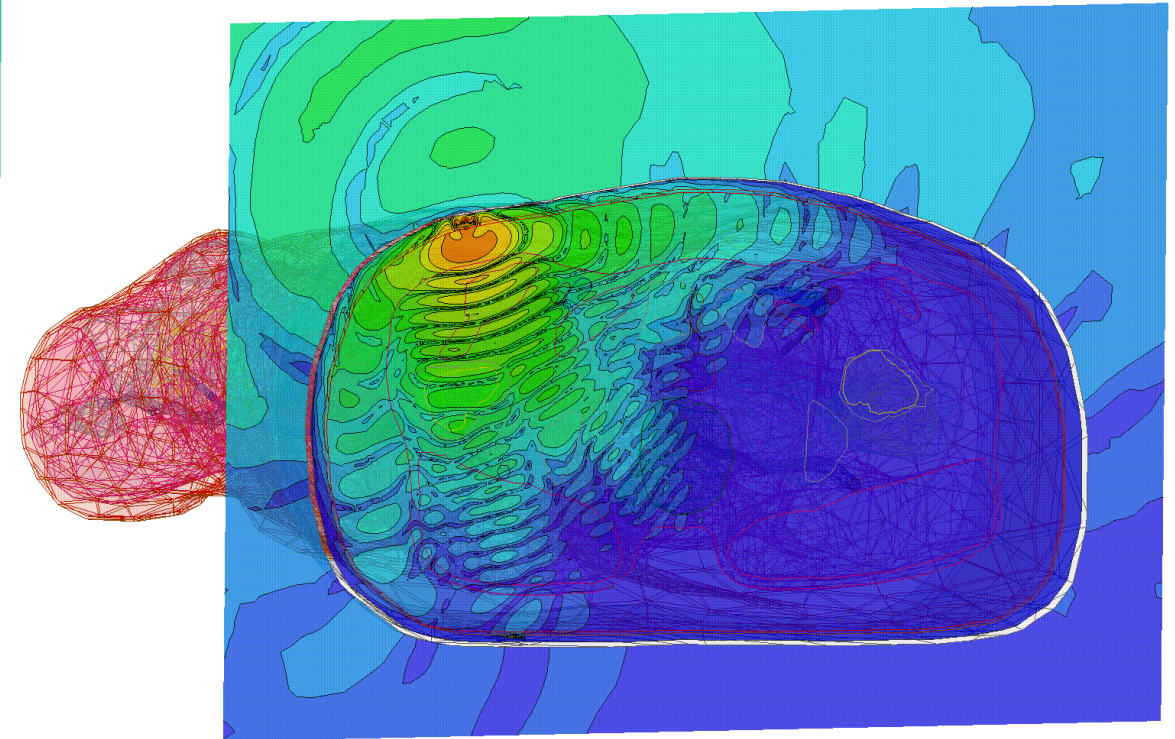
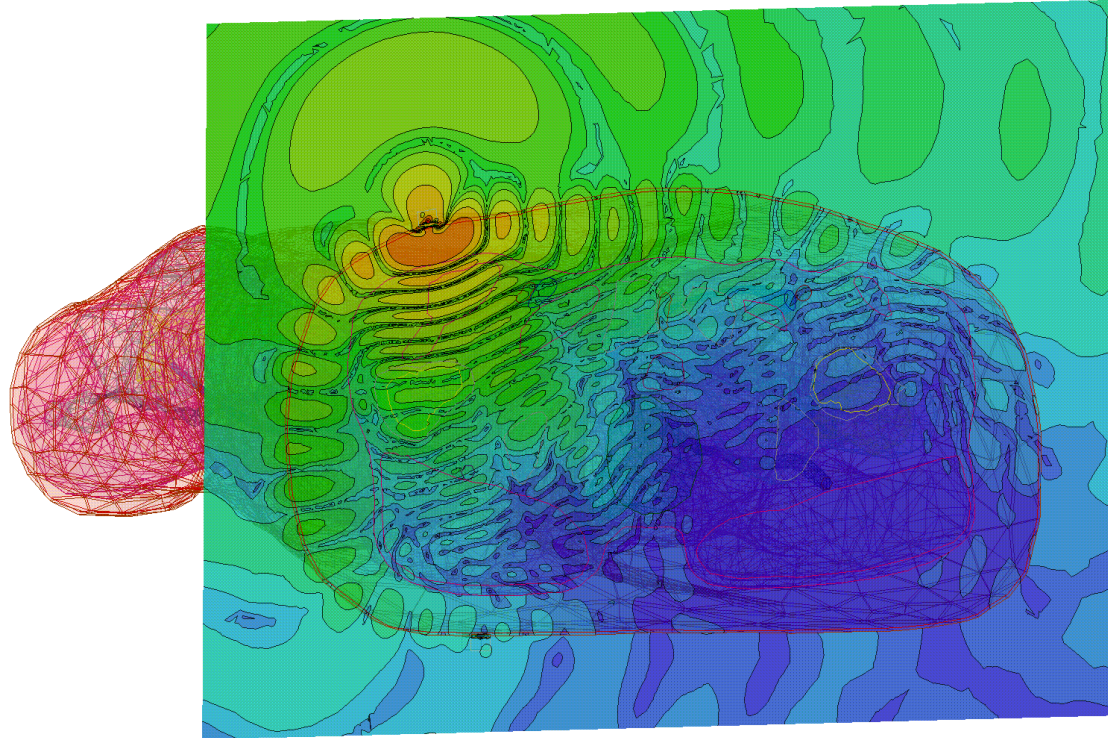
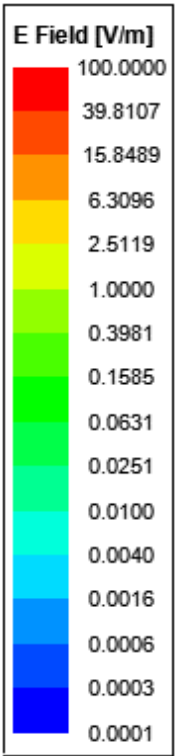
/ Cross-Section View



/ |E| Field vs. Input Excitation Phase – Transverse Plane

No Belt

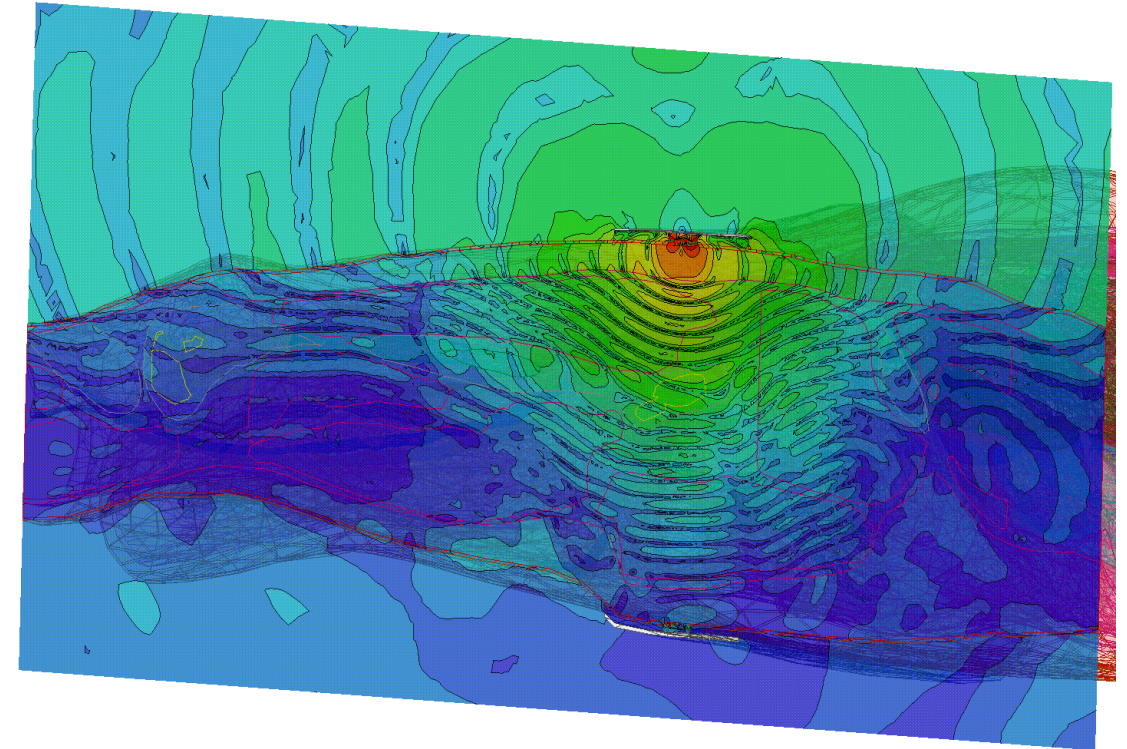
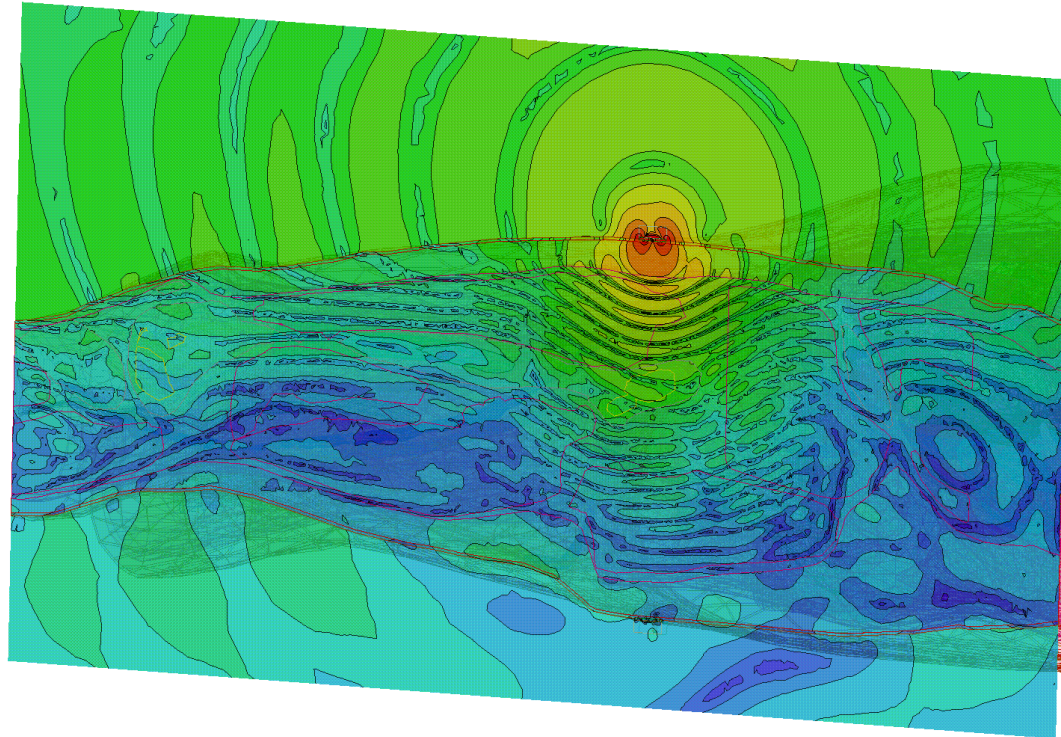
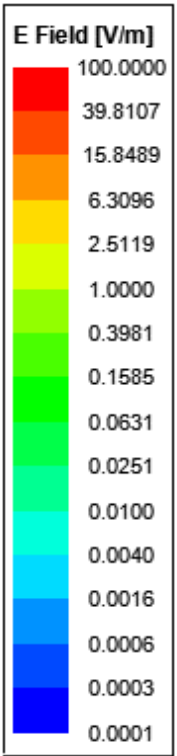
With Belt



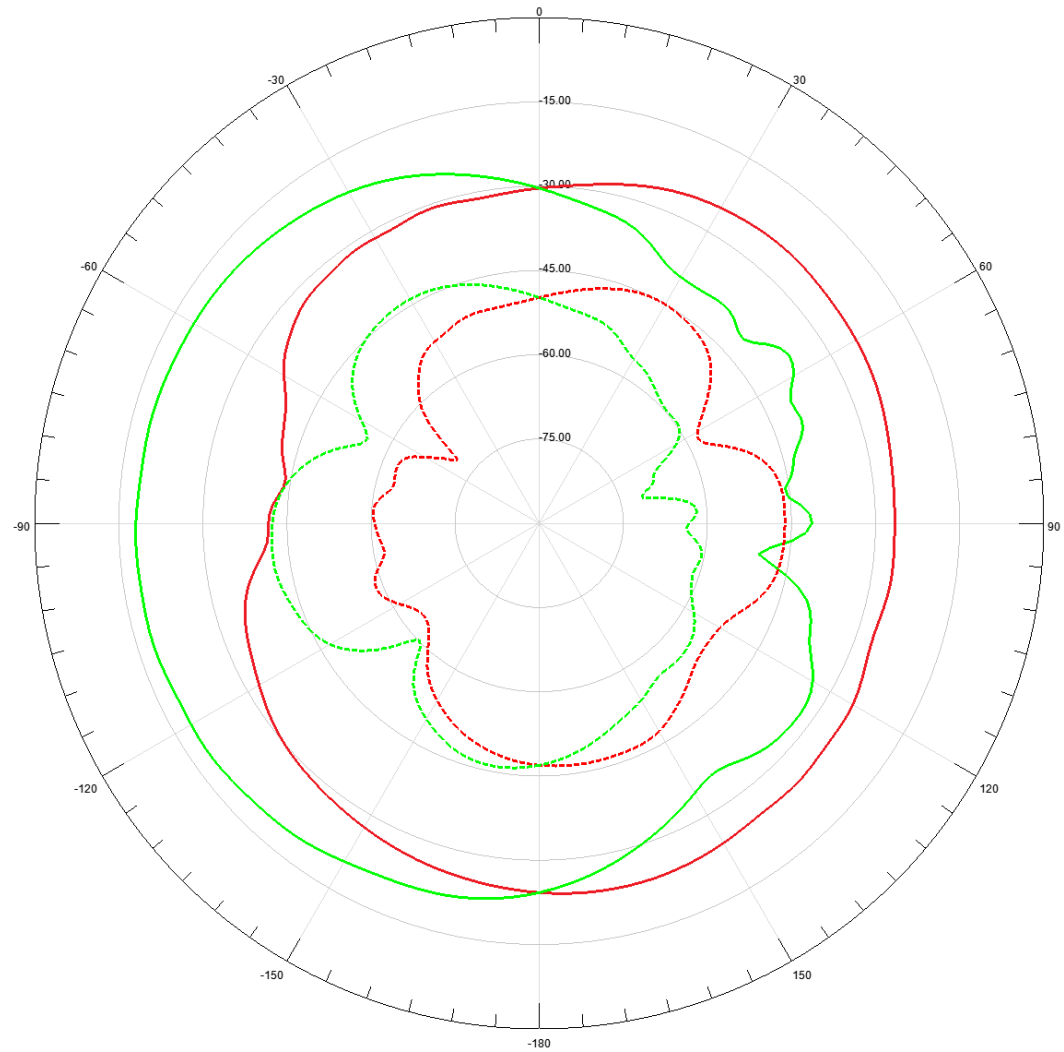
|E| Field vs. Input Excitation Phase – Sagittal Plane

No Belt

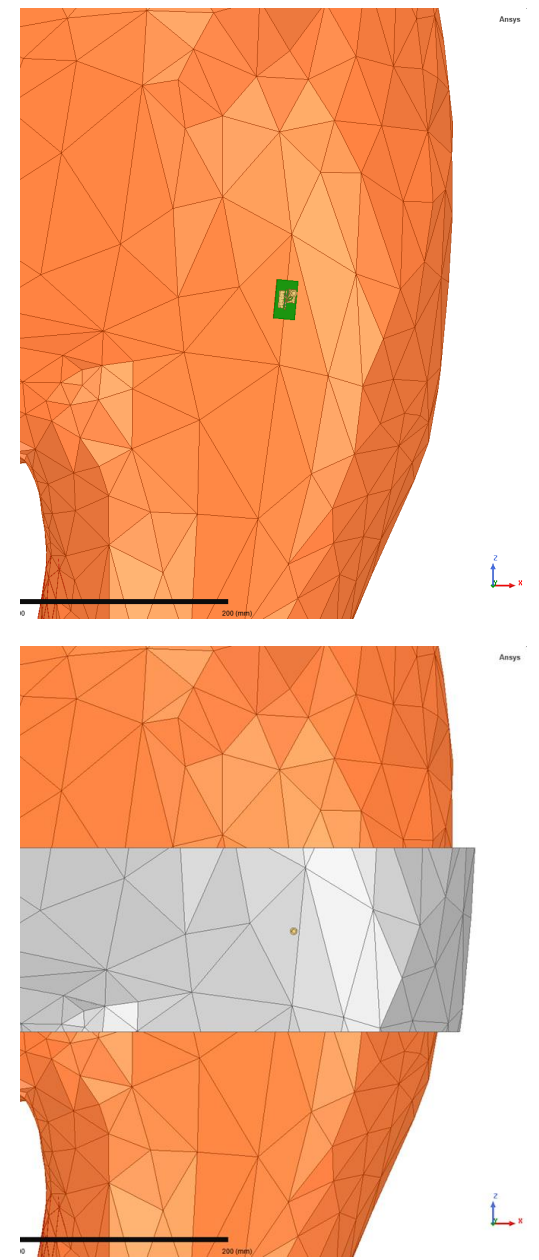
With Belt



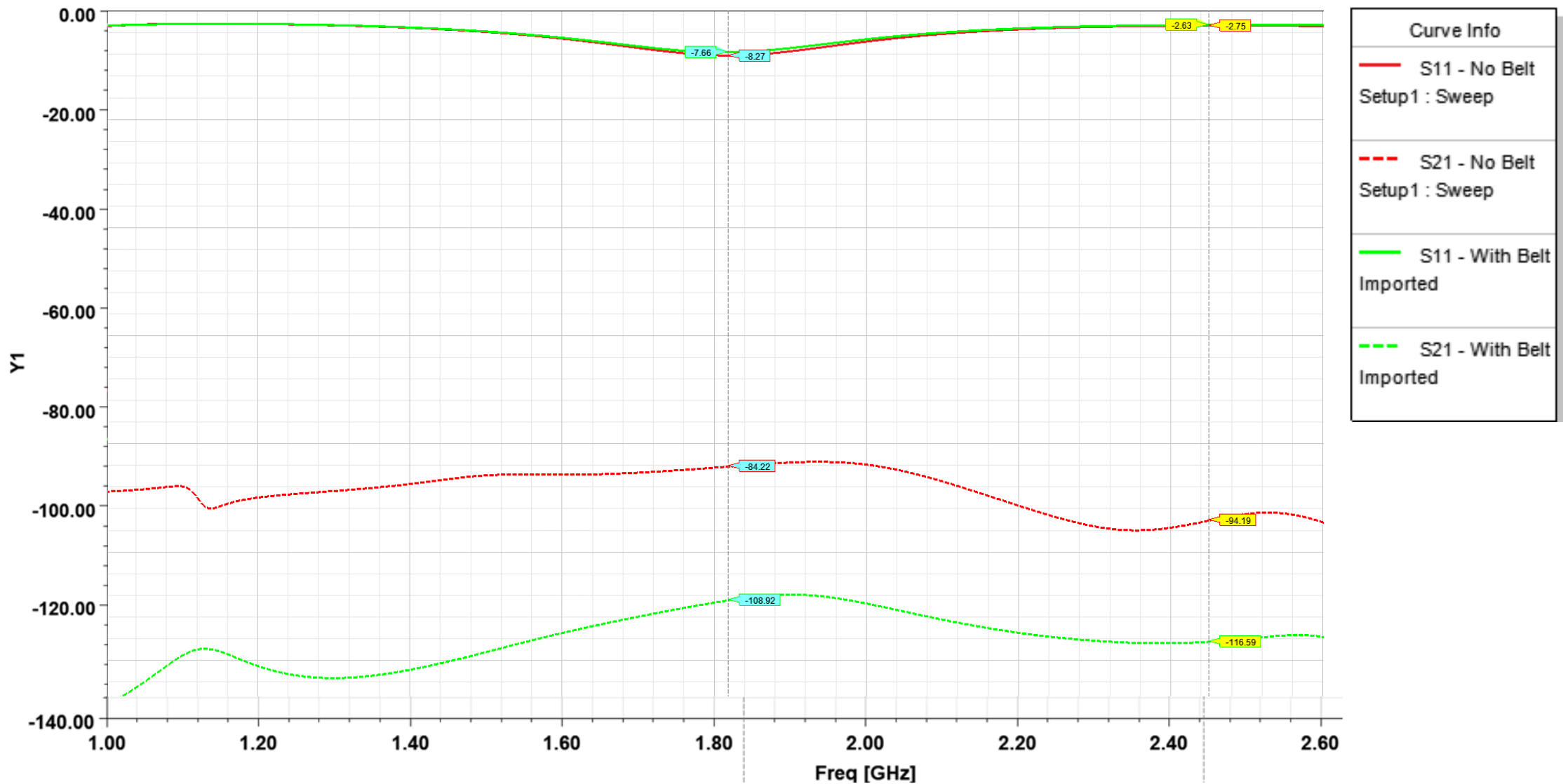
Far Field Gain Pattern



Curve Info	
— (Red)	No Belt
Setup1 : LastAdaptive	
Freq='2.45GHz' Phi='0deg'	
— (Green)	No Belt
Setup1 : LastAdaptive	
Freq='2.45GHz' Phi='90deg'	
- - - (Red)	With Belt
Imported	
Freq='2.45GHz' Phi='0deg'	
- - - (Green)	With Belt
Imported	
Freq='2.45GHz' Phi='90deg'	



S Parameters: Reduced S21 Coupling \propto Increase in SNR



Student Award & IEEE Publication



Reducing Non-Through Body Energy Transfer in Microwave Imaging Systems

Peter Serano¹, Graduate Student Member, IEEE, Johnathan W. Adams², Graduate Student Member, IEEE, Louis Chen, Member, IEEE, Ara Nazarian³, Reinhold Ludwig³, Senior Member, IEEE, and Sergey Makaroff, Senior Member, IEEE

Abstract—On-body antennas for use in microwave imaging (MI) systems can direct energy around the body instead of through the body, thus degrading the overall signal-to-noise ratio (SNR) of the system. This work introduces and quantifies the usage of modern metal-backed RF absorbing foam in conjunction with on-body antennas to dampen energy flowing around the body, using both simulations and experiments. A head imaging system is demonstrated herein but the principle can be applied to any part of the body including the torso or extremities. A computational model was simulated numerically using Ansys HFSS. A physical prototype in the form of a helmet with embedded antennas was built to compare simulations with measured data. Simulations and measurements demonstrate that usage of such metal-backed RF-absorbing foams can significantly reduce around-body coupling from Transmit (Tx) and Receive (Rx) antennas by approximately 10 dB. Thus, the overall SNR of the MI system can be substantially improved using this low-cost and affordable method.

Index Terms—Antennas and propagation, biomedical imaging, electromagnetic propagation in absorbing media, microwave imaging, microwave measurements, numerical simulation, surface waves.

I. INTRODUCTION

MICROWAVE imaging (MI) is a powerful medical diagnostic tool that leverages the changes in internal tissues' dielectric properties due to trauma or illness, to locate and identify the tissue of interest [1]. Its fundamental principle is electromagnetic scattering. A single antenna assembly excites signals toward the tissue's location of interest. If pathology (e.g., a hemorrhage or tumor) is present, the signals can be modulated by the targeted tissue relative to other adjacent normal and healthy tissues. Subsequently the scattered signals are then received by other antenna assemblies at different locations. Through similar RADAR target imaging algorithms, the position

Manuscript received 23 November 2022; revised 29 January 2023; accepted 5 February 2023. Date of publication 7 March 2023; date of current version 31 May 2023. This work was supported by NIH/NIBIB under Grant 5P41EB030006 (PI Bruce Rosen). (Corresponding author: Peter Serano.)

This work involved human subjects or animals in its research. Approval of all ethical and experimental procedures and protocols was granted by WPI IRB-19-0123 on 10/18/2018.

Peter Serano, Johnathan W. Adams, Louis Chen, Reinhold Ludwig, and Sergey Makaroff are with the Worcester Polytechnic Institute, Worcester, MA 01609 USA (e-mail: pserano@wpi.edu; jwadams2@wpi.edu; lgchen@wpi.edu; ludwig@wpi.edu; smakaroff@wpi.edu).

Ara Nazarian is with the Beth Israel Deaconess Medical Center, Harvard Medical School, Boston, MA 02215 USA (e-mail: anazaria@bidmc.harvard.edu).

Digital Object Identifier 10.1109/JERM.2023.3247904

2469-7249 © 2023 IEEE. Personal use is permitted, but republication/redistribution requires IEEE permission. See <https://www.ieee.org/publications/rights/index.html> for more information.

of the targeted tissue may be constructed in a 3D map [2], [3]. In recent years, there have been ongoing developments and innovations in this space to further enhance the accuracy of image captures [4], [5], [6].

One significant issue of concern with MI systems is that the on-body antennas intended to transmit RF energy through the body also inherently transmit energy that flows around the outer surface of the body [7], [8], [9]. This known phenomenon is regularly exploited by designers of on-body RF communication systems [10], [11], [12], [13], [14], [15], [16], [17]. The energy traveling through air and around the surface of the body is considered parasitic in the case of MI systems since it is not modulated by the tissue intended for imaging. Furthermore, the energy which travels outside the body is larger in magnitude and arrives earlier than the energy which travels through the lossy high dielectric human body. Therefore, suppressing transmission of energy that does not flow through the tissue under test is critical to improve the signal-to-noise ratio (SNR) of the detected image in MI systems.

Previous efforts to reduce these so called 'surface waves' have been implemented by special design of the antenna itself, utilizing distributed structures within the substrate [18], [19], [20], electromagnetic band gap (EBG) structures [21], [22], [23], frequency selective surfaces (FSS) [24], [25], [26], and metamaterials [27], [28]. While each of these methods have been shown to reduce surface wave transmission, they are typically limited to a narrow frequency band of operation, require additional care in the design of the antenna, and result in a design with either an increase in physical size, design complexity, and/or cost to manufacture. Another method is use of a liquid-filled bolus between the antenna and body [29], [30], [31]. In this case, there is no air-to-tissue interface for the surface wave to propagate. While this technique offers the additional advantage of wideband antenna impedance matching, it requires the tissue under test to either be fully submerged in a liquid, or a sealed housing to contain the liquid must be factored into the antenna design, again increasing the size, complexity, and cost of the MI system.

This work is the first to propose the novel use of commercially available RF absorbing foams [33], [33] to attenuate energy traveling outside and around the tissue under test in MI systems. The proposed method can be implemented with any MI system utilizing on-body antennas by simply surrounding the tissue volume under test with a layer of RF absorbing foam (with foam

WPI MQP Student Mentoring

Fall Semester '23

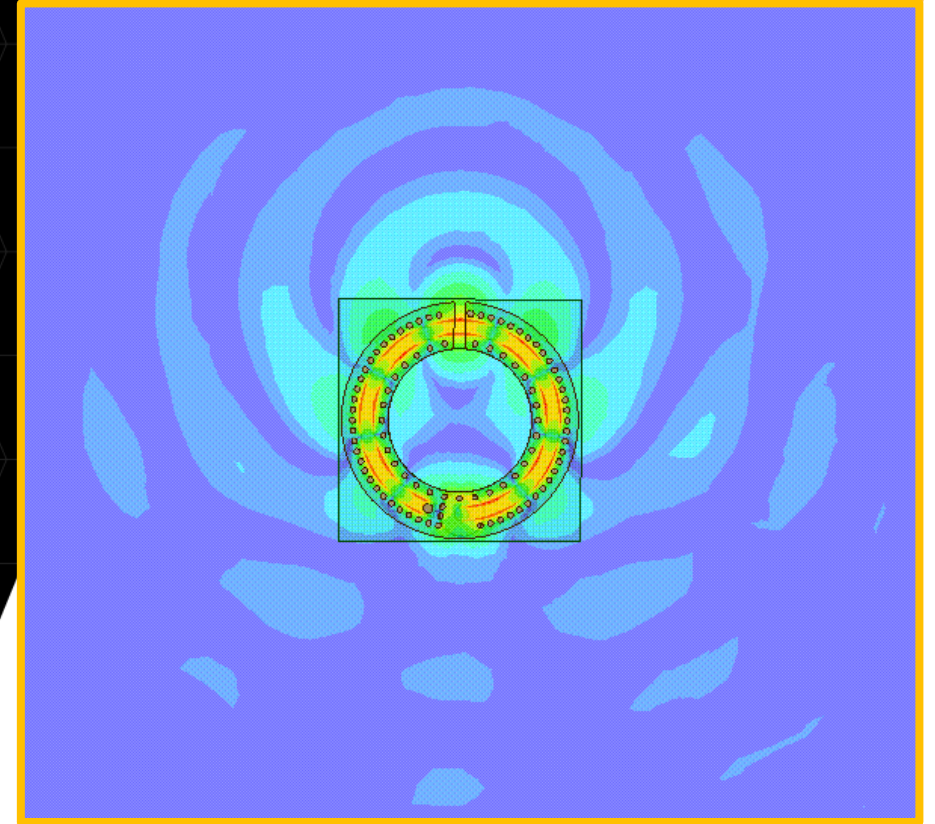
Ph.D. Dissertation Defense
Electrical & Computer Engineering

Peter Serano

PhD Candidate, WPI ECE

Lead Application Engineer, Ansys Inc.

12/14/23

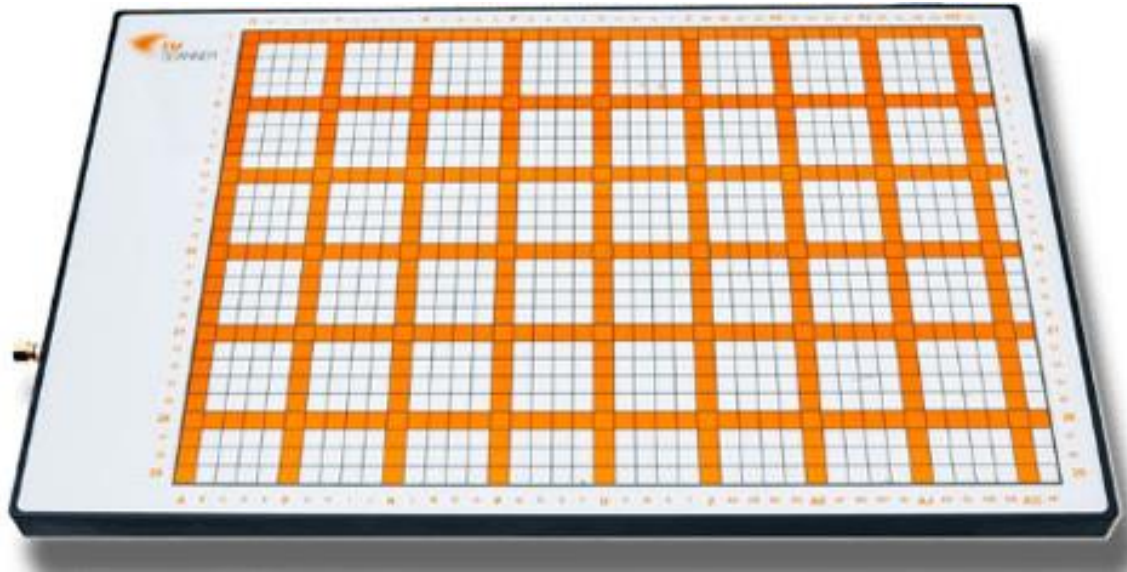


WPI

Ansys

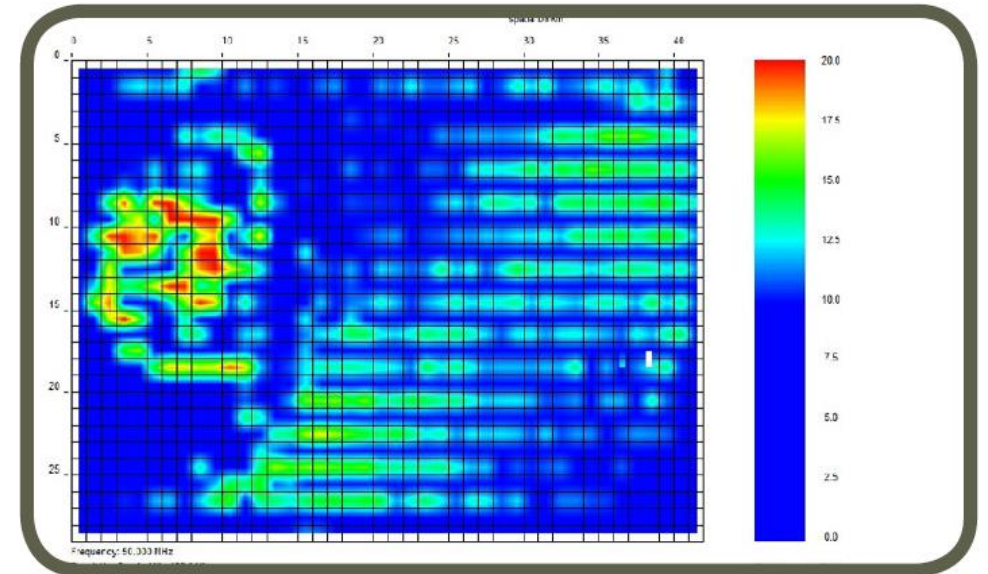
WPI MQP Student Project: Design of an EMI Scanner

- Array of H-Field Loop Probes
- Digitally Multiplexed via Software



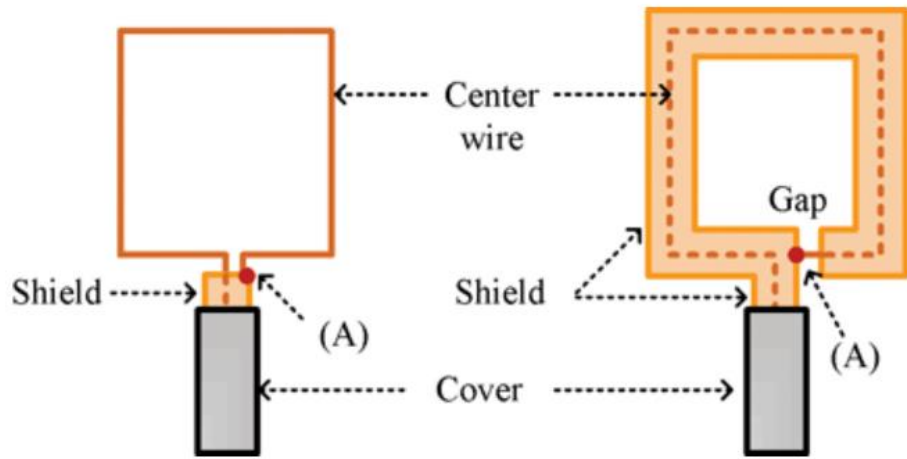
Commercial EMI Scanner: “EMSCAN ERX EMC Scanner”

<https://www.emcfastpass.com/test-equipment/shop/near-field-scanners/near-field-scanner-emxpert-ehx/>



Magnetic Field (H-Field) Loop Probe

Encourage Students to Build DIY Probe:



Square loop from a coax cable unshielded (left) and shielded (right)

“SHIELDED VS. UNSHIELDED SQUARE MAGNETIC FIELD LOOPS FOR EMI/ESD DESIGN AND TROUBLESHOOTING”:

<https://incompliancemag.com/article/shielded-vs-unshielded-square-magnetic-field-loops-for-emiesd-design-and-troubleshooting/>



“A DIY Magnetic Field Probe”:

<https://www.changpuak.ch/electronics/MagneticFieldProbe.php>



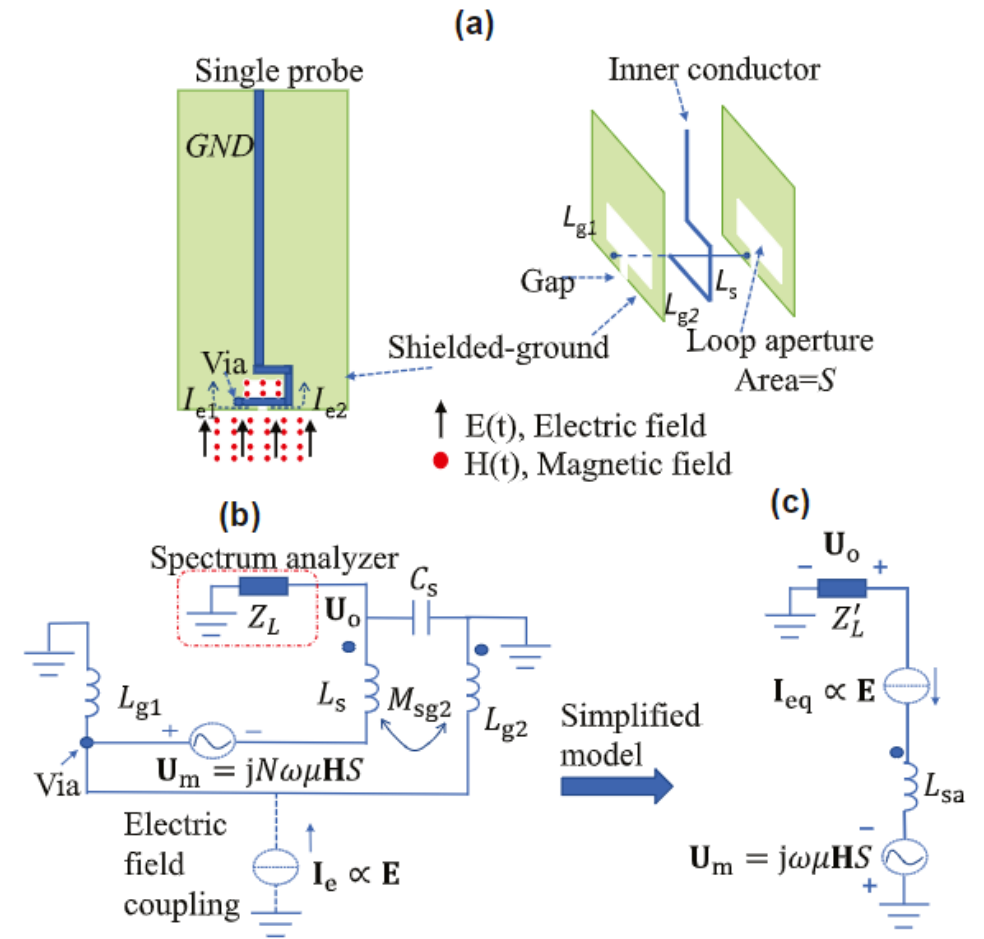
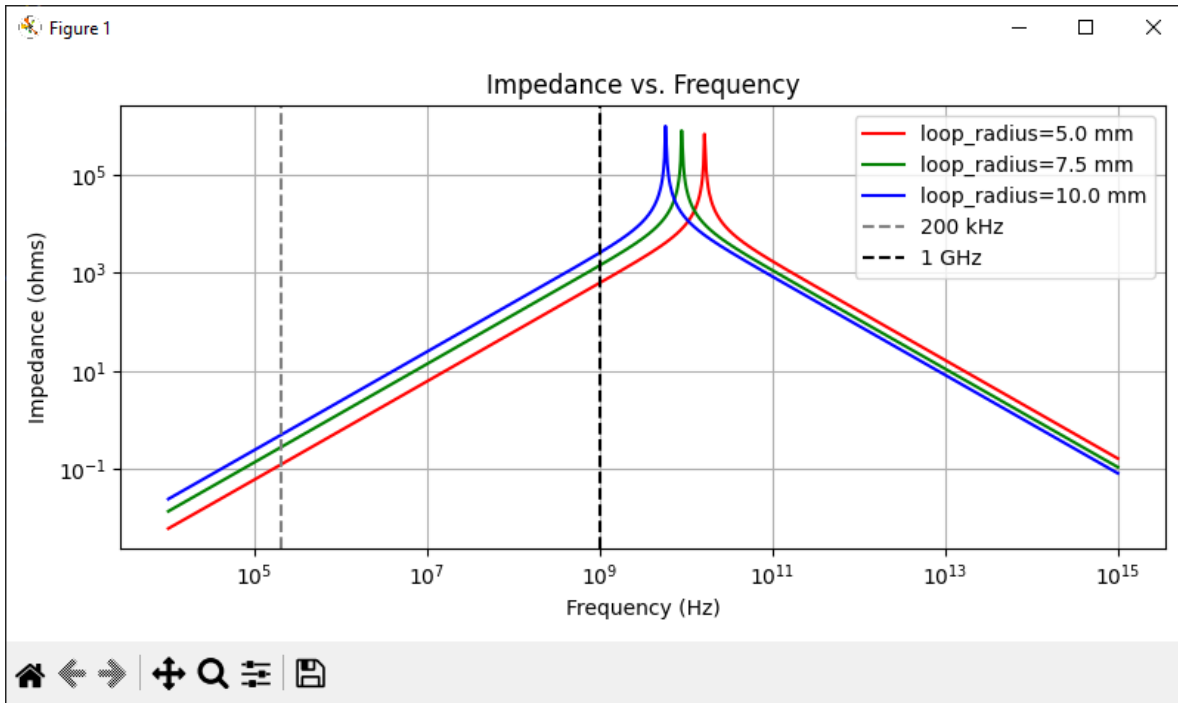
“EEVblog #1178 - Build a \$10 DIY EMC Probe”:

https://www.youtube.com/watch?v=2xy3Hm1_ZqI

Initial Simulation: Lumped Circuit Model

Introduce Students to Python Scripting & Review Lumped vs. Distributed Circuit Theory:

Plot Made Students with NumPy + Matplotlib:

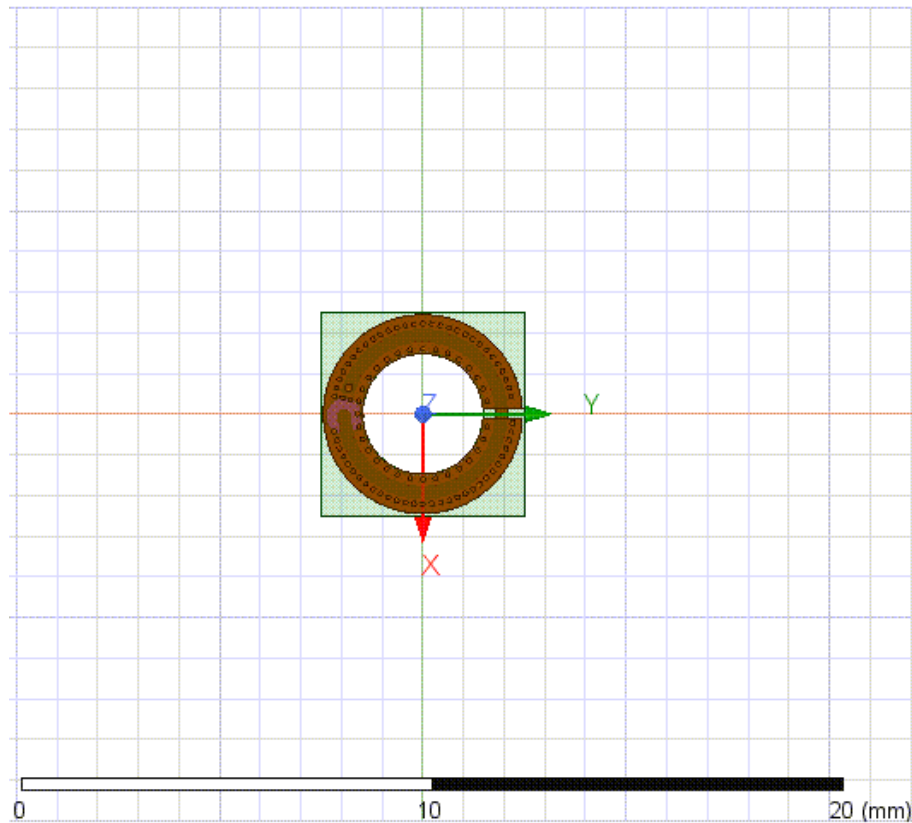


A popular single-shielded-loop magnetic field probe (a), its circuit mode (b) and simplified mode (c)

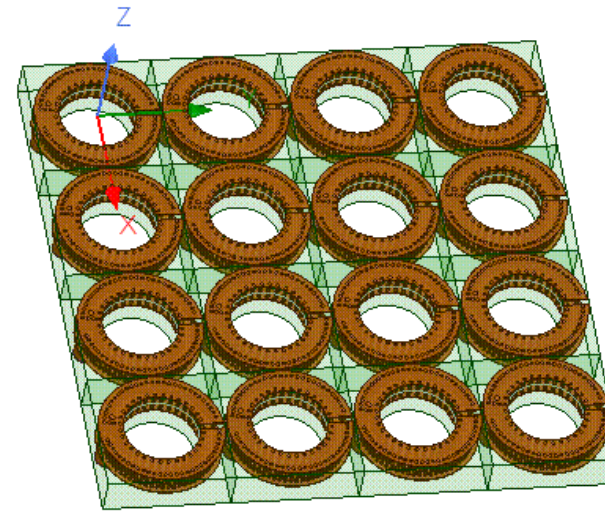
Liu, J., Xiao, M., He, X., Fang, W., Shao, W., Huang, Q., Lu, G., Wang, L., Huang, Y., En, Y. and Yao, R. (2021), Symmetrical double-loop H-field probe with floating shield for improving sensitivity and electric field suppression. IET Microw. Antennas Propag, 15: 464-473. <https://doi.org/10.1049/mia2.12050>

Single Shielded Loop Probe + Array: Implemented on FR-4 Substrate

Introduce Students to Creation of Parameterized CAD & Full-Wave FEM Modeling with Ansys HFSS



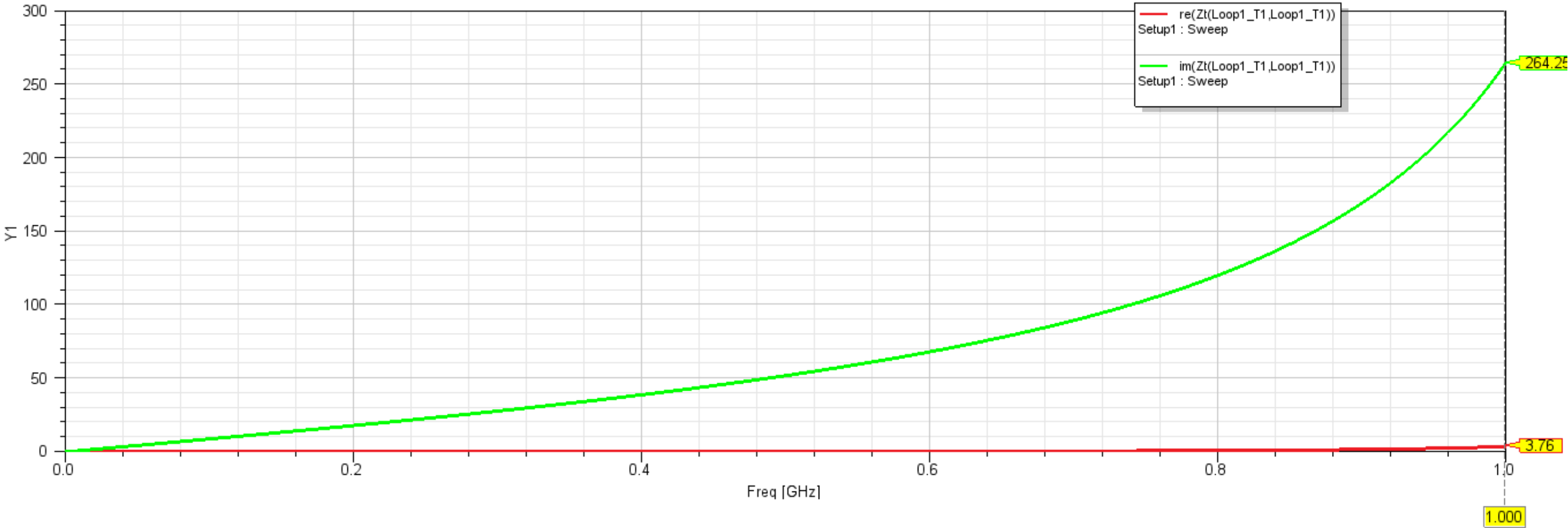
loop_size = 10mm



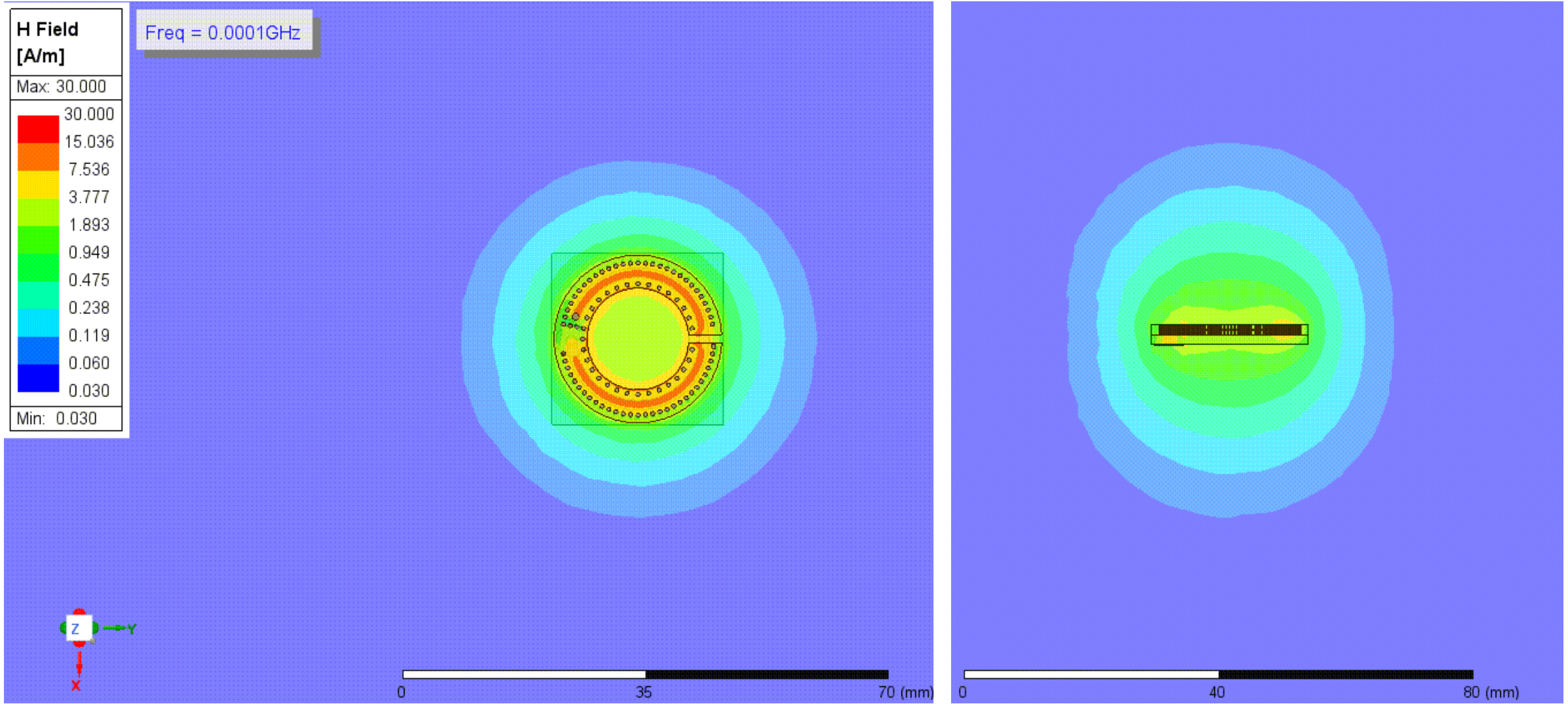
Example Simulation Output: Loop Probe Input Impedance (Z_{11})

Terminal Z Parameter Plot 1

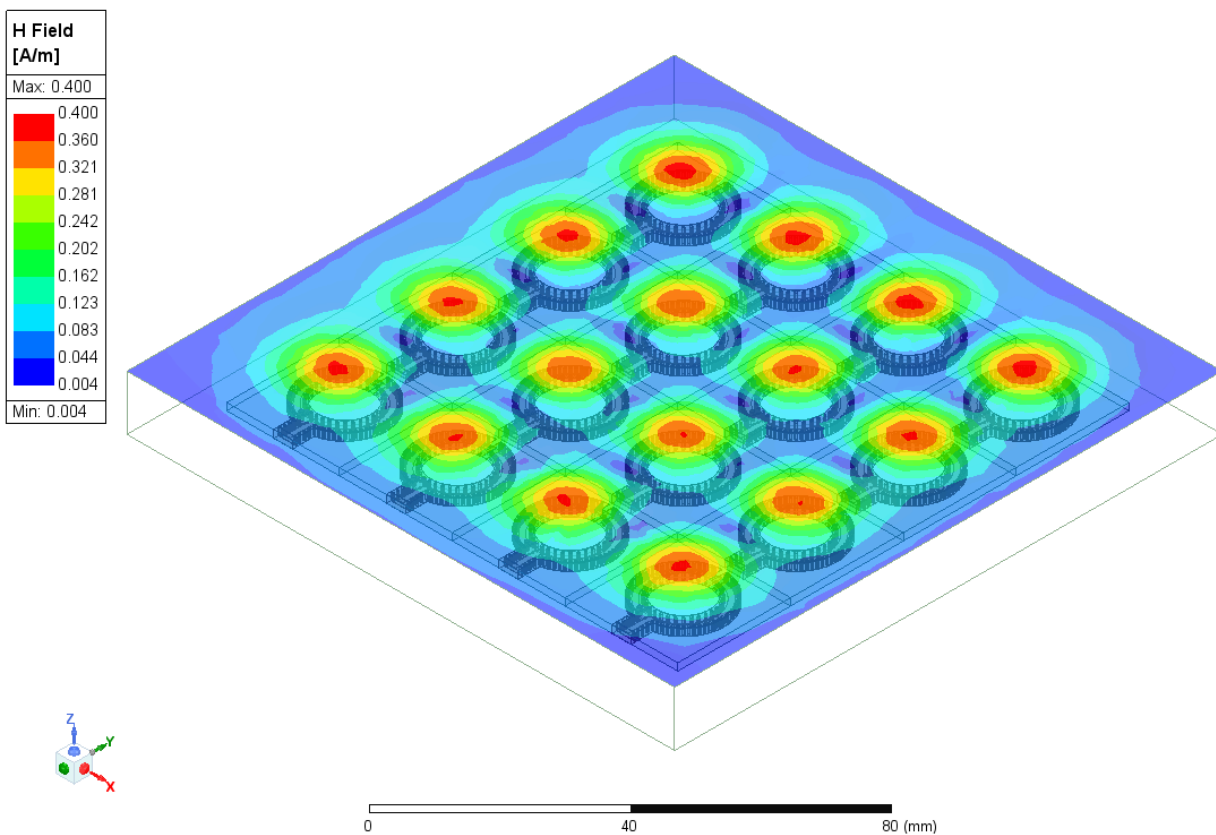
HFSSDesign1
Ansys
2023 R1.1



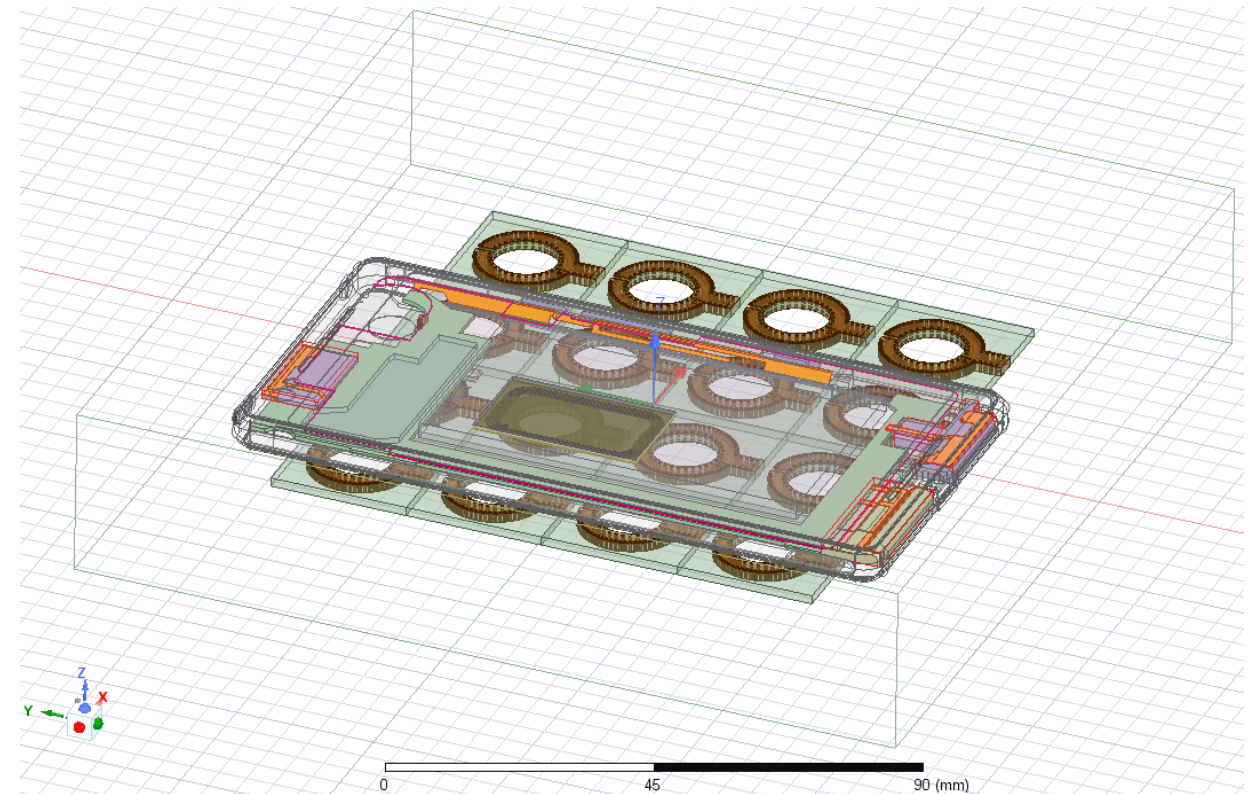
Animation: H-Field Magnitude vs. Input Excitation Frequency



4x4 Array of Loop Probes: Evaluate Loop-to-Loop Coupling

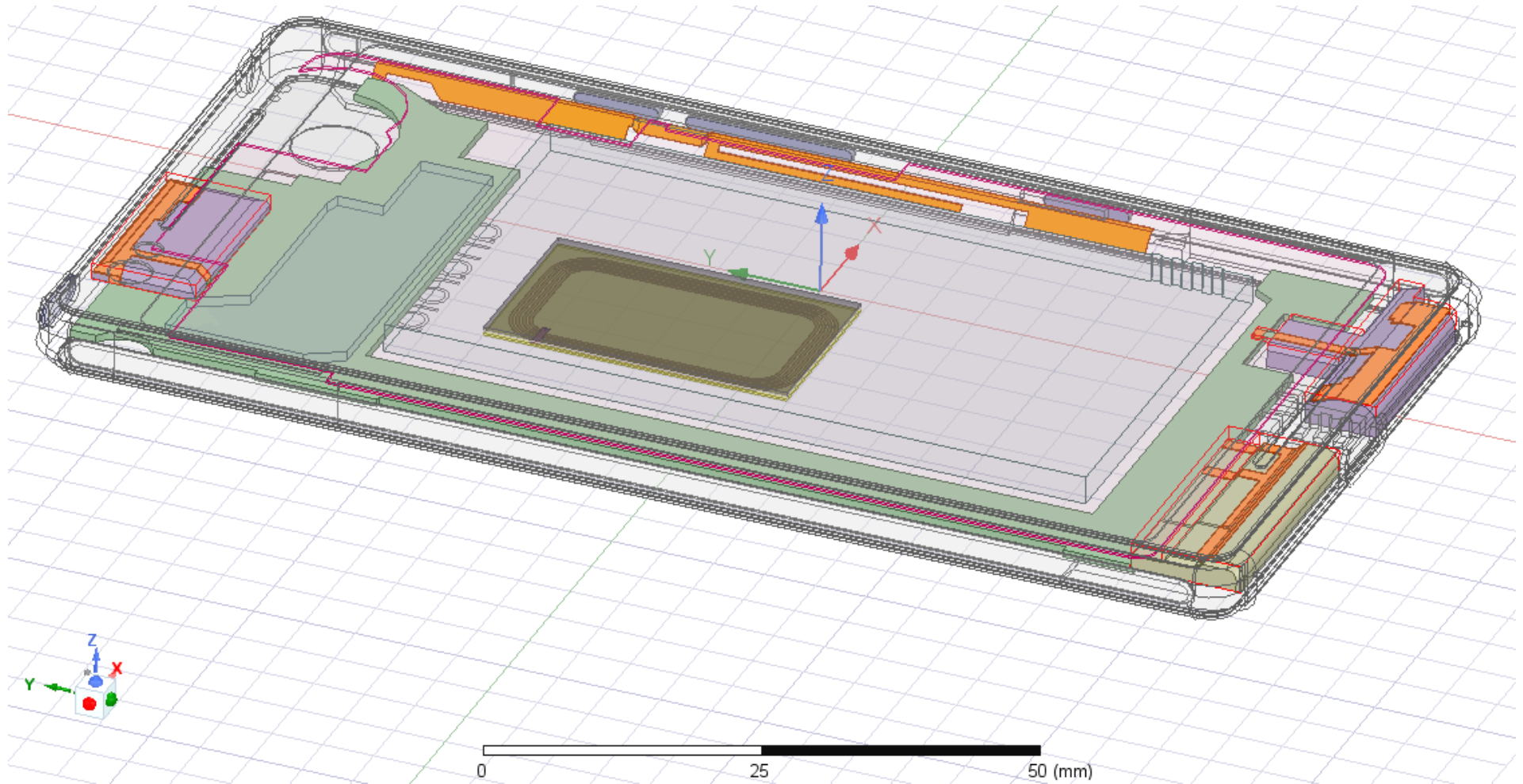


- H-Field Magnitude on XY Plane, 5mm Above Array
 - Evaluate Field Homogeneity

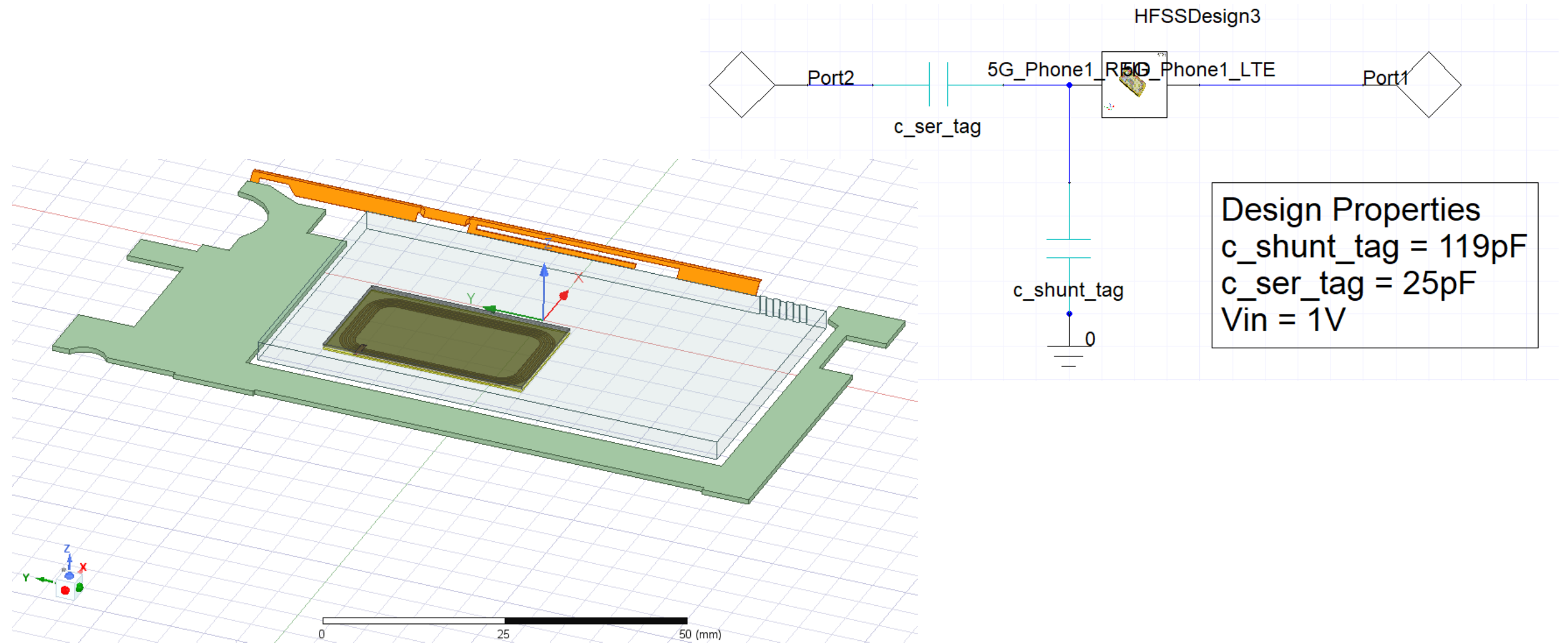


- Add External RF Excitation from Smartphone Antennas
 - Evaluate Phone-to-Array S-Parameter Coupling

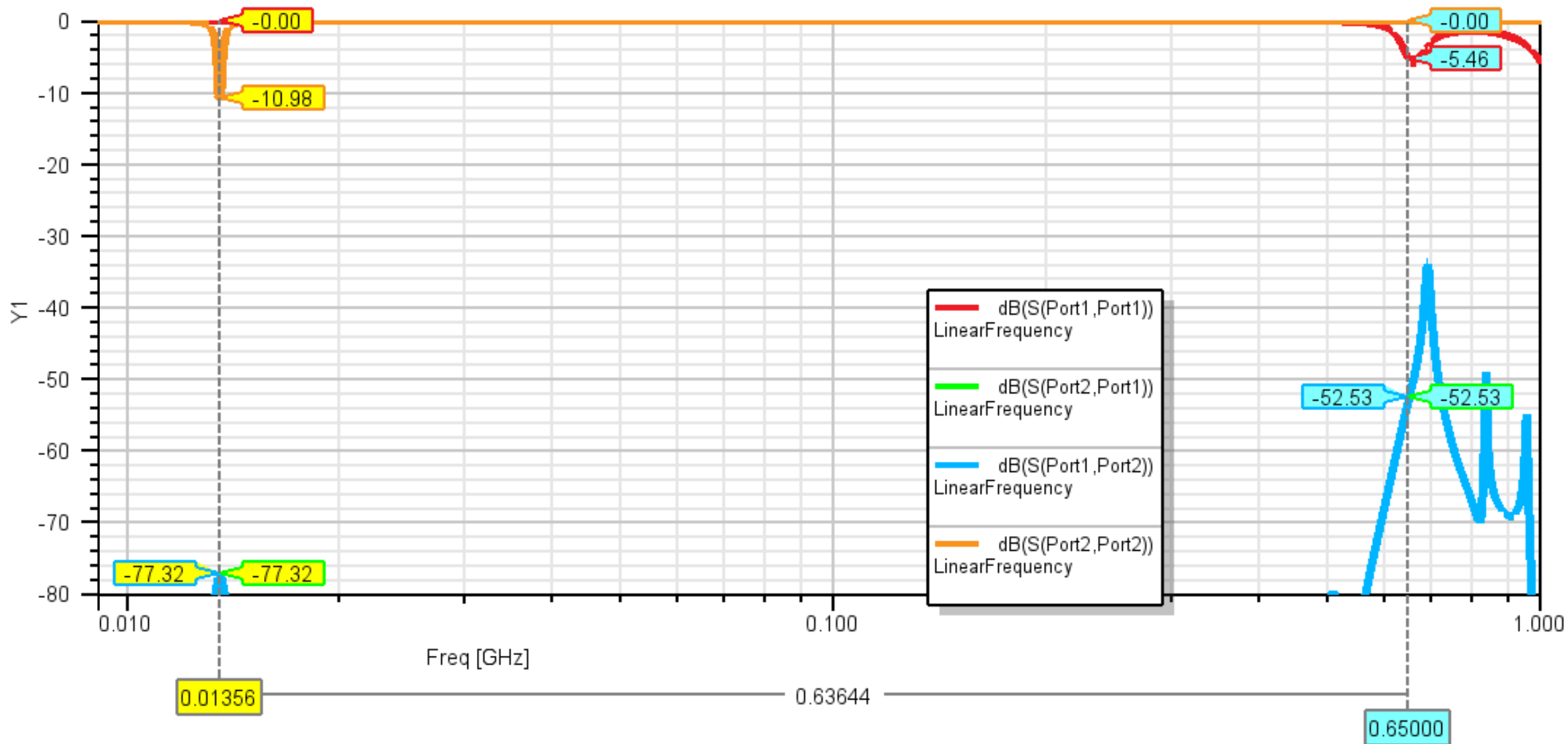
Generic Android Cell Phone w/ LTE Antenna (Provided by Ansys) & NFC Coil (Added by Students)



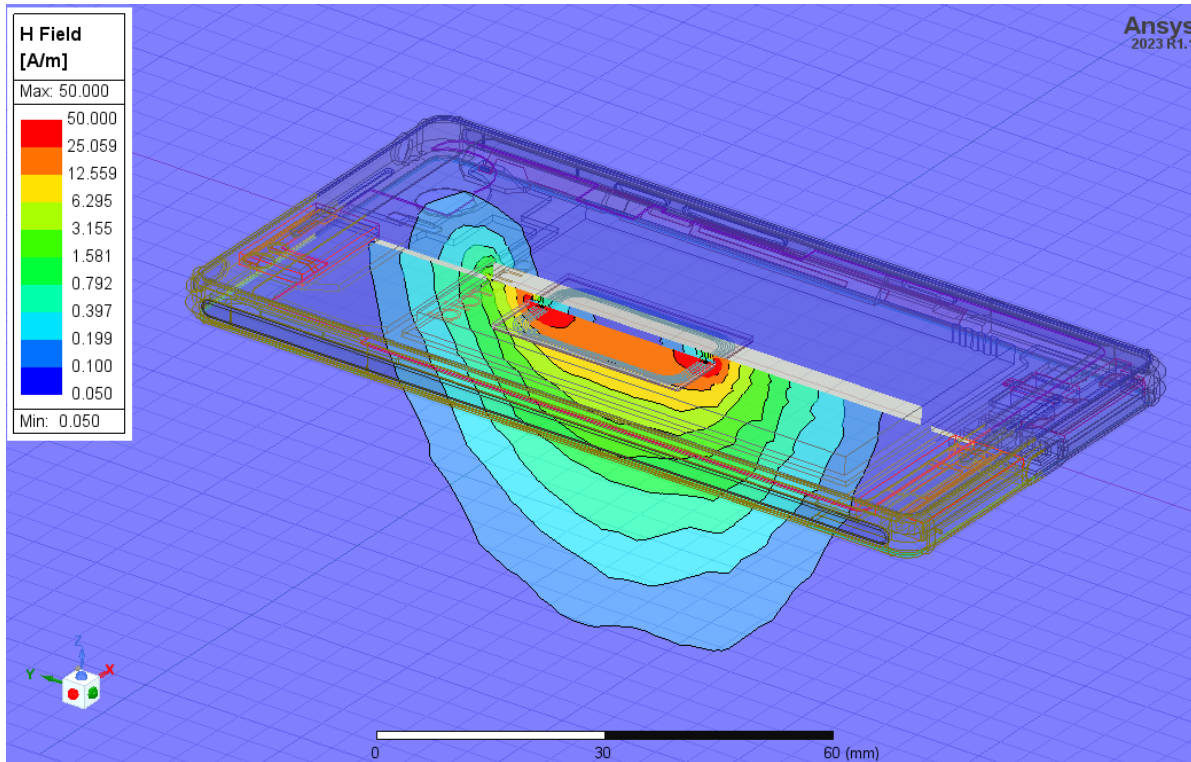
FEM + Circuit Co-Simulation for NFC Coil Matching Network



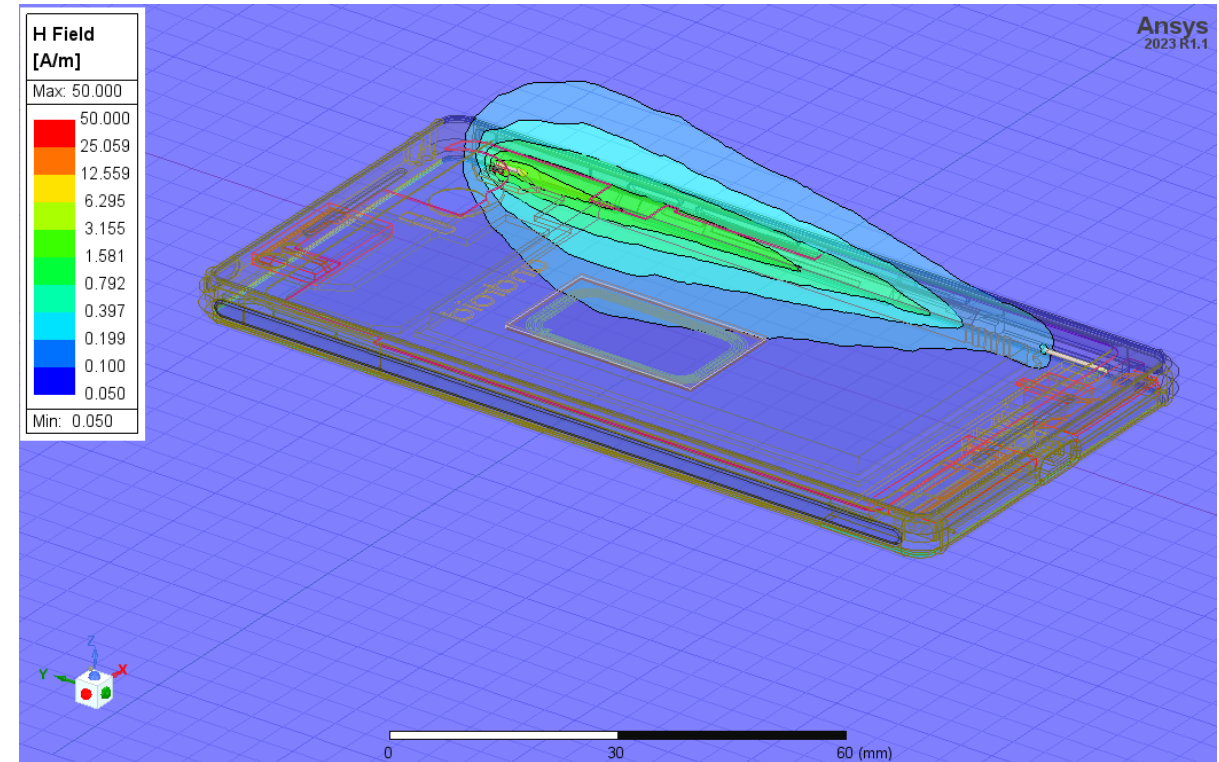
S-Parameters: Phone Antennas in Free Space



H-Field Magnitude Plot Through Cross-Section of Phone

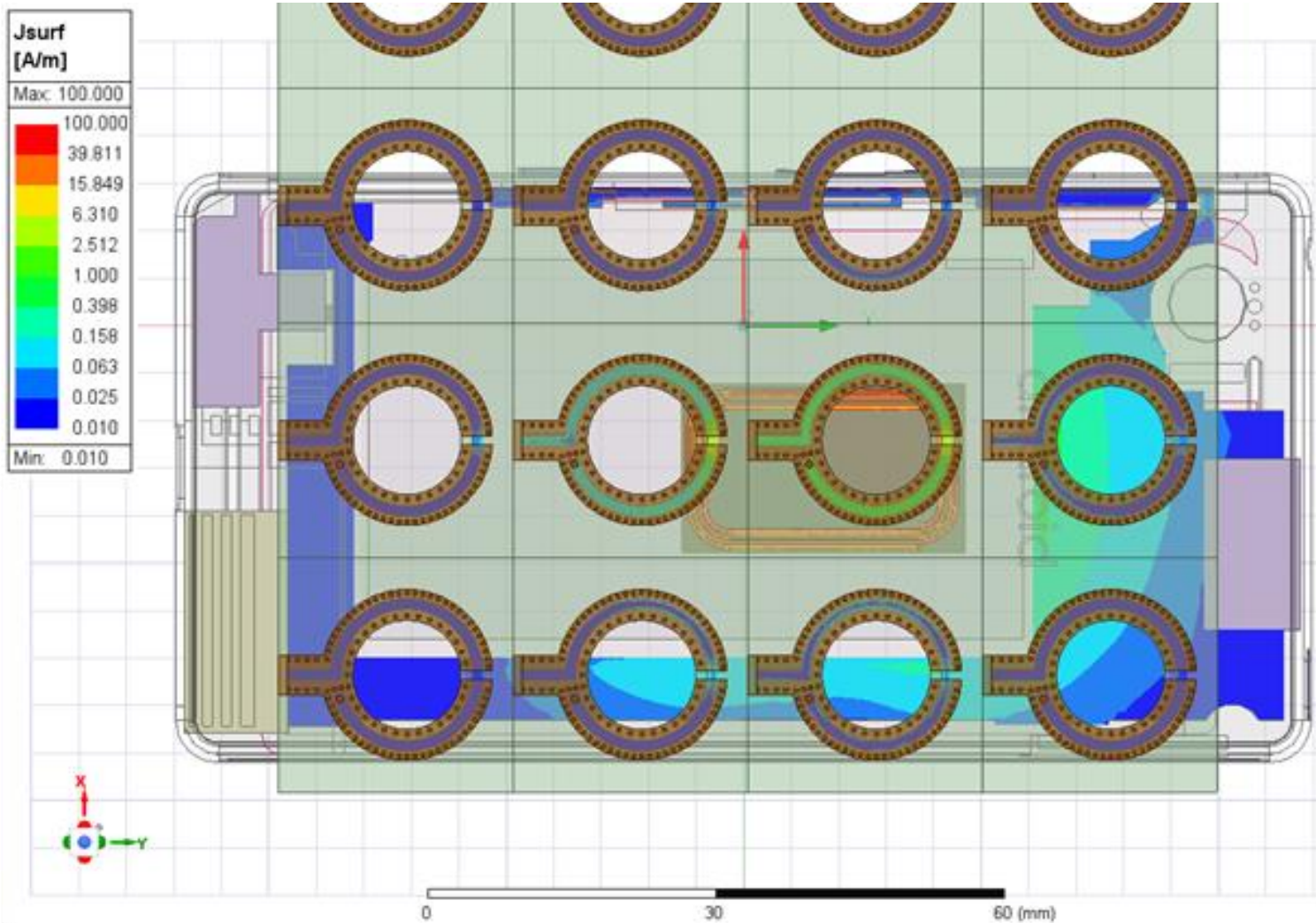


NFC Coil Excited @ 13.56 MHz

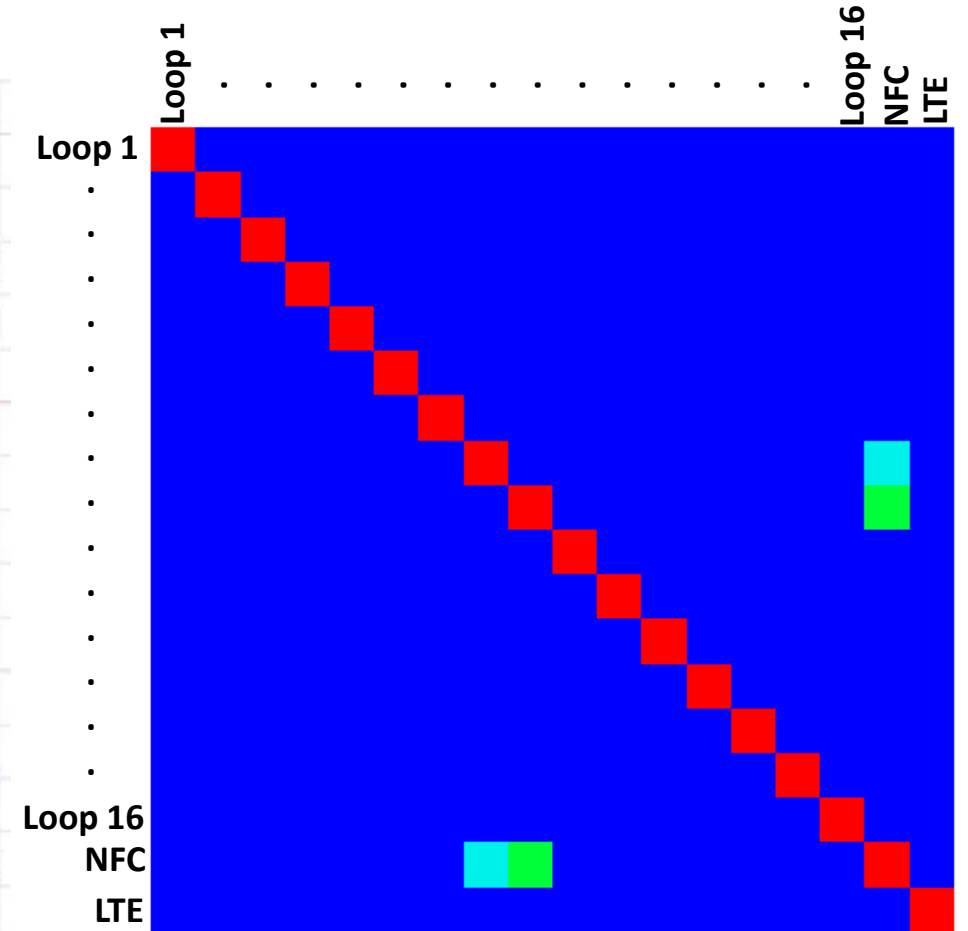


LTE Antenna Excited @ 650 MHz

NFC Coil Excited (13.56 MHz):



Normalized S-Parameter Coupling Magnitude



Proposed Syllabus for New Senior-Level Undergraduate Course: ECE 4114 – ‘Introduction to Computational Electromagnetics’

Week 1: Review of Vector Fields, Vector Calculus Notation, and Maxwell’s Equations

Lab: Introduction to Python Scripting and the PyAEDT Python module

Week 2: Review of Lumped vs. Distributed Models of Electromagnetic Phenomena

Lab: Designing a Capacitive Touch Sensor with Lumped RLGC Parameter Solver Ansys Q3D

Week 3: Numerical Computation Methods Part 1: Electrostatics, Magnetostatics, and Quasi-Static Solutions for Electrically Small Problems

Lab: Designing an Electric Guitar Pickup with Magnetostatic & Quasistatic EM Solver Ansys Maxwell / Near-Field Visualization Techniques

Week 4: Numerical Computation Methods Part 2: Full-Wave Solutions – FEM, MoM, and FDTD

Lab: Designing a Highly Directional Wi-Fi Antenna with Full-Wave FEM Solver Ansys HFSS / Far-Field Visualization Techniques

Week 5: Numerical Computation Methods Part 3: Asymptotic Solutions for Electrically Large Problems

Lab: Optimizing Wi-Fi Signal Propagation in a Home with Asymptotic EM Solver Ansys SBR+ / Ray-Tracing Visualization Techniques

Week 6: RF System Design and Co-Simulation of Models with Lumped Components & Distributed Structures

Lab: Designing a Matching Network for an Electrically Small Bluetooth Antenna with Ansys Circuit + HFSS

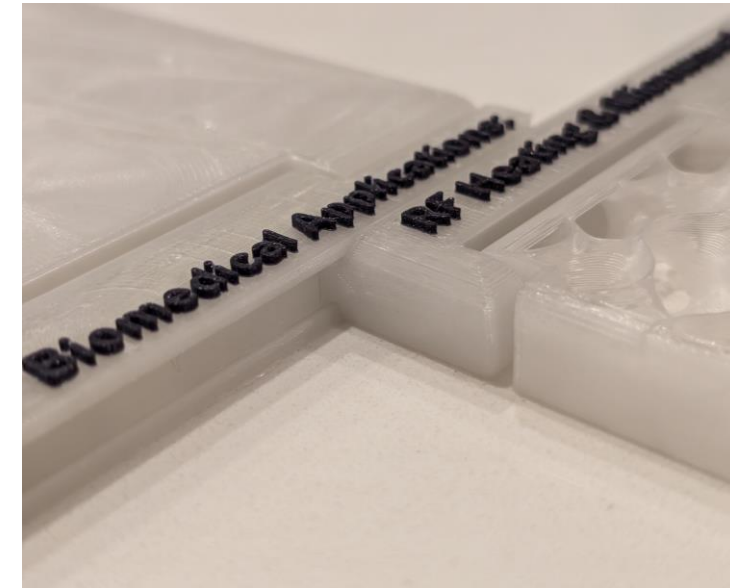
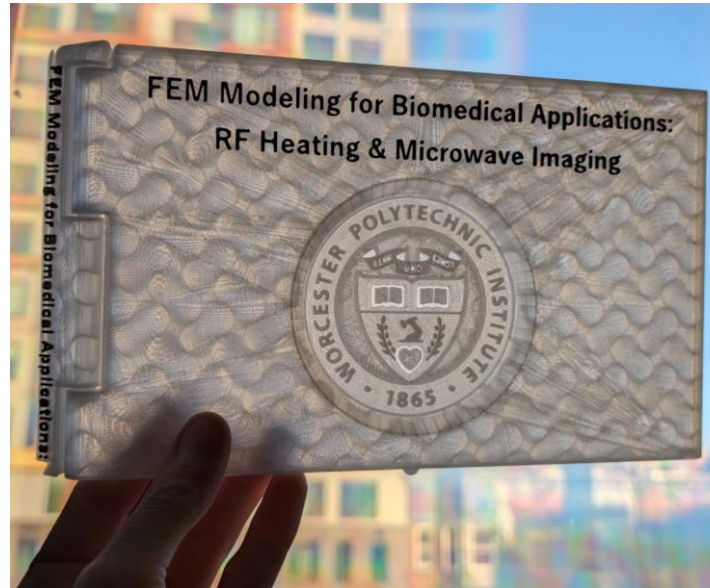
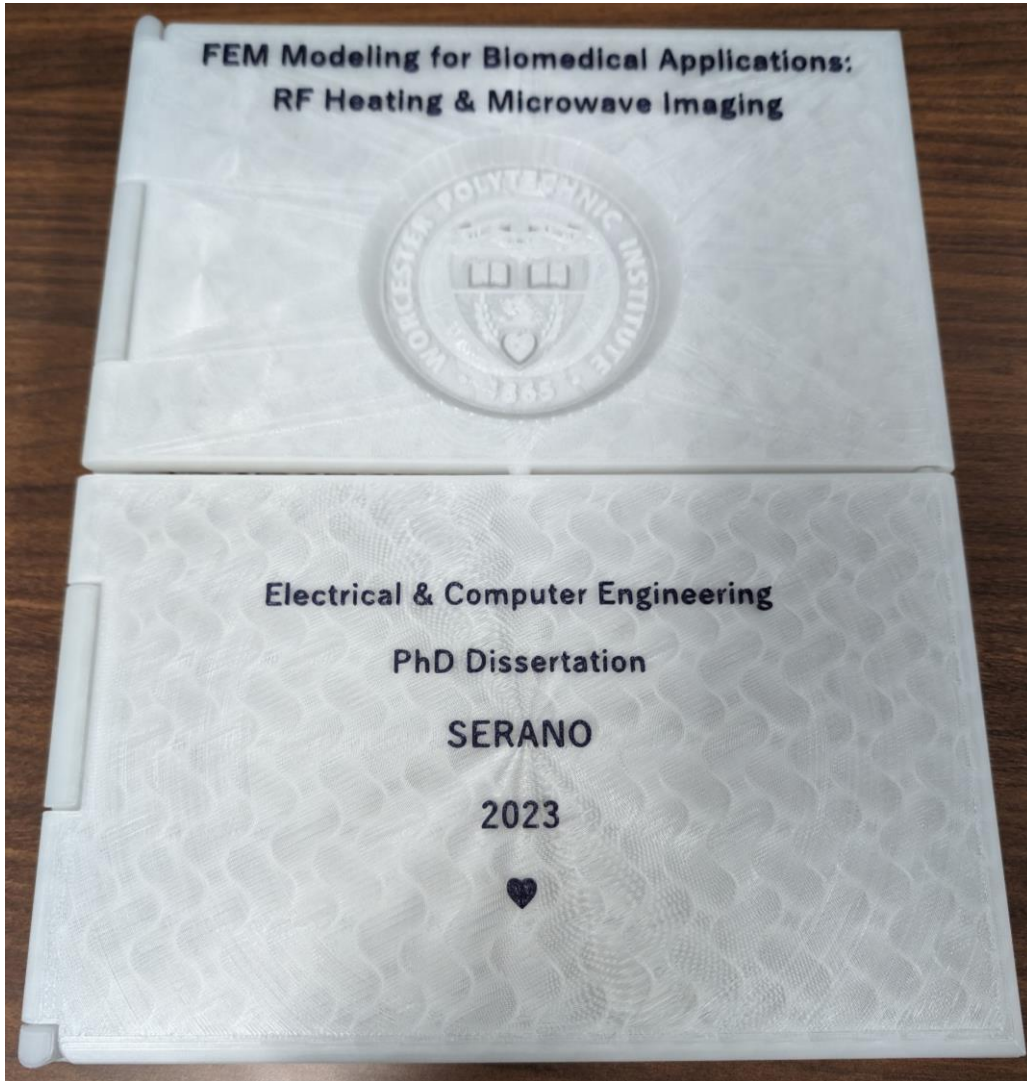
Week 7: Finals Week – Student Project (In Lieu of Final Written Exam)

Students to work in small teams on a computational EM modeling/design project of their own interest.

Extra Credit: Build the device modeled in your simulation and compare to measurements taken with a VNA or other relevant measurement device.

Student Art Competition: Along with their final project, students will submit their favorite animated GIF that demonstrates the power of visualizing EM fields!

3D Printed Lithophane Hardcover for Dissertation Document



- Initial Book Cover CAD w/ Print-in-Place Hinges:
 - <https://www.printables.com/model/10776-book-cover>
- CAD Modified in Ansys HFSS
 - Enlarged for 8.5 x 11" Document
 - Added WPI Seal (PNG > DXF)
 - Split into 4x Pieces w/ Connecting Dovetail Joints
 - Printed with UV-Activated Glow-in-the-Dark PLA

Animation Flip Book Appendix:

Appendix B: Cut-Out Animation Flip Book

The following section may be cut out of this document to create an animation 'flip book'.

These animations were generated as part of the research for:

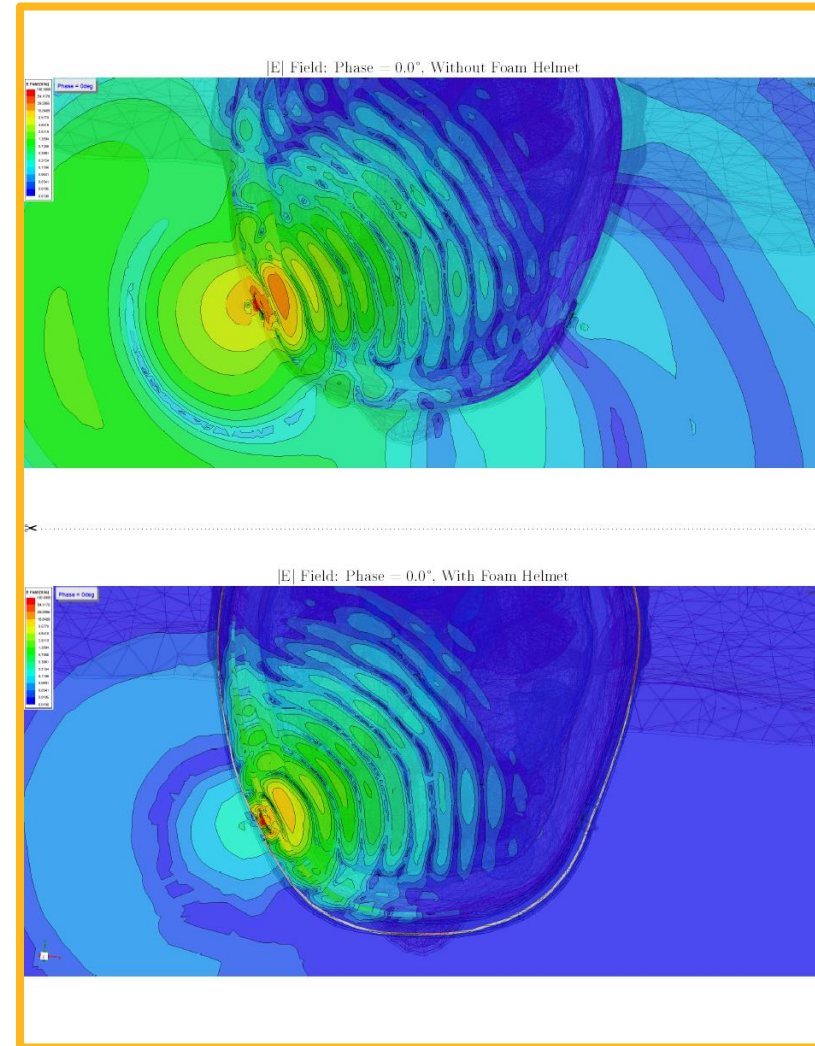
Serano P, Adams JW, Chen L, Nazarian A, Ludwig R, Makaroff SN, Reducing Non-Through Body Energy Transfer in Microwave Imaging Systems. *IEEE Journal of Electromagnetics, RF and Microwaves in Medicine and Biology*, vol. 7, no. 2, pp. 187-192, June 2023, doi: 10.1109/JERM.2023.3247904

Each animation shows the magnitude of the electric field plot through a cross-section of the head and animated vs. the phase of the input excitation:

Upper Animation: Without Foam Helmet

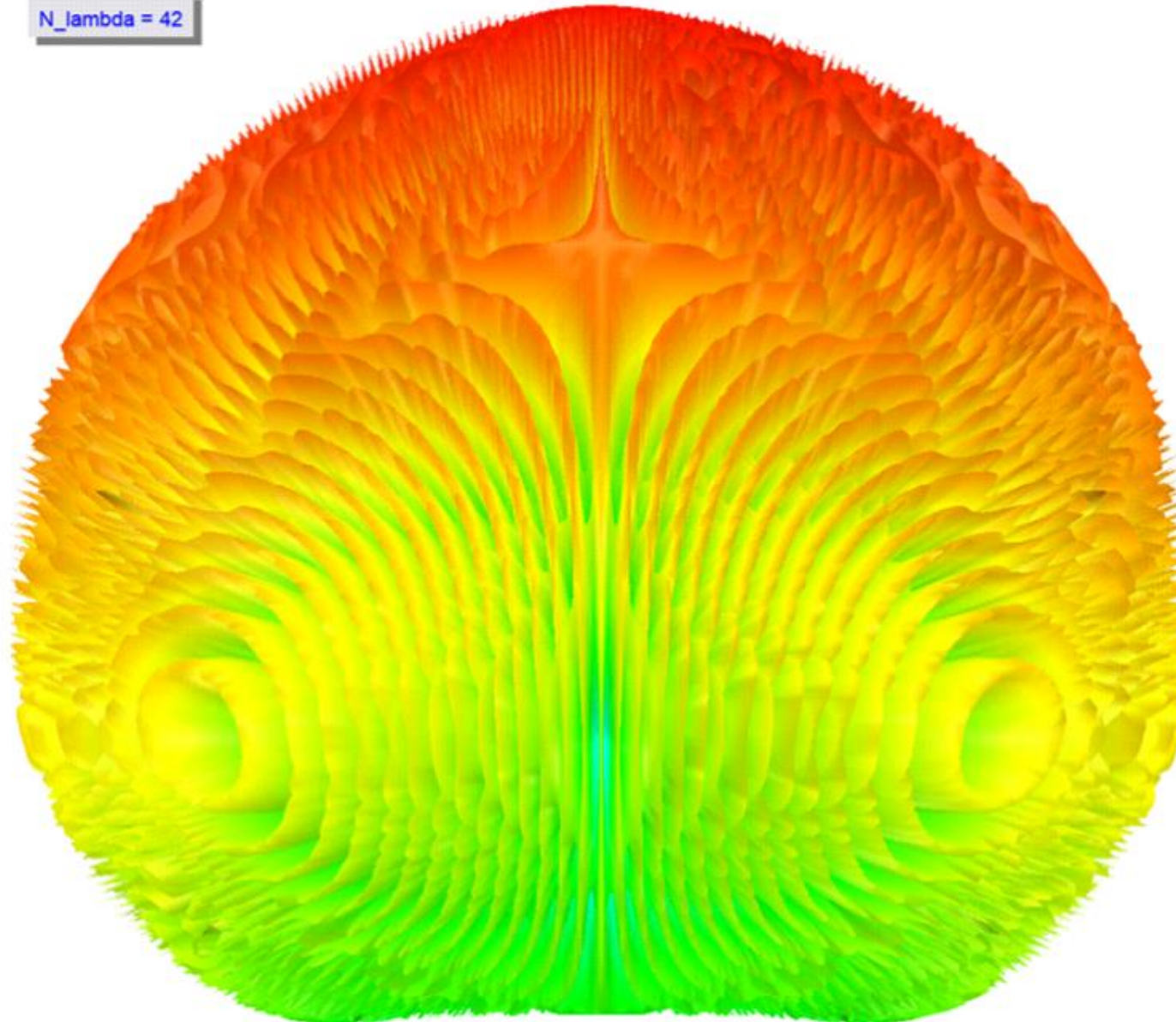
✕

Lower Animation: With Foam Helmet



Thank You!

$N_{\lambda} = 42$



Animation: Combined Far-Field Pattern of Two Antennas vs. Antenna Spacing; Made w/ Ansys HFSS SBR+

Full List of Presenter's Publications: Journal Articles

- [1] **Serano P**, Makaroff SN, Ackerman JL, Nummenmaa AR, Noetscher G. Detailed High-Quality Surface-Based Mouse CAD Model Suitable for Electromagnetic Simulations. *Biomed Phys Eng Express*. 2023 Nov 20. doi: 10.1088/2057-1976/ad0e14. Epub ahead of print. PMID: 37983756.
- [2] Yao J, Kaso A, **Serano P**, Ackerman JL, A Single-Solenoid Double-Resonance Radiofrequency Coil for 1H and 31P Solid State MRI at 1.5 T. - Under Review at *Journal of Medical & Radiation Oncology*, 2023
- [3] Noetscher GM, **Serano P**, Horner M, Prokop A, Hanson J, Fujimoto K, Brown JE, Nazarian A, Ackerman J, Makaroff SN. An In-Silico Testbed for Fast and Accurate MR Labeling of Orthopaedic Implants. *eLife* 2023 Jul 18:2023.07.16.549234. doi: 10.1101/2023.07.16.549234. PMID: 37649909; PMCID: PMC10465017
- [4] **Serano P**, Adams JW, Chen L, Nazarian A, Ludwig R, Makaroff SN, Reducing Non-Through Body Energy Transfer in Microwave Imaging Systems. *IEEE Journal of Electromagnetics, RF and Microwaves in Medicine and Biology*, vol. 7, no. 2, pp. 187-192, June 2023, doi: 10.1109/JERM.2023.3247904
- [5] Adams JW, Chen L, **Serano P**, Nazarian A, Ludwig R, Makaroff SN, Miniaturized Dual Antiphase Patch Antenna Radiating into the Human Body at 2.4 GHz. *IEEE Journal of Electromagnetics, RF and Microwaves in Medicine and Biology*, vol. 7, no. 2, pp. 182-186, June 2023, doi: 10.1109/JERM.2023.3247959
- [6] Noetscher GM, **Serano P**, Wartman WA, Fujimoto K, Makarov SN. Visible Human Project female surface based computational phantom (Nelly) for radio-frequency safety evaluation in MRI coils. *PLoS One*. 2021 Dec 10;16(12):e0260922. doi: 10.1371/journal.pone.0260922. PMID: 34890429; PMCID: PMC8664205
- [7] Bonmassar G, **Serano P**. MRI-Induced Heating of Coils for Microscopic Magnetic Stimulation at 1.5 Tesla: An Initial Study *Frontiers in Human Neuroscience*, 2020 Mar 13;14:53. doi: 10.3389/fnhum.2020.00053. PMID: 32231526; PMCID: PMC7082860
- [8] Golestanirad L, Rahsepar AA, Kirsch JE, Suwa K, Collins JC, Angelone LM, Keil B, Passman RS, Bonmassar G, **Serano P**, Krenz P, DeLap J, Carr JC, Wald LL. Changes in the specific absorption rate (SAR) of radiofrequency energy in patients with retained cardiac leads during MRI at 1.5T and 3T. *Magn Reson Med*. 2019 Jan;81(1):653-669. doi: 10.1002/mrm.27350. Epub 2018 Jun 12. PMID: 29893997; PMCID: PMC6258273.
- [9] Martinez JA, **Serano P**, Ennis DB. Patient Orientation Affects Lead-Tip Heating of Cardiac Active Implantable Medical Devices During MRI Radiology: *Cardiothoracic Imaging*, 2019 Aug 29;1(3):e190006. doi: 10.1148/ryct.2019190006. PMID: 32076667; PMCID: PMC6735361

Full List of Presenter's Publications: Journal Articles

- [10] Atefi SR, **Serano P**, Poulsen C, Angelone LM, Bonmassar G. Numerical and Experimental Analysis of RF Induced Heating vs. Lead Conductivity During EEG-MRI at 3T IEEE Transactions on Electromagnetic Compatibility, 2018, Jun; 61(3):852-859. doi: 10.1109/TEMC.2018.2840050. Epub 2018 Jun 25. PMID: 31210669; PMCID: PMC6579539
- [11] Guérin B, **Serano P**, Iacono MI, Herrington, TM, Dougherty, DD. Realistic Modeling of Deep Brain Stimulation Implants for Electromagnetic MRI Safety Studies Physics in Medicine & Biology, 2018 May 4; 63(9):095015. doi: 10.1088/1361-6560/aabd50. PMID: 29637905; PMCID: PMC5935557
- [12] **Serano P**, Angelone LM, Katnani H, Eskandar E, Bonmassar G. A Novel Brain Stimulation Technology Provides Compatibility with MRI. **Scientific Reports**, 2015 Apr 29; 5:9805. doi: 10.1038/srep09805. PMID: 25924189; PMCID: PMC4413880
- [13] Guérin B, Gebhardt M, **Serano P**, Adalsteinsson E, Hamm M, Pfeuer J, Nistler J, Wald LL. Comparison of simulated parallel transmit body arrays at 3T using excitation uniformity, global SAR, local SAR, and power efficiency metrics. Magnetic Resonance in Medicine, 2014.
- [14] Janssens T, Keil B, **Serano P**, Mareyam A, McNab JA, Wald LL, Vanduffel, W. A 22-channel receive array with Helmholtz transmit coil for anesthetized macaque MRI at 3T. NMR in Biomedicine, 2013.
- [15] Zhao W, Cohen-Adad J, Polimeni J, Keil, B, Guérin B, Setsompop K, **Serano P**, Mareyam A, Hoecht P, Wald L.L. 19-channel Rx array coil and 4-channel Tx loop array for cervical spinal cord imaging at 7T MRI. Magnetic Resonance in Medicine, 2013.
- [16] Poser BA, Anderson RJ, Guérin B, Setsompop K, Deng W, Mareyam A, **Serano P**, Wald LL, Stenger VA. Simultaneous Multislice Excitation by Parallel Transmission. Magnetic Resonance in Medicine, 2013.

/ Full List of Presenter's Publications: Book Chapters

[1] Adams J, **Serano P**, Nazarian A. (2021). Modeling and Experimental Results for Microwave Imaging of a Hip with Emphasis on the Femoral Neck. In Brain and Human Body Modelling 2021. Makarov S, Noetscher G, & Nummenmaa A (eds) Springer, Cham. https://doi.org/10.1007/978-3-031-15451-5_10

[2] Rajan S, **Serano P**, Guag J, Zaidi T, Fujimoto K, Iacono MI and Angelone LM. (2020). RF-Induced Heating in Bare and Covered Stainless Steel Rods: Effect of Length, Covering, and Diameter. In eMagRes (eds R.K. Harris and R.L. Wasylshen). <https://doi.org/10.1002/9780470034590.emrstm1630>

Full List of Presenter's Publications: Conference Proceedings

- [1] Murdock M, Gross D, Leewood A, **Serano P**, Horner M, Nyenhuis J, Afshari P, Moreno D, White J, Alnnasouri R, Ferry P, Ponvianne Y, Kozlov M, Gerber C, Bibiano C, Rajan S, Angelone LM, Computational Modeling of RF-Induced Heating Due to a Titanium-Alloy Rod: An Interlaboratory Comparison for the ASTM F2182 Task Group 27th Annual Meeting of the International Society for Magnetic Resonance in Medicine, Montreal, 2019.
- [2] **Serano P**, Fujimoto K, Iacono M, Angelone LM, Rajan S. Variation in RF Heating Characteristics of Insulated vs. Bare Metal Stents BMES Frontiers in Medical Devices Conference, Washington, 2017.
- [3] Atefi SR, **Serano P**, Poulsen C, Angelone LM, Bonmassar G. Numerical Simulation of Specific Absorption Rate (SAR) Induced in the Head as a Function of EEG Lead Conductivity during 256-channel dEEG/fMRI at 3T 25th Annual Meeting of the International Society for Magnetic Resonance in Medicine, Honolulu, 2017
- [4] Guérin B, **Serano P**, Iacono MI, Herrington, TM, Dougherty, DD. Patient Specific Modeling of Deep Brain Stimulation Patients for MRI Safety Studies 25th Annual Meeting of the International Society for Magnetic Resonance in Medicine, Honolulu, 2017
- [5] Fujimoto K, Angelone LM, Lucano E, **Serano P**, Rajan S, Iacono M.I. Effect of Simulation Settings on Local Specific Absorption Rate (SAR) in Different Anatomical Structures ISMRM Workshop on Ensuring RF Safety in MRI, Mclean, 2017.
- [6] **Serano P**, Iacono, M, Angelone, LM, Rajan S. Increased RF Heating of Implanted Medical Devices Due to the Ground Plane Effect. BMES Frontiers in Medical Devices Conference, Washington, 2016.
- [7] **Serano P**, Iacono M, Angelone LM, Rajan S. RF Induced Heating of Overlapped Stents. Annual Meeting of the International Society of Magnetic Resonance in Medicine, Singapore, 2016.
- [8] **Serano P**, Donaldson F, Coburn J, Kainz W, Song T, Angelone LM, Rajan S, Iacono M. Probabilistic Finite Element Analysis to Assess the RF Safety of Passive Implanted Devices in MRI. BMES Frontiers in Medical Devices Conference, Washington, 2015.
- [9] **Serano P**, Angelone LM, Bonmassar G. Novel Lead Design for Simultaneous Deep Brain Stimulation and Functional Magnetic Resonance Imaging. EMBS BRAIN Grand Challenges Conference, Washington, 2014.

Full List of Presenter's Publications: Conference Proceedings

- [10] **Serano P**, Angelone LM, Bonmassar G. Evaluation of Multi-Section Resistive Tapered Stripline (RTS) Lead Wires to Reduce SAR Near Implanted DBS Electrodes During MRI. Annual Meeting of the International Society of Magnetic Resonance in Medicine, Milan, 2014.
- [11] Bonmassar G, **Serano P**, Angelone LM. Specific Absorption Rate in an ASTM Phantom Containing a Deep Brain Stimulation Lead at 3 Tesla MRI. 6th International IEEE EMBS Neural Engineering Conference, San Diego, 2013.
- [12] Lim C, **Serano P**, Ackerman J. Pre-Amplifiers for a 15 Tesla Magnetic Resonance Imager. IEEE International RF and Microwave Conference, Penang, 2013.
- [13] Guérin B, Gebhardt M, **Serano P**, Adalsteinsson E, Hamm M, Pfeuffer J, Nistler J, Wald LL. Performance comparison of parallel transmit arrays for 3T body imaging under local and global SAR constraints. Annual Meeting of the International Society of Magnetic Resonance in Medicine, Salt Lake City, 2013
- [14] Poser BA, Anderson RJ, **Serano P**, Mareyam A, Guérin B, Deng W, Wald LL, Stenger VA. Simultaneous multi-slice excitation by parallel transmission using a dual-row pTX head array. Annual Meeting of the International Society of Magnetic Resonance in Medicine, Salt Lake City, 2013.
- [15] Guérin B, Gebhardt M, **Serano P**, Adalsteinsson E, Hamm M, Pfeuffer J, Nistler J, Wald LL. Simulation study of parallel transmit arrays for 3T body imaging under local and global SAR constraints. Annual Meeting of the International Society of Magnetic Resonance in Medicine, Melbourne, 2012.
- [16] Zhao W, Cohen-Adad J, Polimeni J, Guérin B, **Serano P**, Mareyam A, Hoecht P, Wald LL. 19-channel Rx array coil and 4-channel Tx loop array for cervical spinal cord imaging at 7T MRI. Annual Meeting of the International Society of Magnetic Resonance in Medicine, Melbourne, 2012.
- [17] **Serano P**, Brevard M, Ludwig R. Reconfigurable electronic tune-detune circuit for RF coil systems. Annual Meeting of the International Society of Magnetic Resonance in Medicine, Honolulu, 2009